STAR CLUSTERS IN M31: I. A CATALOG AND A STUDY OF THE YOUNG CLUSTERS

Nelson Caldwell

Smithsonian Astrophysical Observatory, 60 Garden Street, Cambridge, MA 02138, USA
electronic mail: caldwell@cfa.harvard.edu

Paul Harding

Department of Astronomy, Case Western Reserve University, Cleveland OH 44106-7215
electronic mail: paul.harding@case.edu

Heather Morrison

Department of Astronomy, Case Western Reserve University, Cleveland OH 44106-7215
electronic mail: heather@vegemite.case.edu

James A. Rose

Department of Physics and Astronomy, University of North Carolina, Chapel Hill, NC 27599, USA
electronic mail: jim@physics.unc.edu

Ricardo Schiavon

Gemini Observatory, 670 N. A'ohoku Place , Hilo, HI 96720, USA
electronic mail: rschiavo@gemini.edu

Jeff Kriessler

Department of Astronomy, Case Western Reserve University, Cleveland OH 44106-7215
electronic mail: jeffrey.kriessler@case.edu

ABSTRACT

We present an updated catalog of 1300 objects in the field of M31, including 670 likely star clusters of various types, the rest being stars or background galaxies once thought to be clusters. The coordinates in the catalog are accurate to $0.2''$, and are based on images from the Local Group Survey (LGS, Massey et al. 2006) or from the DSS. Archival HST images and the LGS were inspected to confirm cluster classifications where possible, but most of the classifications are based on spectra taken of ~ 1000 objects with the Hectospec fiber positioner and spectrograph on the 6.5m MMT. The spectra and images of young clusters are analyzed in detail in this paper; analysis of older clusters will appear in a later paper. Ages and reddenings of 140 young clusters are derived by comparing the observed spectra with model spectra. Seven of these clusters also have ages derived from HST color-magnitude diagrams (two of which we present here); these agree well with the spectroscopically determined ages. Combining new V band photometry with the M/L values that correspond to the derived cluster ages, we derive masses for the young clusters, finding them to have masses as great as 10^5 with a median of $10^4 M_\odot$, and a median age of 0.25 Gyr. In comparison therefore, Milky Way open clusters have the lowest median mass, the Milky Way and M31 globulars the highest, and the LMC young massive clusters and the M31 young clusters are in between. The young clusters in M31 show a range of structure. Most have the low concentration typical of Milky Way open clusters, but there are a few which have high concentrations. We expect that most of these young clusters will be disrupted in the next Gyr or so, however, some of the more massive and concentrated of the young clusters will likely survive for longer. The spatial distribution of the young clusters is well correlated with the star-forming regions as mapped out by mid-IR emission. A kinematic analysis likewise confirms the spatial association of the young clusters with the star forming young disk in M31.

Subject headings: catalogs – galaxies: individual (M31) – galaxies: star clusters – globular clusters: general – star clusters: general

1. INTRODUCTION

In the Milky Way, there is a clear separation between known open clusters (which have diffuse structure, generally have low masses and ages, and belong to the disk) and globular clusters (which have a more concentrated structure, higher masses and ages, and in many cases belong to the halo). When the only well-studied globular cluster system was that of the Milky Way, it was generally thought that this separation was because globular clusters were fundamentally different from other star clusters, perhaps because of conditions in the early universe (Peebles & Dicke 1968; Fall & Rees 1985).

However, it is possible to produce this apparent bimodality from clusters formed in a single process, with the same cluster initial mass function. In this picture, cluster disruption mechanisms, which are more effective at destroying low-mass clusters in particular because

of two-body relaxation (Spitzer 1958; Spitzer & Harm 1958), would remove almost all of the low-mass older clusters. If all clusters were born with similar cluster mass functions, then we would expect to see the occasional high-mass young cluster. In fact, we do see these in other galaxies. The "populous blue clusters" of the LMC (Freeman 1980; Hodge 1981; Mateo 1993) have been suggested as examples of young objects which will evolve into globular clusters. M33 also has a few likely massive young clusters (Chandar et al. 1999) , and such clusters have been found in a number of normal isolated spirals (Larsen 2004). It is possible that the seeming absence of such objects in the Milky Way is merely an observational selection effect; recently, there have been discoveries of heavily reddened open clusters such as Westerlund 1, which likely has mass in excess of $10^5 M_\odot$ (Clark et al. 2005).

What of M31's clusters? While its clusters have been studied since the 1960s (eg Kinman 1963; Veteŝnik 1962; van den Bergh 1969) and it was noted even then that some of these clusters had colors indicating young populations, their nature is still not entirely clear. van den Bergh (1969) called them open clusters, while Krienke & Hodge (2007) adopted the simple convention of calling any cluster projected on M31's disk a "disk cluster" until proved otherwise by kinematics. This avoids the question of whether young clusters are fundamentally different from globular clusters in structure, formation, etc. Our detailed study of M31 young clusters, incorporating kinematics, should cast some more light on these questions.

It is only recently that detailed constraints on the mass, kinematics, age and structure of cluster populations in M31 have been obtained, particularly for clusters projected on the inner disk and bulge. Multi-fiber spectroscopy and HST imaging have played an important role here. A number of M31 globular cluster catalogs have been created over the years, giving a very heterogeneous result, with significant contamination by both background galaxies, foreground objects and even non-clusters in M31 itself. While the work of Perrett et al. (2002), Barmby et al. (2000), Galleti et al. (2007), Kim et al. (2007), and Lee et al. (2008) has gone a long way towards cleaning up the catalogs and winnowing out the non-clusters, still more work is needed for both young and old clusters. Here we present a new catalog of M31 star clusters which were originally classified as globular clusters, all with updated high-quality coordinates. We have observed a large number of these clusters with the MMT and the Hectospec multi-fiber system. In this paper we study more than 100 young M31 clusters in detail. In subsequent papers we will address the kinematics, ages and metallicities of the older clusters.

The M31 young clusters have been studied both by authors aiming to study its open clusters (eg Hodge 1979; Hodge et al. 1987; Williams & Hodge 2001a; Krienke & Hodge 2007), and also by others who have aimed to study its globular clusters. For example, Elson & Walterbos (1988) pointed out the existence of young clusters in M31, estimated masses between 10^4 and $10^5 M_\odot$, and drew attention to their similarity to the populous blue clusters in the LMC. Barmby et al. (2000) noted the existence of 8 clusters with strong Balmer lines in their spectra, which they tentatively classified as young

globular clusters. Beasley et al. (2004) (confirmed with a later sample by Puzia et al. 2005) added more clusters, and commented that HST imaging (then unavailable) was needed to distinguish between structure typical of open and globular clusters. Burstein et al. (2004) added more new young clusters, bringing the total to 19, and Fusi Pecci et al. (2005) increased the sample to 67. In general, authors have associated these young clusters with M31's disk, although Burstein et al. (2004) invoke an accretion of an LMC-sized galaxy by M31.

Observations are particularly challenging for clusters projected on M31's disk: many of the early velocities had large errors, and there were issues with background subtraction. Here we discuss high-quality spectroscopic measurements of kinematics and age for the young clusters, supplemented with HST imaging to delineate the structural, spatial and kinematical properties of these young clusters. We find that while they are almost all kinematically associated with M31's young disk, and their age distribution will allow us to test suggestions that M32 has had a recent passage through M31's disk (Gordon et al. 2005; Block et al. 2006). The young clusters have structure and masses which range all the way from the low mass Milky Way open clusters to higher mass, more concentrated globular clusters, although they are dominated by the lower concentration clusters. We will also discuss the likelihood that these clusters will survive.

2. REVISED CATALOG OF M31 CLUSTERS

The starting point for our cluster catalog was the Revised Bologna Catalog (RBC) (Galleti et al. 2004, 2007), itself a compilation of many previous catalogs. Coordinates from this catalog were used to inspect images from the Local Group Survey (LGS) images (Massey et al. 2006), which cover a region out to 18 kpc radius on the major axis and 2.8 kpc away from the major axis, HST archival WFPC2 and ACS images, and the DSS for the outermost clusters. The LGS images have median seeing $\sim 1\,''$. We also added in some new clusters, found visually by ourselves on the LGS images and on HST images (discussed below). Even a casual inspection of the LGS images, particularly the I band images, reveals the presence of a vast number of uncataloged faint disk clusters, presumably similar to the galactic open clusters (Krienke & Hodge 2007, estimate 10000 such clusters from HST images) . We have elected not to take on the enormous task of cataloging and measuring those clusters in this paper; rather we choose to deal with the more massive clusters for which some information, however fragmentary, already exists. At a later stage in the project, the catalogs of Kim et al. (2007), extracted from KPNO 0.9m images, and Krienke & Hodge (2007), from HST images became available, from which we collected objects not already in our own catalog and subjected them to the same editing as we now describe. The archival images were thus used to answer the following questions from the catalog we created from the RBC and our own additions.

First, did the catalog coordinates correspond to a unique object? In cases where the identification of the cluster on the Local Group Survey was ambiguous or unclear, we consulted the original papers and finding charts where these were available (Veteŝnik 1962; Baade & Arp

1964; Sargent et al. 1977; Battistini et al. 1980, 1987, 1993; Crampton et al. 1985; Racine 1991; Auriere et al. 1992; Mochejska et al. 1998; Barmby & Huchra 2001). In some cases, there is no clear object that can be associated with the published coordinates, or the nearest object in fact already had a different ID. The large number of Hectospec fibers meant that we were able to verify classifications of many low-probability candidates. The cataloging and observation parts of this program occurred in a feedback fashion, allowing some target names and/or coordinates to be changed for the succeeding observations. As a result, we had some objects whose identifications were incorrect; to these we add an "x" to their original name in our tables below.

Second, were the existing coordinates accurate? In general, the answer was no. Our final catalog contains 1200 objects from the RBC, without considering the newer candidates of Kim et al. (2007) and Krienke & Hodge (2007). 830 of those required coordinate corrections larger than $0.5''$ to place them on the FK5 system used in the DSS and the LGS images. The median error in coordinates is $0.8''$, with the largest error being of order $10''$; at which point the identification of the actual object becomes uncertain. Similarly, there are 379 objects in the Kim et al. (2007) catalog found within $2''$ of an LGS object. For these, the median error is $0.8''$ offset, where the largest error is $1.9''$. Many of the discrepant velocities between us and the RBC or Kim et al. (2007) tabulations reported here are likely due to inaccurate coordinates used in previous spectroscopic work. The coordinates newly derived from the LGS images are accurate to $0.2''$ rms.

Third, were the targets really clusters? The LGS V and I band images, and WFPC2 or ACS images taken with non-UV filters were used to confirm the cluster nature of the objects, by visual inspection as well as the automated image classifier contained in the SExtractor code (Bertin & Arnouts 1996). A number of cluster candidates were stellar on the LGS images; all of these were later confirmed as stars in our spectra, from either the spectral characteristics or the velocities, in regions of M31 where there is no confusion between the local M31 velocity field and the velocity distribution of foreground galactic stars. We found that about 90 of the Kim et al. (2007) candidates listed as new, probable and possible (indicating that they appeared non-stellar in their KPNO 0.9m images) appeared stellar on the LGS or HST images. Objects for which we have no new classification data are kept in the catalog, but noted as still in question in our table.

The large majority of the misclassified objects are stars (foreground galactic or M31 members); more than 130 objects considered to be clusters as recently as 2007 by Galleti et al. (2007) are in fact stars. Quite a number of cataloged objects are background galaxies, and a few are either unidentifiable, or are accidental clumpings of galactic or M31 member stars.

Cohen et al. (2005) have recently stated that four clusters that were classified as disk clusters by Morrison et al. (2004) are "asterisms". They note that in their Adaptive Optics (AO) images there was no cluster visible – generally there were only a few bright stars. However, for young clusters, red supergiants would dominate the light at infrared wavelengths and the hotter main-sequence stars would appear much fainter. We would need to use multi-wavelength data to classify these objects correctly. We show below that the optical spectra of those four clusters are indeed consistent with clusters of massive, main-sequence stars, and although the magnitudes, and hence masses, of these few objects were certainly overestimated, the objects will still be considered as clusters in our catalog, at least until HST images show otherwise. Figure 1 shows this complication for one cluster, by comparing the high resolution, but long wavelength AO image with the LGS I band image. A star cluster is clearly visible in the I band, and even more prominent at bluer wavelengths - the object is indeed a young star cluster, though certainly not a globular and not very massive. Our own HST images do reveal two cataloged clusters as asterisms: these are comprised of a small number of OB stars and late supergiants, resulting in a distinctive integrated spectrum with strong Balmer and He I lines in the blue, and TiO bands in the red. Even if these two are real clusters, the derived masses are small enough to exclude them from a list of massive clusters.

Some cataloged objects have no real object even within a generous radius. In a few cases, a nearby background galaxy had also led to confusion in previous papers (though not in the most recent version of the RBC), whereby an actual cluster was labeled as background. Thus, while for the most part we have removed objects from the list of clusters, we have also restored a few objects to the cluster list.

Table 1 lists all objects believed to be clusters. For object names, we use the naming convention of Barmby et al. (2000) where possible, where the name consists of a prefix with the RBC number followed by the number of the object from the next most significant catalog. Objects for which we have no new information other than improved coordinates, and which have not been convincingly shown to be clusters by previous workers, are italicized. Objects in the RBC which we did not observe and for which our coordinates are within $0.5''$ of the RBC coordinates are not listed here, nor are the Williams & Hodge (2001a); Kim et al. (2007) or Krienke & Hodge (2007) cluster candidates that we did not observe. Some objects that we did not observe could of course still be background even though they have non-stellar profiles, but these, few in number, are still listed here.

A rough classification based on the spectra is included in this table, for objects with good quality spectra. "Young" clusters are those with ages less than 1 Gyr, "interm" refers to those with ages between 1 and 2 Gyr, and "old" refers to clusters older than that. A subsequent paper will provide a detailed analysis and evidence that few if any of these "old" clusters have ages less than 10 Gyr. "HII" indicates the spectrum is emission-line dominated. "na" appears for objects known to be clusters from an HST image, but for which we have no spectrum, or cases where the spectrum is too poor to determine the age, even in a coarse manner. The V magnitudes come from this paper, using the aperture size listed (see 5.3) or otherwise as indicated. Column C describes what information was used to classify the target as a cluster. The possibilities are "S", where our spectrum clearly indicates a star cluster, "L", where the LGS image is non-stellar, and/or "H", where an HST image indicates a star cluster.
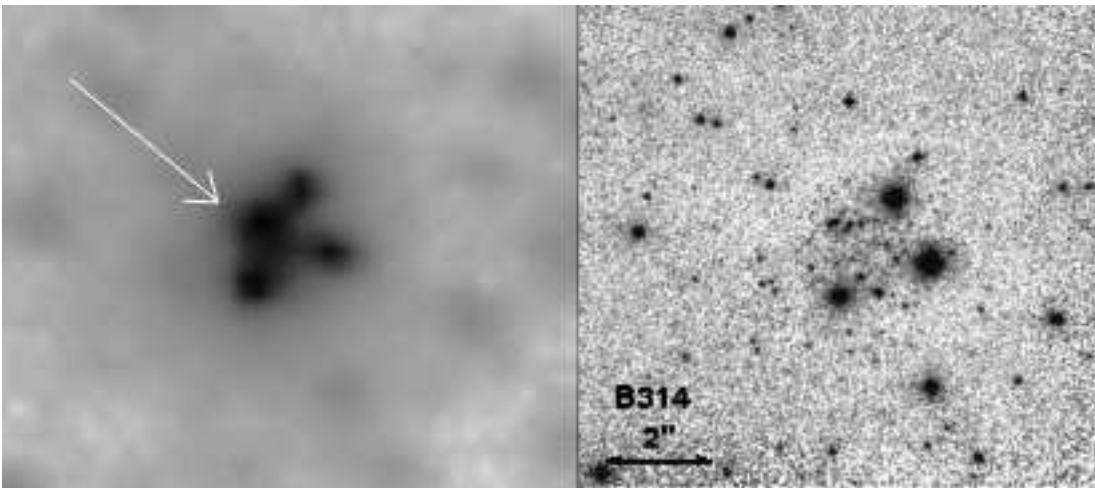
Fig. 1.— The disputed cluster B314-G037. The LGS I band image is shown on the left, next to the Cohen et al. (2005) AO image, taken in the K´ band. The I band reveals the star cluster clearly (arrow), though the magnitude measured for the cluster previously using a large aperture was certainly too bright.

Table 2 gives a list of those clusters that have ages less than 2 Gyr. (Sections 4, 5 and 6.4 of this paper will discuss the measurement of ages and masses for these clusters.) Table 3 lists objects from previous cluster catalogs that are in fact stars. Many of these had also been classified as stars by previous workers. Asterisms are also listed here. Table 4 gives a list of possible stars. In these cases, the Local Group Survey imaging indicates a stellar profile, but either we have no spectrum, or the spectrum is ambiguous. Note that some of the stars in Tables 3 and 4 are certainly members of M31. Objects thought to be clusters in the Kim et al. (2007) catalog but which have stellar profiles in the LGS images are listed in 4, with coordinates derived from the LGS. Table 5 lists background galaxies. Table 6 lists cataloged objects where there was no obvious object within a reasonable distance of the previously published coordinates, which are listed here again.

As a commentary on the difficulty experienced by all of those who have endeavored to collect true M31 star clusters (including us), here is a brief summary of the contents of the most recent version of the RBC, excluding the additions of Kim et al. (2007); Williams & Hodge (2001a); Huxor et al. (2005) and Krienke & Hodge (2007), but including the lists compiled by other astronomers starting with Edwin Hubble. The RBC, restricted as just mentioned, contains 1170 entries. We here, and others (particularly Barmby et al. 2000), have provided classifications for 991 of these. Only 620 entries are actually star clusters, while 20 more could be considered clusters though the large amount of ionized gas present indicates the clusters may still be forming. 270 entries are stars, mostly foreground, and 224 entries are background galaxies or AGN. At least 2 objects are chance arrangements of luminous M31 stars, together which appear as clusters from the ground.

In the Kim et al. (2007) catalogs, there 113, 258 and 234 "new", "probable" and "possible" clusters, respectively. The LGS survey contains images of 94, 152 and 105 members of those catalogs, respectively. Of those subsets, 79, 106, and 129, respectively have non-stellar profiles in the LGS, some of which were observed with Hectospec.

3. HECTOSPEC OBSERVATIONS

The Hectospec multi-fiber positioner and spectrograph is ideally suited for this project, in that its usable field is 1 degree in diameter, and the instrument itself is mounted on the 6.5m MMT telescope. We obtained data in observing runs in the years 2004 to 2007, and now have high-quality spectral observations of over 400 confirmed clusters in M31, and lower quality spectra of 50 more. We used the 270 gpm grating (except for a small number of objects taken with a 600 gpm grating), which gave spectral coverage from 3650–9200Å and a resolution of ~5Å. The normal operating procedure with Hectospec, and other multi-fiber spectrographs, is to assign a number of fibers to blank sky areas in the focal plane, and then combine those in some fashion to allow sky subtraction of the target spectra. For instance, the 4-5 fibers nearest on the sky to the target may be combined. These methods are satisfactory for our outer M31 fields, but not for the central areas where the local background is high relative to the cluster targets. For those fields, we alternated exposures on-target and off-target to allow local background subtraction to be performed. Many of the discrepancies between our bulge cluster velocities and those of previous workers might be explained by their lack of proper background subtraction, and/or inaccurate target coordinates.

We obtained exposures for 25 fields, with total exposure times varying between 1800s and 4800s. The signal/noise ratios for the 500 objects we classified as clusters have a median of 60 at 5200Å and 30 at 4000Å, with more than 100 clusters having a ratio at 5200Å better than 100. Figure 2 shows the locations and types of objects observed in all of these fields.

The multifiber spectra were reduced in a uniform manner. For each field, or configuration, the separate exposures were debiased and flat fielded, and then compared before extraction to allow identification and elimination of cosmic rays through interpolation. Spectra were then extracted, combined and wavelength calibrated. Each fiber has a distinct wavelength dependence in throughput, which can be estimated using exposures of a continuum source or the twilight sky. The object spectra were thus corrected for this dependence next, followed by a
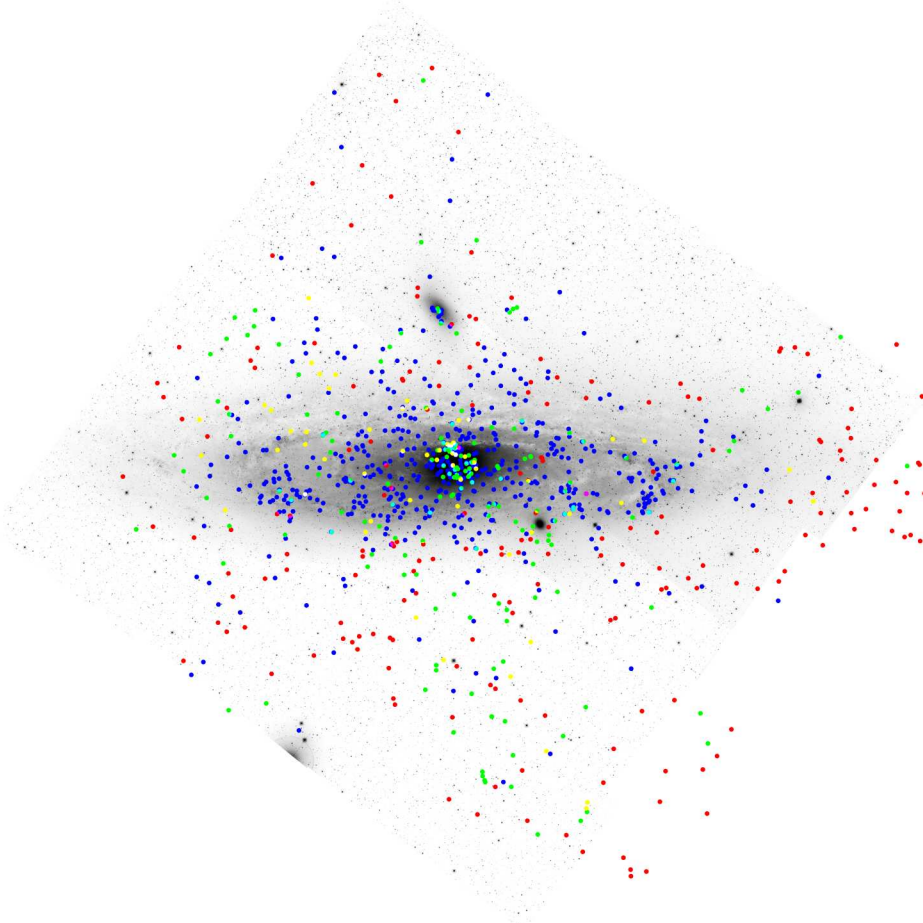
FIG. 2.— Locations of the spectra taken with Hectospec of M31 cluster candidates. Confirmed clusters, stars, possible stars and background galaxies are shown in blue, green, yellow and red, respectively.

correction to put all the spectra on the same exposure level. The latter correction was estimated by the strength of several night sky emission lines. Sky subtraction was performed, using object-free spectra as near as possible to each target. For the targets where local M31 background was high, the method was reversed, such that only sky spectra far from the disk of M31 were used. An offset exposure for such fields, taken concurrently, was reduced in a similar way (thus contemporaneous sky subtraction was performed for on- and off-target exposures), and then the off-target spectra were subtracted from the on-target. This process increased the resultant noise of course, but we deemed it essential for targets in the bulge and disk of M31. The off-target exposures have the additional advantage of giving measurements of the unresolved light in over 800 locations over the entire disk of M31.

Velocities were measured using the SAO xcsao software. Given the wide variety of spectra in this study, it was deemed necessary to develop new velocity templates, from the spectra themselves. The procedure was to derive an initial velocity of all spectra using library templates (typically a K giant star). The spectra were shifted to zero velocity, and sorted into three different spectral types, A, F and G type spectra. The best spectra in each group were combined to make new templates, and the procedure was repeated now using the new templates. By using these templates we have assured that all

the M31 targets are on the same velocity system. They are tied to an external velocity in the initial step, whose accuracy depended on the accuracy of the initial set of templates used. A good test of the internal accuracy was provided by repeat measurements of clusters. We have 386 repeat measurements (on different nights) for 224 clusters. The median difference in velocity for these repeats was 0.5 km s^{-1}, with an implied median single measurement error of 11 km s^{-1} (smaller than our formal errors listed in the tables). We will present external comparisons in a subsequent paper, but note that the cluster velocities agree very well with the HI rotation curve (see 6.3). Velocities for the young clusters, stars and galaxies are presented in Tables 2, 3, 4, and 5. Velocities for the old clusters will presented in a subsequent paper.

The spectra were corrected to relative flux values, using observations of standard stars (the MMT F/5 optics system employs an atmospheric dispersion compensator, ADC). The flux correction has been determined to be very stable over several years. Thus, observations of the same targets taken in different seasons can be combined where available.

4. USING HST IMAGES TO DETERMINE CLUSTER CLASSIFICATION

Cohen et al. (2005) highlighted the heterogeneous quality of the M31 cluster catalogs when they claimed, us-
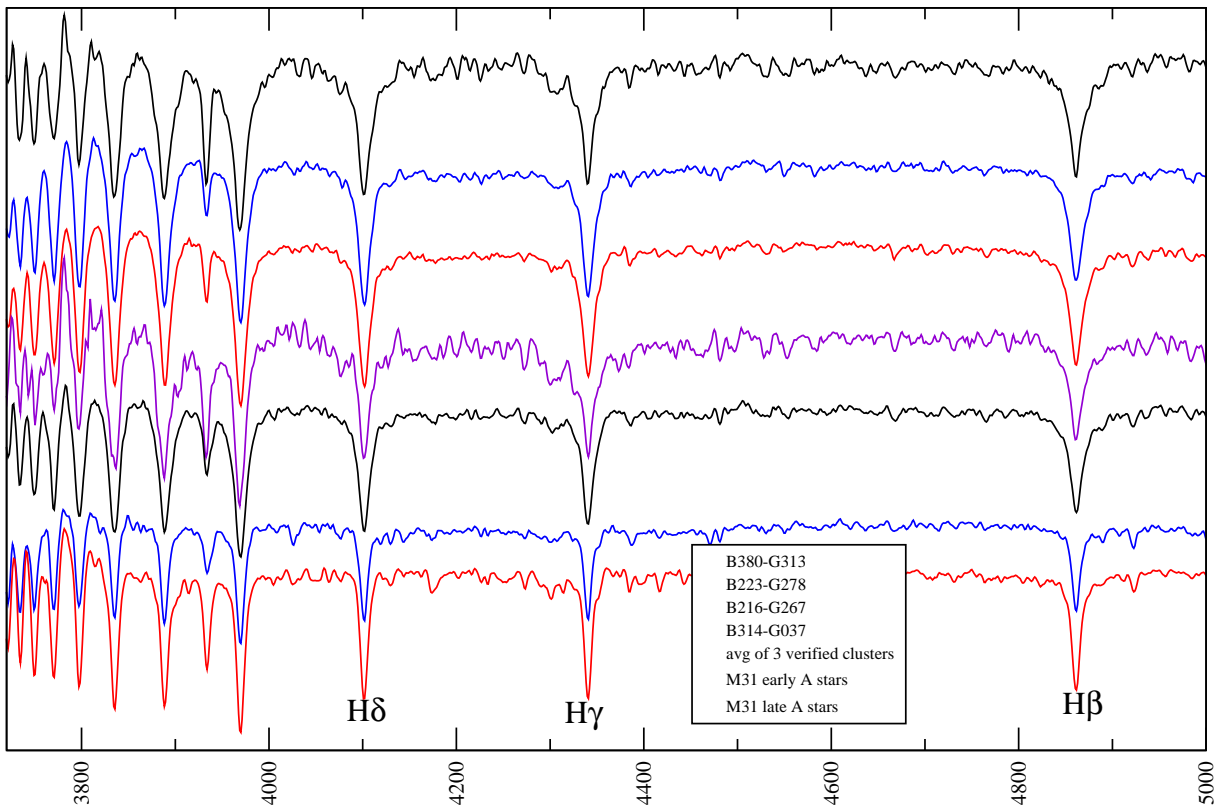
FIG. 3.— Hectospectra of young clusters in M31. Shown are spectra of clusters disputed as real by Cohen et al. (2005), the average of three young clusters verified by ACS images, and the average of single, blue supergiant stars as a comparison. If the disputed clusters were in fact merely a few stars mistaken for a cluster, their absorption line widths, particularly the Balmer lines, would be narrow as seen in the blue supergiant spectra. These spectra have been gaussian smoothed and have had their continuum shapes removed for ease of display.

ing AO techniques at K´ , that four out of six observed young clusters were in fact asterisms. Figure 3 shows, from top to bottom, spectra of the four disputed clusters, the average of three genuine young clusters verified by ACS images, and the average spectra of single supergiant stars (these were verified to be stars from the LGS images, and members of M31 from their velocities). If the disputed clusters were in fact merely a few stars, those stars would have to be supergiant stars, whose absorption line widths would be as narrow as seen in our blue supergiant spectra. This is not the case for the four disputed clusters (note in particular the Hβ and Hδ widths, narrow in the stars and wide in the other spectra), and we conclude that those objects are true clusters and not asterisms. To be sure, these particular clusters are not globular clusters either, and, additionally, are perhaps not massive enough to be considered young, populous clusters.

High spatial resolution imaging can both check for asterisms and also explore the clusters' spatial structure: is their concentration low, like typical Milky Way open clusters, or high, like globular clusters?

There are ACS or WFPC2 images available for 25 of the clusters with ages less than 2 Gyr. Two of these show no evidence of an underlying cluster, but the remaining 23 are clearly not asterisms. Figure 4 shows the range of structure seen in these young clusters. While many of them show the low-concentration structure typical of Milky Way open clusters, a number of them, such as B374-G306 and B018-G071, are quite centrally concentrated, like the majority of the Milky Way globular

clusters.

Barmby et al. (2007) have measured the structure of M31 clusters with available HST imaging at the time of publication. There are 70 clusters in their sample which we have classified as old, and 7 of our young clusters. It is straightforward to compare the structure of the clusters they study with the Milky Way globulars, because they use the same technique as McLaughlin & van der Marel (2005), who have produced a careful summary of the structure of the Milky Way globular clusters. However, it should be noted that their fitting technique (fitting ellipses to cluster isophotes) is not well-suited to very low-concentration clusters, and in fact one of our young clusters, B081D, is omitted from their analysis because of its low density.

Figure 5 compares their results for old clusters from our sample with the structure of Milky Way globulars (from the work of McLaughlin & van der Marel 2005). It can be seen that the concentration parameter[1] for the old clusters in M31 has a similar distribution to the Milky Way globulars. We note that although there are no old clusters in our sample with concentration greater than 2.2, such clusters are definitely present in the Barmby et al. (2007) sample so this absence is unlikely to be significant. The similarity in structure is interesting, because at first sight it would seem that the M31 clusters with high concentration would be preferentially discovered in surveys. Perhaps the M31 globular cluster surveys (which, as we have seen above, include a large number of non-globular

[1] $c = \log(r_t/r_0)$ for King model fits, Binney and Tremaine (2008) p. 307
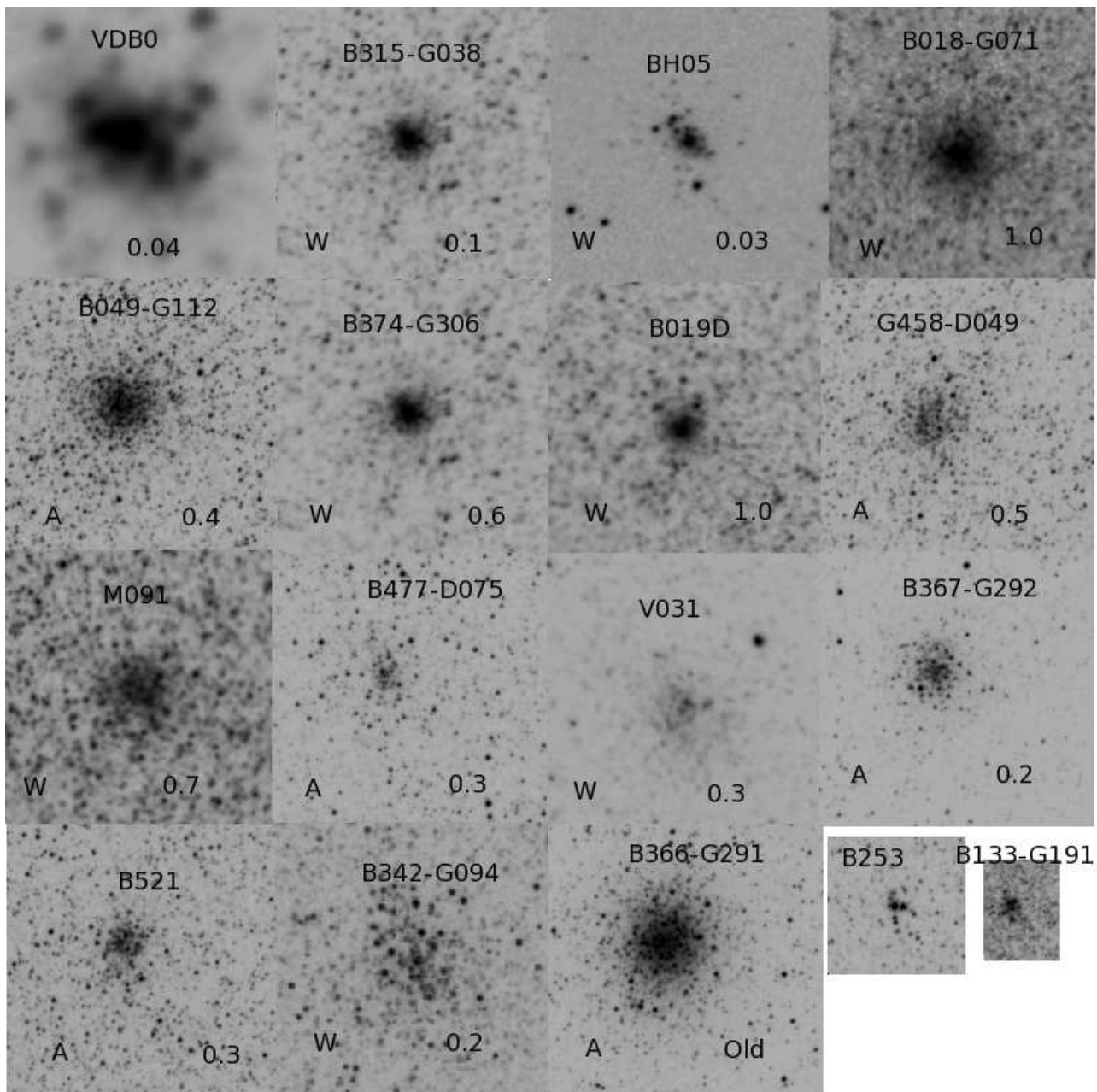
FIG. 4.— HST ACS or WFPC2 images of a selection of clusters with ages less than 2 Gyr, except for VDB0 whose image is from the LGS V band. The HST images were taken in either F555W or F606W. The spectroscopically determined ages in Gyr are listed for each image, as is the camera used ("A"=ACS, "W"=WFPC2), to aid in comparison since in general the ACS images are deeper. A comparison old M31 globular cluster is shown, as are two candidates that turned out to be asterisms. The scale is the same for all images; except for the two small ones, each image is 10″ on a side. The images are ordered by descending mass, starting at the top left.

clusters, as well as the low-concentration young clusters) are now sufficiently thorough that they are not strongly affected by this bias.

Although only seven of our young M31 clusters were analyzed by Barmby et al. (2007), it can be seen from Figure 5 (where they are marked by asterisks and five-pointed stars in the top panel) that their concentrations cover the whole range of the older clusters in M31 and in the Milky Way. (The five-pointed star represents Hubble V from NGC 205.) Our observational selection biases may over-emphasize high-concentration clusters, but it is still interesting to see that three of the young clusters have quite high concentration parameters. How does their structure compare with the Milky Way open clus-

ters? It is quite difficult to answer this question because the available samples of Milky Way open clusters are severely incomplete, and it is a challenging task to fit King models to the known open clusters, because cluster membership is hard to determine. The 2MASS database (Beichman et al. 1998; Jarrett et al. 2000) has been used by Bonatto & Bica (2005); Santos et al. (2005); Bonatto & Bica (2007); Bica et al. (2006); Bica & Bonatto (2008) to measure the structure of 21 open clusters. They used a CMD-fitting technique to remove contamination from disk field stars. We have also used data from Eigenbrod et al. (2004), who used radial velocity to decide member-ship. Because of the high background in all these cases, it is possible that the "limiting radius" given by the au-
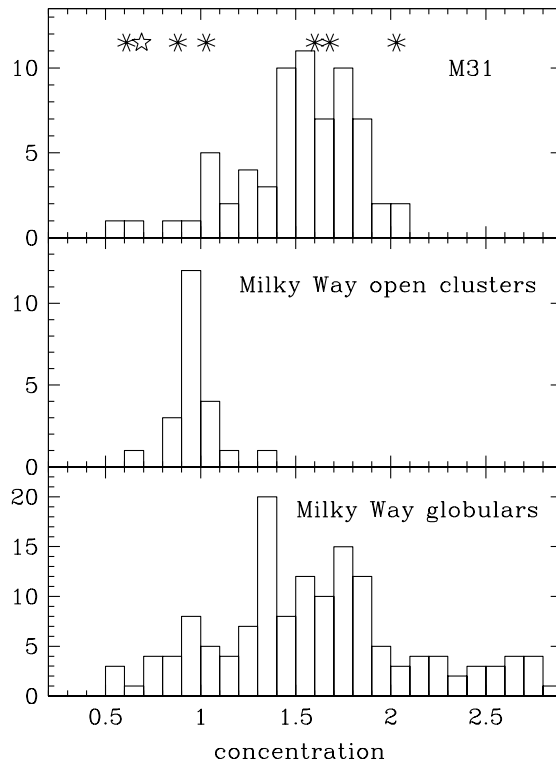
FIG. 5.— Histograms of the concentration parameter from King model fits for (top panel) old M31 clusters (young clusters shown by asterisks, the young cluster in NGC 205 by a 5-pointed star), (middle panel) Milky Way open clusters and (bottom panel) Milky Way globular clusters. It can be seen that the M31 old clusters resemble the Milky Way globulars in their concentration, while the M31 young clusters cover the range of both open and globular clusters.

thors is in fact smaller than the tidal radius, in which case the cluster concentrations would be smaller than those plotted. It can be seen in the middle panel of Figure 5 that all these open clusters have quite low concentrations. However, the sample of clusters with concentration measurements is quite small, and it is quite possible that there are a few open clusters in the Milky Way which are yet to be discovered and have high concentrations, like the two M31 young clusters.

In summary, the young clusters in M31 show a range of structure. Most have the low concentration typical of Milky Way open clusters, but there are a few which have high concentrations, like most Milky Way globulars. We note that any survey of M31 clusters will preferentially discover ones with high concentrations. In addition, the incompleteness of Milky Way open cluster samples and the difficulty of measuring cluster concentration in crowded fields means that we cannot rule out the existence of such clusters in the Milky Way.

5. AGES OF THE YOUNG CLUSTERS

In this section, we describe methods for determining ages from the spectra and color magnitude diagrams for the verified clusters. Since the emphasis in this paper is on the younger clusters, and more specifically, on their M/L ratios, our task is first to distinguish young from old clusters, and then to obtain accurate age measurements among the younger clusters. A more refined age determination (for clusters older than 2 Gyr) is postponed for a later paper.

5.1. Ages from Spectra

The methods for obtaining ages for young stellar populations from their integrated spectra are similar to those used for older stellar populations, except that instead of employing empirical stellar libraries (e.g., Worthey 1994), modelers focussing on younger stellar populations have used synthetic spectra, partly due to a lack of empirical spectra of young stars over a range of metallicities. Here we have made use of the Starburst99 stellar population modeling program (SB99, Leitherer et al. 1999).

To distinguish young from old clusters, we compared our cluster spectra with two external sets of spectra, which served as population templates. One set was the sample of 41 MW globular spectra obtained by Schiavon et al. (2005), covering the abundance range of $-2 <$[Fe/H]< 0. These spectra have a wavelength coverage from 3500 to 6300Å , a dispersion of 1Å/pixel and a resolution of about 4.5 Å, and served as our old population templates. Our young population templates were created from the SB99 program using the Padova Z=0.05 interior models and Z=0.04 stellar atmospheres, since it seemed likely the young clusters have supersolar abundances. Using a solar abundance set of isochrones in the models has the net effect of increasing the derived ages for clusters older than 0.1 Gyr, in a logarithmic scaling such that a 1 Gyr supersolar model and a 2.5 Gyr solar abundance model have nearly the same resultant spectra. A grid of 40 high resolution spectra was created for ages from zero to 2 Gyr, with a logarithmic time step of 0.07 between models.
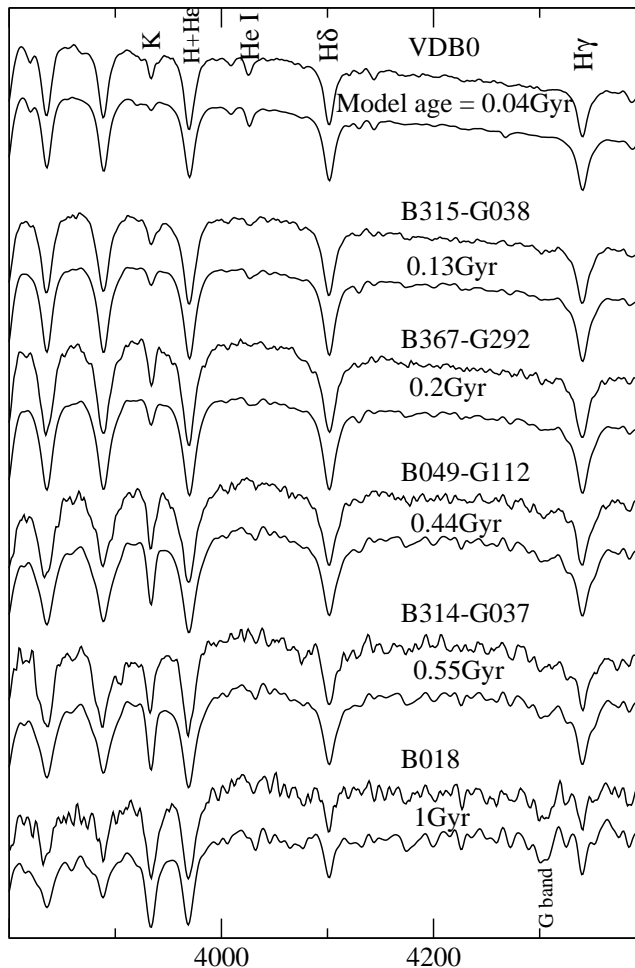
FIG. 6.— Spectra of a sample of young clusters, ranging in ages from 0.04 to 1 Gyr. Each object spectrum is shown with the best matching SB99 model spectrum. The object spectra have been smoothed with a gaussian with a sigma of 1.1Å and have been corrected for the reddening determined in this paper, which was itself determined by matching the continuum shapes of objects and models.

Our approach then was to simplify the old populations by only using a set of MW globular cluster templates, and to simplify the young populations by restricting ourselves to a single metal-rich chemical composition. The evolution of integrated spectra is essentially logarithmic with time; for example, the difference between a 5 and 12 Gyr population is relatively small compared to the large changes which occur over the first 1 Gyr. Thus our simplification seems warranted, particularly since in this paper we are concerned only with identifying the younger clusters and then studying them in detail. The major issue, as seen below, in separating old from young clusters, is the potential degeneracy between very metal-poor old populations and young populations, both of which are dominated by Balmer lines in their integrated spectra.

Both sets of template spectra were rebinned to the same resolution and dispersion as the M31 set, and then each template spectrum and M31 spectrum had a low order fit subtracted. The significance of this step was that we did not use the continuum shape to help determine the best matching template. A scaling factor was then determined between each template and all the available M31 cluster spectra, and the reduced χ^2 calculated over the spectral ranges of 3750-4500, 4750-5000, and 5080-5360 Å. These ranges were chosen to exclude spectral regions where there are few lines, as well as where the MW cluster spectra have no data due to bad columns in

the CCD used for that set. Specifically included were the Balmer lines from Hβ to Hζ, the Mg b lines, Ca II H&K, and the He I lines at 4009 and 4026Å, the last being prominent in OB stars and thus strong in the youngest clusters. The noise used in the reduced χ^2 calculations was that calculated from the spectra themselves.

A few logic decisions had to be made in analyzing the resultant list of reduced χ^2 values. For most cases, the lowest reduced χ^2 occurred clearly either in the SB99 set or the MW cluster set, thus allowing a particular cluster to be identified as young or old. For the young clusters, the age chosen was the average of ages where the reduced χ^2 was within 10% of the lowest value. About 10% of the clusters were equally well fit by a MW cluster, typically a metal-poor one with [Fe/H] < −1, and a metal-rich SB99 model. Nearly all of these are low S/N, and thus the poor fits were not surprising. Visual inspection of the spectrum clarified 11 of these as being very young (with very blue continuum shapes), and the remaining 48 we grouped as old.

Figure 6 compares the data and best-fitting models for a range of determined ages. We estimate the errors in determined ages for the young clusters to be about a factor of two, which leads to M/L uncertainties of 50%.

The model M/L values for each chosen age then allowed masses to be estimated from the cluster integrated V band photometry, which is described in 5.3. To allow a
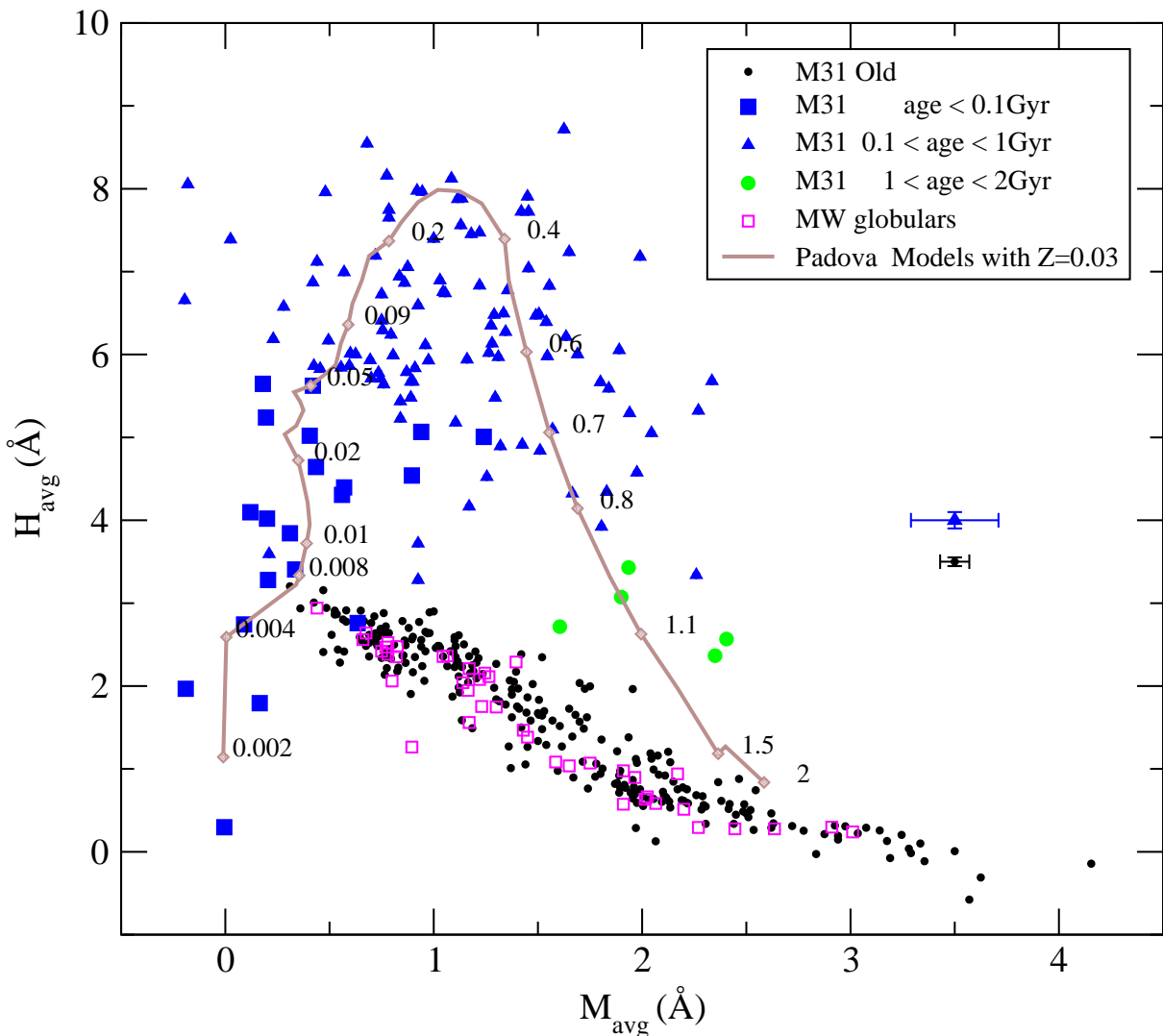
FIG. 7.— M_{avg} vs H_{avg} for M31 cluster spectra, with different types identified. Model indices derived from SB99 models using Padova Z=0.03 isochrones are also shown as a solid curve. Ages in Gyr are marked at selected areas along the curve. Median error bars are shown at the right for young and old clusters separately. The maximum errors on points in this plot are 0.45 for M_{avg} and 0.19 for H_{avg}.

comparison of young clusters to be made, we also calculated spectroscopic M/L values for the old M31 clusters from the models in Leonardi & Rose (2003), by obtaining estimates of [Fe/H] for each cluster via Fe and Mg line indices and assuming an age of 12 Gyr for each. The detailed analysis of the old cluster spectra will be presented in future paper.

Many readers may be more familiar with extracting ages from diagrams that plot a largely age-sensitive index versus a largely metallicity-sensitive index. To help demonstrate the efficacy of the χ^2 approach we show two such diagrams. Figure 7 is a plot of a Balmer line index versus a metal line index. We have defined M_{avg}=(Fe5270+Mgb)/2 and H_{avg}=(Hδ_F+ Hγ_F+Hβ)/3, all Lick indices (Worthey & Ottaviani 1997). These indices are equivalent widths: units are Å. For clarity in these diagrams, a signal-to-noise ratio cutoff was made, which eliminated 20% of the clusters from being plotted. Different symbols represent MW globular clusters (data from Schiavon et al. 2005), and four age bins for M31 clusters, which were determined by the χ^2 method: very young (< 0.1 Gyr), young (0.1 < age < 1 Gyr), intermediate (1 < age < 2 Gyr), and old. Clearly, there is a se-

quence of M31 clusters that closely matches the sequence of MW globular clusters, and a large spray of clusters that fall mostly in regions of higher Balmer equivalent width. Clusters with younger ages will of course have stronger Balmer absorption, until the very youngest ages are reached, at which point the Balmer strength declines again.

The second diagram (figure 8) uses indices defined in Leonardi & Rose (2003), namely the ratio of residual light in the Hδ line to the nearby Fe4045 line, and the ratio of the line at 3969Å which contains both Hϵ and CaII H, to the CaII K line. The indices are unitless. This diagram also shows the old cluster metallicity sequence and again distinguishes them from the young clusters, again excepting for the extremely young clusters.

The shortcoming of using such diagrams is that occasionally, due to the nature of real data, one index will be bad, causing the cluster to look young or old in one diagram, and the opposite in another. We are thus more confident in a fitting procedure that uses many diagnostic lines, but are gratified that in the vast majority of cases, these two diagrams verify the ages assigned by the χ^2 method.
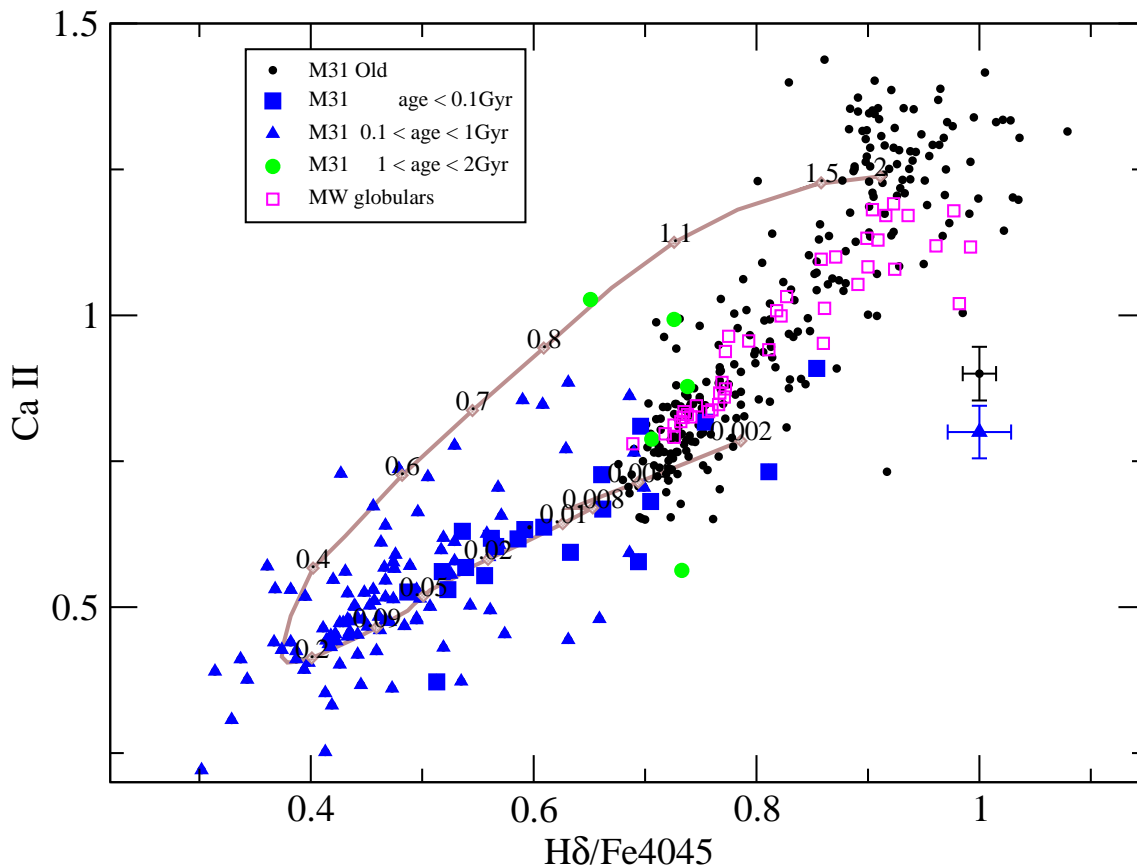
FIG. 8.— Same as Figure 7 for Hδ/Fe4045 and CaII. Maximum errors on points in this plot are 0.2 for both indices.

5.2. *Ages from HST/ACS color magnitude diagrams*

Williams & Hodge (2001a,b) estimated ages of many young disk clusters in M31 from WFPC2 color-magnitude diagrams (CMD) and isochrone fitting to the main sequence or to luminous evolved stars. Four of their clusters are bright enough to be in our spectroscopic study. Their ages agree quite well with ours (Table 7). Additionally, as part of HST GO proposal 10407, we obtained ACS images of several young clusters, three of which we report on here.

The multidrizzle package (Koekemoer et al. 2002) was used to combine the 3 individual exposures taken in the F435W and F606W filters (corresponding to B and V, respectively). Stellar photometry was obtained using the DAOPHOT package of Stetson (1987), modeling the spatially variable PSFs for each of the combined images separately, using only stars on those images. PSFs were constructed using 5-10 bright stars which had no pixels above a level of 20,000 counts, the point at which an ostensible non-linearity set in and the PSF no longer matched those of fainter stars. Aperture corrections were also measured using these stars, to determine any photometric offset between the psf photometry and the aperture magnitude within 0.5″. Sirianni et al. (2005) have provided aperture corrections from that aperture size to infinity, in all ACS filters. Generally, two passes of photometry were run. First, a star list was made and entered into ALLSTAR, which aside of the photometry, produces a star-subtracted image. Stars missed in the first round were located in the subtracted image and added to the original list. The original frame was then measured

again by ALLSTAR. The photometry was then placed on the standard Johnson/Kron-Cousins VI system using the aperture corrections and synthetic transformations provided in Sirianni et al. (2005). To lessen the severe problems with crowding in these clusters, only stars that fall in an annulus with radii of 15 and 50 pixels (0.75 and 2.5″) are shown in the color-magnitude diagrams (figure 9). The background field shown has the same area as the cluster fields, and refers to an annulus around B049-G112 with inner radius of 60 pixels. Isochrones with super solar abundances from the Padova group (Cioni et al. 2006a,b) have been placed in the diagrams to allow age determination, using a distance modulus of M31 of 24.43 and the reddenings determined above for these two clusters (0.25 for both). These CMDs and that of a third we have worked on (B367-G292) give ages in reasonable agreement with those from the spectroscopic analysis (Table 7).

5.3. *Cluster integrated photometry*

Multicolor photometry for most of the clusters in this project is already collated in Barmby et al. (2000), but enough clusters are missing to warrant remeasuring all the clusters, to allow the photometry to be used with the spectroscopic M/L values to obtain masses. The LGS survey of M31 consisted of 10 separate but overlapping fields. Stellar photometry from these fields using psf-fitting has been reported in Massey et al. (2006), but the aperture photometry needed for resolved star clusters has not yet been reported. To limit the scope of the work, we elected to measure objects in our catalogs only in the V

B049-G112   B458-D049   Background
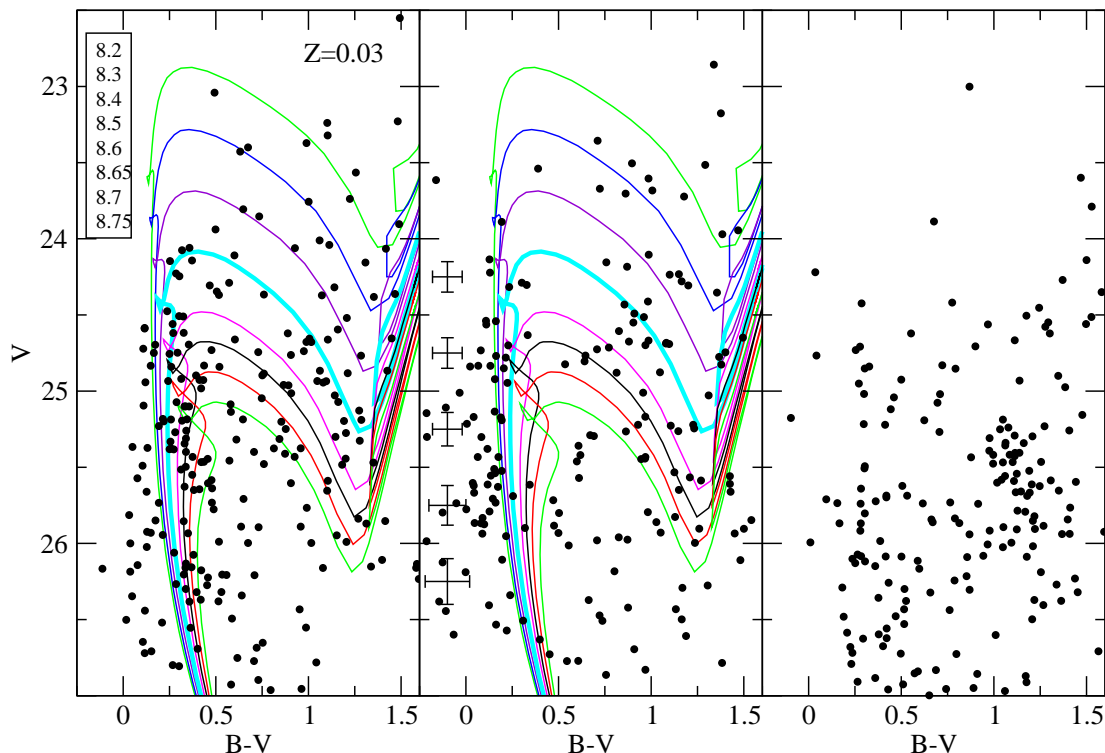
FIG. 9.— Color magnitude diagrams obtained from HST/ACS F435W and F606W images. Shown are two young clusters and the background field for B048-S112. Isochrones for a range of ages at supersolar metallicity come from Cioni et al. (2006a,b). The inset legend lists the isochrone ages shown, in log years. A distance modulus of 24.43 and reddenings of 0.25 mag have been assumed in positioning the isochrones. Median photometric errors at the five indicated magnitudes are shown in the middle panel, but refer to all three panels. From these diagrams, we have derived an age of 0.35 Gyr (log age=8.55) for B049-G112, and 0.25 Gyr (8.4) for B458-D049.

band. Targets from our entire catalog were located on the images, and photometry for 12 separate apertures ranging from 0.7 to 16″ (spaced logarithmically) was collected using DAOPHOT. Growth curves from these apertures were constructed, and used in an automatic fashion to estimate the aperture which enclosed the total light of the cluster. These apertures were then inspected on the images and increased, if the clusters were in fact larger, or decreased for cases where the apertures included substantial light from objects clearly not part of the clusters. The local background was measured in annuli with inner radii 1 pixel larger than the outer radius of the aperture for the object. The apertures used are listed in Table 1. Extraneous stars remaining in the apertures were accounted for by measuring their magnitudes separately, and subtracting their contribution to the cluster aperture magnitudes. The resultant instrumental magnitudes were then placed on the standard V system using stars from the Massey et al. (2006) tables which we were measured in the same way as the clusters. The color term in the V mag transformation (described in Massey et al. 2006) was ignored, as it was smaller than the errors we report. Tables 1, 3, and 4 list the results from this work. The formal errors in the standardized photometry were less than 0.03 mag, set by the uncertainties in the transformations. However, since our goal was actually cluster total magnitudes, our calculated uncertainties refer to the uncertainty in setting the proper apertures and correcting for extraneous objects within those apertures.

Specifically, the uncertainties were set to be equal to the difference in the magnitude of the aperture chosen as best representing the limiting radius of the cluster, and that of the next larger aperture in our logarithmic spacing of aperture sizes. In practice this means that clusters in crowded fields have larger uncertainties than those in less dense areas. The tables also list photometry from other sources for the objects that are outside of the LGS images; we do not list the errors in such cases.

Comparing our aperture magnitudes with those collected from various sources and listed in the RBC, we find excellent agreement over the magnitude range of 14 to 18, with an rms in the differences of 0.18 mag in the set of 200 objects in common; this in spite of the fact that no effort was made to insure that the apertures used in the two data sets were the same. Between V=18 and 20, our photometry tended to be fainter by 0.2 mag and the scatter increased to 0.5 mag, some of which was likely due to differences in object identification. A further comparison was made with the 58 V magnitudes measured for M31 clusters from archival HST images in Barmby et al. (2007). Aside of one cluster whose V magnitude appears to be a typo (B151-G205), the rms of the differences of that set with the magnitudes presented here is 0.28, with no apparent systematics.

6. THE NATURE OF THE YOUNG CLUSTERS

6.1. Misclassified globular clusters

Morrison et al. (2004) misclassified 15 of the young

clusters as old disk globular clusters (17% of their disk globulars). This was pointed out by Beasley et al. (2004). In some cases this was due to the low S/N of the WYF-FOS spectrum, in others the problem was misinterpretation of the spectra. Our new study of the clusters has resolved most of this confusion and changed the classification of a number of clusters from old and massive to younger, not very massive. However, we still find clusters with significant masses, above $10^4 M_\odot$, and with ages less than 150 Myr (see Table 2). Of the 10 clusters with those physical characteristics, the HST or LGS images of three confirm them as clusters similar in appearance to the populous clusters of the LMC (these are B315-G038, B318-G042, and VDB0, the latter still the most massive, young cluster known in M31, van den Bergh (1969)). Five appear more like OB associations, and thus may not survive as bound clusters (B319-G044, B327-G053, B442-D033, B106D and BH05). The case for the other two (B040-G102, B043-G106) is not as clear, but their LGS images are more similar to the cases like B315-G038 than to the OB associations.

6.2. *Position*

Figure 10 shows a Spitzer/MIPS 24μ mosaic of M31 (Gordon et al. 2005) with the positions of the young clusters overlaid. Clusters younger than 0.1 Gyr, between 0.1 and 0.32 Gyr, and 0.32 and 2 Gyr are shown in different colors. The latter two groupings divide the clusters older than 0.1 Gyr into two equal parts. It can be seen that the spatial distribution of the young clusters is well correlated with the star-forming regions in M31, with the majority associated with the 10 kpc "ring of fire". The comparison of these young clusters and the warm dust emission is distinct from the comparison of the latter with the location of HII regions, as we have excluded the clusters embedded in HII regions from our sample.

Gordon et al. (2005) and Block et al. (2006) use the curious appearance of the mid-IR ring - the split near the location of M32, creating the appearance of a "hole" in between, and the possible offset of the ring from the nucleus - to suggest a recent encounter of M32 and M31. Both groups suggest that the split is caused by M32's passage through the disk, and their models also produce rings offset from M31's center, albeit not as extreme as is observed (Gordon et al. 2005, produce an offset of $1'$, not $6'$). An examination of our Figure 10 shows that the cluster distribution favors the outer parts of the hole, and is generally quite symmetric about M31's nucleus. Most models of an offset ring assume that the inner part of the split in the observed ring is the one which should be traced by star formation. However, this is not where most of the clusters are found.

Gordon et al. (2005) need a very recent interaction between M32 and the disk (their model has the disk passage occurring 2×10^7 years ago) because the passage of M32 through the disk in their model results in a burst of star formation that propagates outward through the disk. However, we do not see any radial trends with cluster age, which might be expected with a propagating ring of star formation (Figure 11).

Block et al. (2006) prefer a collision about 2×10^8 years ago, which triggers expanding density waves. Our young cluster ages range from 0.04 Gyr to 1 Gyr, but most are between 10^8 and 10^9 years. If the "ring of fire" was pro-

duced by a single event, as modeled by the above authors, we might expect the age distribution of clusters associated with it to be more peaked. The ages of the younger clusters presented in Williams & Hodge (2001a) range from around 2×10^7 to 2×10^8 years, and there is little evidence of a peak in star formation in this age range either. These results seem to suggest that star formation has been fairly high in this region of M31 for 1 Gyr or more. In summary, we see no evidence of enhancement in star formation rate or any spatial age separation, as we might expect from the M32 disk passage.

6.3. *Kinematics*

Do the kinematics of the young clusters bear out the disk origin suggested by their close association (in projection) with star forming regions in M31's disk? M31's inner disk kinematics are more complex than originally supposed, due to M31's bar (Beaton et al. 2007; Athanassoula & Beaton 2006). The velocities from our many sky fibers, taken both as a part of regular observing and also from entire exposures devoted to offset sky in the crowded inner regions, give us a new way of quantifying disk rotation throughout the inner regions where the young clusters are found. (We plan to use these data in a study of bar kinematics, Athanassoula et al. in preparation). Figure 12 shows the disk mean velocity field.

We also use kinematics of HII regions that we observed as fillers in the Hectospec fields to give us an indication of the kinematics of young disk objects. These data will be published in Athanassoula et al. (in preparation).

Figure 13 shows the kinematics of the mean disk light, the young clusters, and HII regions, versus major axis distance X, in kpc. We have split the sample into objects which are close to the major axis (< 1 kpc) and those projected from $1 - 2$ kpc from the major axis, because the projection of a circular orbit looks different in these two cases. Objects on the major axis in circular orbits have all of their velocity projected on the line of sight; as we move further away from the major axis, less of the circular velocity is projected on the line of sight and so the tilt of the distance-velocity line becomes smaller. This can be seen clearly in Figure 13 for all types of objects.

The curious flattening of the mean velocities from absorption line spectra for major axis distances between 3 and 10 kpc is likely to be caused by the bar. It can be seen that the young clusters follow the disk mean velocity curve from absorption spectra quite well, and show an even better correlation with the kinematics of the youngest objects: HII regions and sky fibers showing emission spectra.

This kinematic analysis confirms our spatial association of the young clusters with the star forming young disk in M31.

6.4. *Masses of the clusters*

The M/L values obtained from the spectroscopic age estimates can be combined with the V band photometry to derive masses of all the observed M31 clusters, young and old. Reddening values are of course also needed, and a large number of E(B–V) values were derived from photometry in Barmby et al. (2000). They and we consider only the total reddenings, foreground and internal to M31. The methodology used in Barmby et al. (2000)
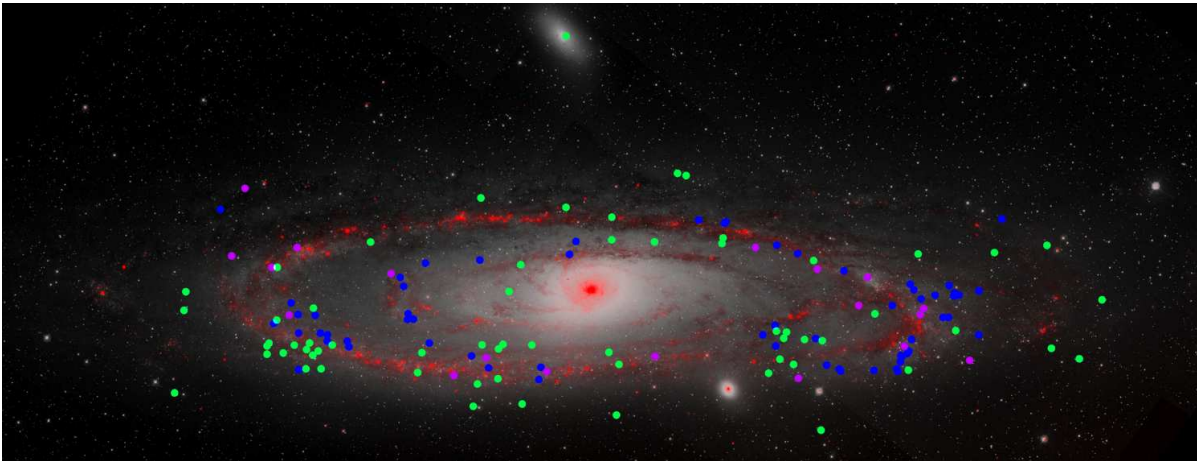
FIG. 10.— Spitzer/MIPS 24 micron imaging (in red on top of the optical DSS image), showing the location of clusters with ages less than 0.1 Gyr as violet, between 0.1 and 0.32 Gyr as blue, and between 0.32 and 2 Gyr as green.
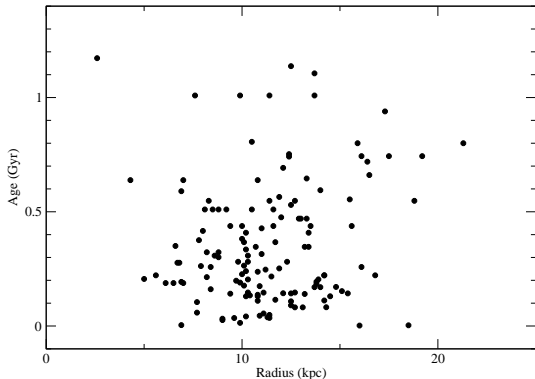
FIG. 11.— Ages of young clusters as a function of distance from the center of M31, in the plane of its disk.

meant that the reddenings would only be valid for old clusters, and indeed few of the clusters we have identified here as young were included in their study, thus reddenings for those objects are needed. Therefore, we elected to rederive the reddenings for all of the clusters in our study, young and old.

In the case of the young clusters we compared the fluxed spectra with the SB99 model spectra of the appropriate age. As described above, the ages were obtained by matching spectral line features in the observed and model spectra, not by comparing the continua shapes. Once the ages have been found in this way, differences in the continua shapes may be assumed to be due to reddening, except for a few cases where a late-type star, whether member or not, clearly dominates the redder wavelengths as evidenced by the presence of TiO bands. For those cases, we use the mean reddening for the young clusters of 0.28.

For the old clusters we did not use models, but rather the sample of spectra themselves. Initial values of reddenings were obtained from Barmby et al. (2000), and were used to deredden the spectra of those clusters with E(B−V)< 0.4, about 190 in number (there are about 350 old clusters in our spectroscopic sample). These spectra were ordered in metallicity, which was estimated from the spectral line indices as mentioned above, rebinned to a coarse grid in wavelength, and normalized to have the same intensity at the arbitrary wavelength of 5000Å. Interpolation formulae were developed from these spectra,

via a least squares method to avoid bad spectra, for intensity as a function of both wavelength and metallicity. As a result, a cluster spectrum of arbitrary metallicity could be created, dereddened to the accuracy of the Barmby et al. (2000) reddenings. The individual spectra in this low reddening sample were then compared with the appropriate interpolated spectra, and reddenings were adjusted as needed to bring their continua shapes closer to that of the expected template shape. The method is thus similar to methods that use the metal abundance to predict the intrinsic broad band colors, and then require the derived reddening to reproduce the observed colors.

The overall goal in working with the low reddening sample was to retain the mean value of the reddenings found in Barmby et al. (2000), but to correct those that varied significantly. After cleaning up those reddenings, the interpolation formulae were then used to derive reddenings for the 150 clusters for which we have spectra and whose reddenings were not measured in Barmby et al. (2000). Thus while we have not improved upon the absolute levels of the M31 old cluster reddenings, we believe we have improved the precision of the values in a relative sense, and as well have nearly doubled the number of reddenings available. About 10% of the spectra were taken during nights when the ADC was not operating properly, thus we can't use the continuum shape to estimate reddenings. For objects whose only spectra were taken on those nights, we assume the average reddening of 0.28.

A comparison of our derived E(B−V) values (which range up to 1.4 mag) and those in Barmby et al. (2000) results in a scatter of 0.17 mag rms, which is good enough for our overall goal of comparing the M31 cluster system in bulk with that of other galaxies. Interestingly, both the young cluster and old cluster groups have clusters with E(B−V)> 0.5, though the highest measured value (E(B−V)=1.4) is still found in the old cluster B037-V327, probably a selection effect since that cluster also has the highest luminosity in all of M31. The young cluster reddenings are listed in Table 2; those of the old clusters will be presented in a subsequent paper. By using the position of blue-plume stars in the color-magnitude diagram, Massey et al. (2007) estimated the average reddening for young stars in M31 to be 0.13 mag, significantly lower than the mean of the clusters younger than 100
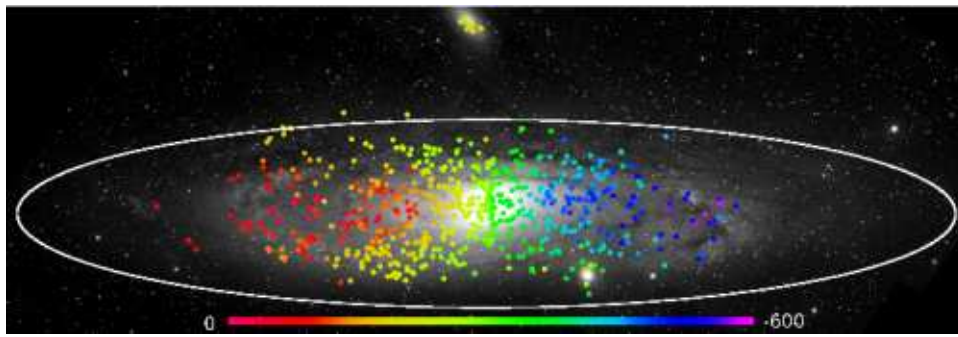
FIG. 12.— Disk mean velocity field, obtained from sky fibers. The color bar at bottom shows the velocity scale in km/s.
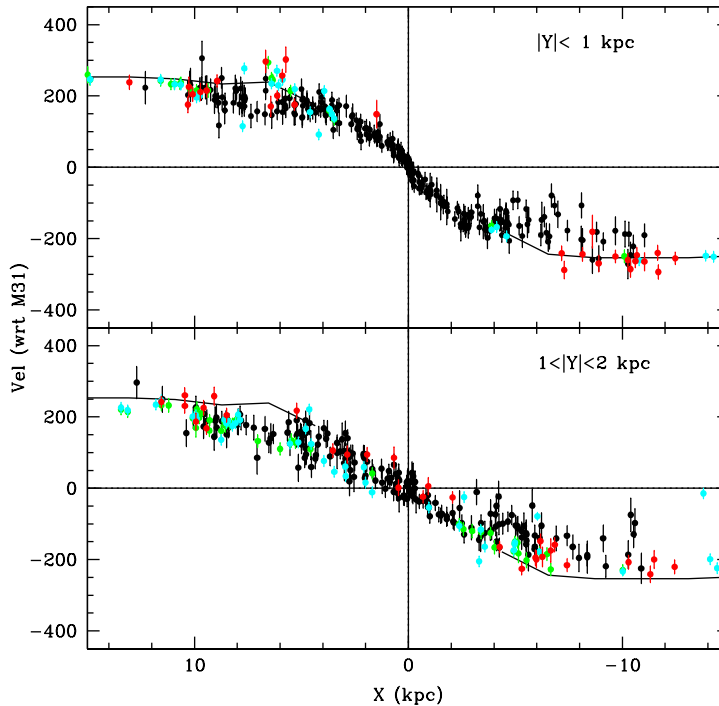
FIG. 13.— Plot of major axis distance X vs velocity with respect to M31, for objects within 1 kpc of the major axis (upper panel) and for objects between 1 and 2 kpc from the major axis (lower panel). Mean disk velocities obtained from sky fibers which show absorption spectra are shown in black, from sky fibers which show emission in green. HII region velocities are shown in cyan and young cluster velocities (from Table 2) in red. The rotation curve from Kent (1989) is shown as a solid line.

Myr presented here, which may place a constraint on the accuracy of the values presented here.

The mass histogram for the all of the young clusters is shown in Figure 14. We have also shown the mass distribution of Milky Way open clusters within 600 pc of the Sun. This is based on the sample of Kharchenko et al. (2005), with mass calculations by Lamers et al. (2005). The Kharchenko catalog is the most homogeneous and complete catalog of open clusters in the solar neighborhood currently available, and is based on a stellar catalog complete to V=11.5. The cluster masses were estimated by counting the number of cluster members brighter than the limiting magnitude, then correcting for the stars fainter than this using a Salpeter mass function and a lower mass limit of 0.15 $M_\odot$. This catalog does not include the most massive clusters in the Galaxy because of its relatively small sample size; for example, there have been recent discoveries of more distant young

clusters which may have masses as high as $10^5 M_\odot$ (e.g. Clark et al. (2005)), and we add Westerlund 1 to the histogram as an example. The Milky Way globular and LMC young massive cluster histograms are shown in the bottom two panels (from McLaughlin & van der Marel 2005). These mass estimates are based on King model fits.

Obviously, M31 clusters with masses less than $\approx$ $10^3 M_\odot$ and ages greater than a few $\times 10^7$ years are too faint to be part of this study, and await a future study. Krienke & Hodge (2007) estimate over 10000 such clusters in the disk of M31; these would form the low mass tail in the mass distribution of Figure 14.

Nonetheless, there is a trend in cluster mass, with the Milky Way open clusters having the lowest median mass, the Milky Way and M31 globulars the highest, and the LMC young massive clusters and the M31 young clusters in between. This trend is consistent with a single cluster
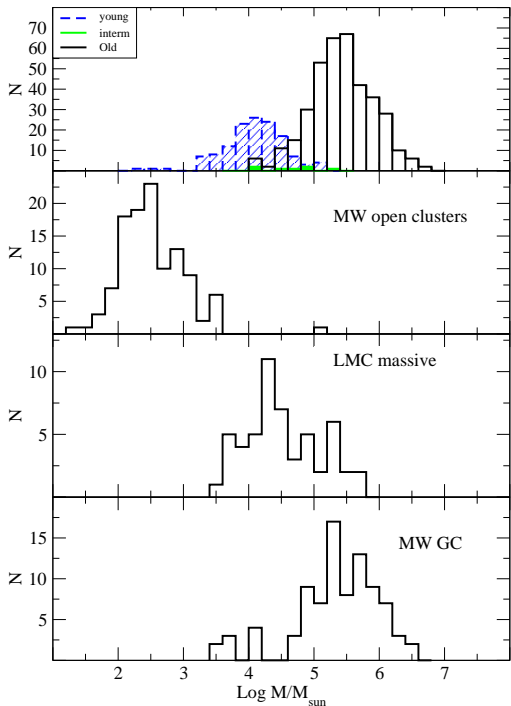
Fig. 14.— Mass histograms, from top to bottom, M31 clusters (young, intermediate and old), Milky Way open clusters, LMC massive clusters and Milky Way globular clusters. The young M31clusters are shown in a hatched histogram, the intermediate as solid, and the old as open.

IMF plus disruption, taking into account the small size of the volume searched for clusters in the Milky Way.

6.5. Cluster survival

Would we expect these young M31 clusters to survive as they age, or to disrupt? One of the main processes that leads to cluster disruption is 2-body relaxation enhanced by an external tidal field (Spitzer & Harm 1958). The lower-mass clusters suffer more strongly from relaxation effects. Another property of the cluster itself which will affect its survival is its density — lower-density clusters will disrupt more quickly (Spitzer 1958). Thus we would expect that massive, concentrated clusters such as B018 and BH05 would be more likely to survive.

Boutloukos & Lamers (2003) derive an empirical expression for the disruption of clusters as a function of their mass, studying cluster populations in the solar neighborhood, the SMC, M33 and M51. Whitmore et al. (2007) point out that observational selection effects could mimic the decrease in the number of clusters with age which Boutloukos et al. ascribe to cluster disruption. However, this is almost certainly not true of the solar neighborhood open clusters studied by Lamers et al. (2005) using a similar analysis. We show the age-mass diagram for the young M31 clusters in Figure 15. While our sample is clearly very incomplete below 10^8 years, the diagram shows some similarity to the LMC cluster age-mass diagram of de Grijs & Anders (2006) in the age range we cover. Unfortunately, we do not expect our catalog to be complete enough to permit an analysis using the techniques of Boutloukos et al.

Environmental effects also control the tidal stripping of the cluster. For stars whose orbits are mostly confined to the disk, encounters with giant molecular clouds
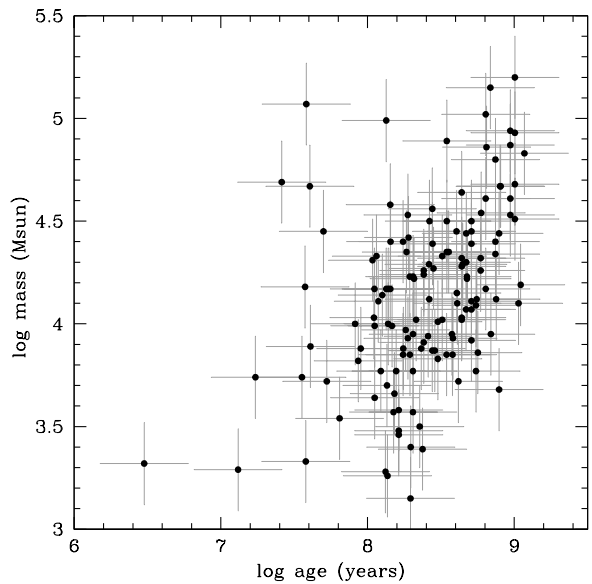
Fig. 15.— Age-mass diagram for our young and intermediate-age clusters.

and spiral arms contribute to their disruption (Spitzer 1958; Gieles et al. 2007). For clusters whose orbits are not confined to the disk, bulge and disk shocking are more important (Ostriker et al. 1972; Aguilar et al. 1988). The similarity of the M31 young cluster kinematics to that of other young disk objects suggests strongly that these clusters are confined to M31's disk plane, so giant molecular clouds should be the relevant external disruptor. Gieles et al. (2008) show that disruption times for clusters in galaxies ranging in size from M51 to the SMC, scale with molecular gas density in the expected way. M31's molecular gas density is highest near the "ring of fire" where many of our clusters are found (Loinard et al. 1999). This density is similar to the molecular gas density in the solar neighborhood (Dame 1993). Thus we would expect the survival due to giant molecular cloud interactions of the M31 young clusters to be similar to that of the solar neighborhood open clusters.

We expect that most of these young clusters will be disrupted in the next Gyr or so (Lamers et al. 2005, derive a disruption time of 1.3 Gyr for a cluster of mass $10^4 M_\odot$ in the solar neighborhood). However, some of the more massive and concentrated of the young clusters will likely survive for longer.

7. SUMMARY

We present a new catalog of 670 M31 clusters, with accurate coordinates. In this paper we focus on the 140 clusters (many originally classified in the literature as globular clusters) which have ages less than 2 Gyr: most have ages between 10^8 and 10^9 years. Using high-quality MMT/Hectospec spectra, excellent ground based images, and in some cases, HST images, we explore the nature of these clusters. With the exception of NGC 205's young cluster, they have spatial and kinematical properties consistent with formation in the star-forming disk of M31. Many are located close to the 10 kpc "ring of fire" which shows active star formation. The age distribution of our clusters, plus that of the younger clusters of Williams & Hodge (2001a), shows no evidence for a peak in star for-

mation there between 2×10^7 and 10^9 years ago, which we might expect if the ring was created by a recent passage of M32 through the disk, as suggested by Gordon et al. (2005) and Block et al. (2006).

We have estimated their masses using spectroscopic ages and M/L ratios, (in some cases) ACS color-magnitude diagrams, and new photometry from the Local Group Survey. The clusters have masses ranging from 250 to 150,000 $M_\odot$. These reach to higher values than the known Milky Way open clusters, but it must be remembered that our sample of open clusters in the Milky Way is far from complete. The most massive of our young clusters overlap the mass distributions of M31's old clusters and the Milky Way globulars.

Interestingly, although most of the young clusters show the low-concentration structure typical of the Milky Way open clusters, a few have the high concentrations typical of the Milky Way globulars and the old M31 clusters. We estimate that most of these young clusters will disrupt in $1 - 2$ Gyr, but the massive, concentrated clusters may well survive longer.

REFERENCES

Athanassoula, E., & Beaton, R. L. 2006, MNRAS, 370, 1499

Auriere, M., Coupinot, G., & Hecquet, J. 1992, A&A, 256, 95

Aguilar, L., Hut, P., & Ostriker, J. P. 1988, ApJ, 335, 720

Baade, W., & Arp, H. 1964, ApJ, 139, 1027

Barmby, P. et al. 2000, AJ, 119, 727

Barmby, P., & Huchra, J. P. 2001, AJ, 122, 2458

Barmby, P., McLaughlin, D. E., Harris, W. E., Harris, G. L. H., & Forbes, D. A. 2007, AJ, 133, 2764

Battistini, P., Bonoli, F., Braccesi, A., Fusi-Pecci, F., Malagnini, M. L., & Marano, B. 1980, A&AS, 42, 357

Battistini, P., Bonoli, F., Braccesi, A., Federici, L., Fusi Pecci, F., Marano, B., & Borngen, F. 1987, A&AS, 67, 447

Battistini, P. L., Bonoli, F., Casavecchia, M., Ciotti, L., Federici, L., & Fusi-Pecci, F. 1993, A&A, 272, 77

Beasley, M. A. et al. 2004, AJ, 128, 1623

Beaton, R. L., et al. 2007, ApJ, 658, L91

Beichman, C. A., Chester, T. J., Skrutskie, M., Low, F. J., & Gillett, F. 1998, PASP, 110, 480

Bertin, E., & Arnouts, S. 1996, A&AS, 117, 393

Bica, E., Bonatto, C., & Blumbeqrg, R. 2006, A&A, 460, 83

Bica, E., & Bonatto, C. 2008, MNRAS, 384, 1733

Binney, J. and Tremaine, S., 'Galactic Dynamics', second edition, Princeton University Press, Princeton NJ

Block, D. L., et al. 2006, Nature, 443, 832

Bonatto, C., & Bica, E. 2005, A&A, 437, 483

Bonatto, C., & Bica, E. 2007, A&A, 473, 445

Boutloukos, S. G., & Lamers, H. J. G. L. M. 2003, MNRAS, 338, 717

Burstein, D., et al. 2004, ApJ, 614, 158

Chandar, R., Bianchi, L., & Ford, H. C. 1999, ApJ, 517, 668

Cioni, M.-R. L., Girardi, L., Marigo, P., & Habing, H. J. 2006, A&A, 448, 77

Cioni, M.-R. L., Girardi, L., Marigo, P., & Habing, H. J. 2006, A&A, 452, 195

Clark, J. S., Negueruela, I., Crowther, P. A., & Goodwin, S. P. 2005, A&A, 434, 949 K., & Cameron, P. B. 2005, ApJ, 634, L45

Cohen, J. G., Matthews, K., & Cameron, P. B. 2005, ApJl, 634, L45

Crampton, D., Cowley, A. P., Schade, D., & Chayer, P. 1985, ApJ, 288, 494

Dame, T. M. 1993, Back to the Galaxy, 278, 267

Dubath, P., & Grillmair, C. J. 1997, A&A, 321, 379

Eigenbrod, A., Mermilliod, J.-C., Clariá, J. J., Andersen, J., & Mayor, M. 2004, A&A, 423, 189

Elson, R. A., & Walterbos, R. A. M. 1988, ApJ, 333, 594

Fall, S. M., & Rees, M. J. 1985, ApJ, 298, 18

Freeman, K.C. 1980, in Star Clusters, IAU Symposium 85, edited by J. Hesser (Reidel, Dordrecht), p317

Friel, E. D. 1995, ARA&A, 33, 381

Fusi Pecci, F. et al. 2005, AJ, 130, 554

Galleti, S., Federici, L., Bellazzini, M., Fusi Pecci, F., & Macrina, S. 2004, A&A, 416, 917

Galleti, S., Bellazzini, M., Federici, L., Buzzoni, A., & Fusi Pecci, F. 2007, A&A, 471, 127

Gieles, M., Athanassoula, E., & Portegies Zwart, S. F. 2007, MNRAS, 376, 809

Gieles, M., Lamers, H. J. G. L. M., & Baumgardt, H. 2008, IAU Symposium, 246, 171

Gordon, K. D., et al. 2006, ApJL, 638, L87

de Grijs, R., & Anders, P. 2006, MNRAS, 366, 295

Jarrett, T. H., Chester, T., Cutri, R., Schneider, S., Skrutskie, M., & Huchra, J. P. 2000, AJ, 119, 2498

Hodge, P.W. 1981, in Astrophysical Parameters for Globular Clusters, IAU Colloquium 68, edited by A.G.D. Phillip and D.S. Hayes (Schenectady, Davis)

Hodge, P. W. 1979, AJ, 84, 744

Hodge, P. W., Mateo, M., Lee, M. G., & Geisler, D. 1987, PASP, 99, 173

Hubble, E. 1932, ApJ, 76, 44

Huxor, A. P., Tanvir, N. R., Irwin, M. J., Ibata, R., Collett, J. L., Ferguson, A. M. N., Bridges, T., & Lewis, G. F. 2005, MNRAS, 360, 1007

Kharchenko, N. et al. 2005, A&A, 438, 1163

Kennicutt, R. C., Jr., & Chu, Y.-H. 1988, AJ, 95, 720

Kent, S. M. 1989, AJ, 97, 1614.

Kinman, T. D. 1963, ApJ, 137, 213

Kim, S. C., et al. 2007, AJ, 134, 706

Koekemoer, A. M., Fruchter, A. S., Hook, R. N., & Hack, W. 2002, The 2002 HST Calibration Workshop : Hubble after the Installation of the ACS and the NICMOS Cooling System, Proceedings of a Workshop held at the Space Telescope Science Institute, Baltimore, Maryland, October 17 and 18, 2002. Edited by Santiago Arribas, Anton Koekemoer, and Brad Whitmore. Baltimore, MD: Space Telescope Science Institute, 2002., p.337, 337

Krienke, O. K., & Hodge, P. W. 2007, PASP, 119, 7

Krienke, O. K., & Hodge, P. W. 2008, PASP, 120, 1

Lamers, H. J. G. L. M. et al. 2005, A&A, 441, 117

Larsen, S. S. 2002, Extragalactic Star Clusters, IAUS 207, 421

Larsen, S. S. 2004, The Formation and Evolution of Massive Young Star Clusters, 322, 19

Lee, M. G., Hwang, H. S., Kim, S. C., Park, H. S., Geisler, D., Sarajedini, A., & Harris, W. E. 2008, ApJ, 674, 886

Leonardi, A. J., & Rose, J. A. 2003, AJ, 126, 1811

Leitherer, C., et al. 1999, ApJS, 123, 3

Loinard, L., Dame, T. M., Heyer, M. H., Lequeux, J., & Thaddeus, P. 1999, A&A, 351, 1087

McLaughlin, D. E., & van der Marel, R. P. 2005, ApJS, 161, 304

Mateo, M. 1993, The Globular Cluster-Galaxy Connection, 48, 387

Massey, P. et al. 2006, AJ, 131, 2478

Massey, P., Olsen, K. A. G., Hodge, P. W., Jacoby, G. H., McNeill, R. T., Smith, R. C., & Strong, S. B. 2007, AJ, 133, 2393

Mochejska, B. J., Kaluzny, J., Krockenberger, M., Sasselov, D. D., & Stanek, K. Z. 1998, Acta Astronomica, 48, 455

Morrison, H. L., Harding, P., Perrett, K., & Hurley-Keller, D. 2004, ApJ, 603, 87

Ostriker, J. P., Spitzer, L. J., & Chevalier, R. A. 1972, ApJ, 176, L51

Peebles, P. J. E., & Dicke, R. H. 1968, ApJ, 154, 891

Perrett, K. M., Bridges, T. J., Hanes, D. A., Irwin, M. J., Brodie, J. P., Carter, D., Huchra, J. P., & Watson, F. G. 2002, AJ, 123, 2490

Puzia, T. H., Perrett, K. M., & Bridges, T. J. 2005, A&A, 434, 909

Racine, R. 1991, AJ, 101, 865

Racine, R., & Harris, W. E. 1992, AJ, 104, 1068

Santos, J. F. C., Jr., Bonatto, C., & Bica, E. 2005, A&A, 442, 201

Sargent, W. L. W., Kowal, C. T., Hartwick, F. D. A., & van den Bergh, S. 1977, AJ, 82, 947

Schiavon, R. P., Rose, J. A., Courteau, S., & MacArthur, L. A. 2005, ApJS, 160, 163

Sirianni, M., et al. 2005, PASP, 117, 1049

Spitzer, L. J., & Harm, R. 1958, ApJ, 127, 544

Spitzer, L. J. 1958, ApJ, 127, 17

Spitzer, L. J., & Shapiro, S. L. 1972, ApJ, 173, 529

Stetson, P. B. 1987, PASP, 99, 191

van den Bergh, S. 1969, ApJS, 19, 145

Vázquez, G. A., & Leitherer, C. 2005, ApJ, 621, 695

Vetešnik, M. 1962, Bulletin of the Astronomical Institutes of Czechoslovakia, 13, 180

Whitmore, B. C., Chandar, R., & Fall, M. 2007, AJ, 133, 1067

Williams, B. F., & Hodge, P. W. 2001, ApJ, 559, 851

Williams, B. F., & Hodge, P. W. 2001, ApJ, 548, 190

Worthey, G. 1994, ApJS, 95, 107

Worthey, G., & Ottaviani, D. L. 1997, ApJS, 111, 377

TABLE 1
CLEANED CLUSTER CATALOG

Object	RA	Dec	V	type	S[a]	Ap ″	P[b]	C[c]
		2000						
SH01	0:32:41.44	40:01:41.4	15.82				G	
G001-MII	0:32:46.53	39:34:40.6	13.75	old	B		B	H
G002-MIII	0:33:33.77	39:31:18.9	15.81	old	B		B	
B290	0:34:20.94	41:28:18.1	17.14	old	P		B	
BA21	0:34:53.83	39:49:40.5	16.64				G	
B412	0:34:55.28	41:32:26.4	17.36				G	
B413	0:35:13.00	41:29:07.8	18.12				G	
BA22	0:35:13.60	39:45:37.1						
B134D	0:35:30.29	40:44:24.8	18.19				G	
B291-G009	0:36:04.97	42:02:09.3	16.59	old	HS		B	S
B292-G010	0:36:16.66	40:58:26.5	17.00	old	B		B	
B293-G011	0:36:20.86	40:53:37.2	16.30	old	B		B	
B138D	0:36:21.66	41:28:33.1	16.87				G	
B139D	0:36:24.67	39:45:07.4	18.59				G	
B140D	0:36:30.78	41:21:52.8	17.67				G	
B141D	0:36:30.99	41:28:38.5	17.43				G	
B142D	0:36:33.83	41:09:07.9	18.63				G	
B144D	0:36:36.64	41:37:03.6	17.72				G	
B147D	0:36:44.40	41:08:27.0	17.96				G	
B295-G014	0:36:46.73	40:19:42.1	16.72	old	HS		B	S
B148D-SH3	0:36:50.17	41:07:10.7	16.31				G	
B150D	0:36:59.91	41:25:30.1	17.67				B	
B156D	0:37:26.32	41:19:02.2	18.16				G	
B420	0:37:28.43	41:35:44.2	17.85				G	
B157D	0:37:35.27	40:57:52.3	17.83				G	
B422	0:37:38.45	41:59:59.2	18.11	old	HS		B	S
B423	0:37:56.66	40:57:35.9	17.87				B	
B298-G021	0:38:00.22	40:43:55.8	16.59	old	B		B	H
B165D	0:38:04.41	40:55:32.1	17.62				G	
B426-D018	0:38:19.80	41:14:30.7	16.35				G	
B301-G022	0:38:21.59	40:03:37.0	16.93±0.26	old	HS	3.8	L	SL
B167D	0:38:22.48	41:54:35.0	17.95	old	HS		B	S
B302-G023	0:38:33.5	41:20:52.2	16.68	old	HS		B	S
GC7	0:38:49.4	42:22:48.0	17.99±0.1	old	HS		H	SH
B303-G026	0:38:50.55	40:27:31.1	18.00±0.15	young	HS	7.7	L	SL
B176D	0:38:53.15	41:29:03.0	17.96				G	
DAO23	0:38:54.19	40:26:33.9	19.42±0.19			3.8	L	L
B431-G027	0:38:54.76	40:34:56.4	18.00±0.20	young	HS	7.7	L	SL
B304-G028	0:38:56.94	41:10:28.4	16.83	old	HS		B	S
B305-D024	0:38:58.85	40:16:32.1	17.49±0.16	old	HS	11.6	L	SL
B306-G029	0:39:08.70	40:34:21.2	16.46±0.15	old	HS	7.7	L	SL
DAO27	0:39:16.48	40:41:05.4	18.60±0.18	HII	HS	11.6	L	SL
B307-G030	0:39:18.46	40:32:58.2	17.74±0.29	interm	HS	7.7	L	SL
B309-G031	0:39:24.62	40:14:29.1	17.41±0.24	old	HS	7.7	L	SL
B310-G032	0:39:25.75	41:23:33.1	17.04	old	HS		B	S
B436	0:39:30.67	40:18:20.6	18.20±0.20	old	HS	5.1	L	SL
B181D	0:39:30.85	41:28:26.4	17.72	old	HS		G	S
B311-G033	0:39:33.72	40:31:14.7	15.50±0.10	old	HS	11.6	L	SLH
SH07	0:39:37.36	42:09:57.1						
B312-G035	0:39:40.17	40:57:02.4	15.58	old	HS		B	S
B314-G037	0:39:44.59	40:14:08.1	17.52±0.27	young	HS	7.7	L	SL
B313-G036	0:39:44.60	40:52:55.2	16.45±0.18	old	HS	11.6	L	SL
B315-G038	0:39:48.52	40:31:30.6	16.24±0.03	young	HS	15.4	L	SLH
DAO30	0:39:50.78	40:18:14.9	17.81±0.04	young	HS	11.6	L	SL
B001-G039	0:39:51.02	40:58:10.6	16.92±0.03	old	HS	15.4	L	SL
B316-G040	0:39:53.58	40:41:39.2	16.90±0.03	interm	HS	15.4	L	SL
B317-G041	0:39:55.29	41:47:45.9	16.55	old	HS		B	SH
KHM31-22	0:39:58.71	40:35:23.6	20.10±0.09	young	HS	3.8	L	SLH
WH2	0:39:59.99	40:33:27.0	20.65±0.54	young	HS	1.8	L	SLH
B318-G042	0:40:00.85	40:34:08.1	17.13±0.17	young	HS	5.1	L	SLH
B186D	0:40:02.25	39:23:12.1	17.84				G	
B002-G043	0:40:02.57	41:11:53.5	17.54	old	HS		B	S
B319-G044	0:40:03.07	40:33:58.6	17.59±0.12	young	HS	7.7	L	SLH
B003-G045	0:40:09.40	41:11:05.6	17.57	old	HS		B	S
BH02	0:40:10.29	40:36:26.2	19.39±0.14			5.1	L	L
KHM31-37	0:40:10.99	40:36:11.6	18.09±0.10	young	HS	5.1	L	SLH
B188D	0:40:14.03	39:41:30.8	17.92				G	
B321-G046	0:40:15.37	40:27:46.2	18.00±0.17	young	HS	5.1	L	SL
B189D-G047	0:40:15.49	40:39:59.5	18.47±0.08	young	HS	5.1	L	SL
B322-G049	0:40:17.27	40:39:04.7	18.10±0.23	young	HS	3.8	L	SL
B004-G050	0:40:17.92	41:22:40.2	16.95	old	HS		B	S
B323	0:40:18.28	40:32:44.6	18.11±0.26	young	HS	7.7	L	SL
B442-D033	0:40:19.40	40:37:28.9	18.17±0.14	young	HS	7.7	L	SL
B005-G052	0:40:20.33	40:43:58.3	15.66±0.08	old	HS	5.1	L	SL

TABLE 1 — *Continued*

Object	RA	Dec 2000	V	type	S^a	Ap ″	P^b	C^c
B324-G051	0:40:20.47	41:40:49.3	16.91	young	HS		B	SH
B443-D034	0:40:20.79	40:33:22.0	19.01±0.35	young	HS	2.5	L	SL
BH03	0:40:22.63	41:40:44.4	18.28	na			G	H
B325	0:40:23.09	40:30:47.4	17.47±0.44	young	HS	11.6	L	SL
B327-G053	0:40:24.10	40:36:22.4	16.64±0.10	young	HS	7.7	L	SL
B328-G054	0:40:24.52	41:40:23.1	17.57	old	HS		B	SH
B003D	0:40:25.02	41:12:23.5	18.50				G	
B330-G056	0:40:25.58	41:42:53.6	17.69	old	HS		B	SH
B331-G057	0:40:26.10	41:42:03.9	18.20	old	HS		B	SH
B006-G058	0:40:26.48	41:27:26.7	15.52	old	HS		B	SH
B244	0:40:26.49	41:18:35.5	18.26	old	HS		B	S
BH04	0:40:27.2	41:42:23.9	19.69	old	HS		G	SLH
VDB0-B195D	0:40:29.43	40:36:14.8	15.19±0.30	young	HS	11.6	L	SL
B333	0:40:29.58	41:40:26.7	19.13	old	HS		B	SH
B008-G060	0:40:30.28	41:16:08.7	16.52	old	HS		B	SH
BH05	0:40:30.51	40:45:29.3	16.03±0.19	young	HS	3.8	L	SLH
BH06	0:40:30.62	40:44:53.9	18.14±0.40	na		1.8	L	LH
B009-G061	0:40:30.70	41:36:55.6	16.91	old	HS		B	SH
B010-G062	0:40:31.56	41:14:22.5	16.66	old	HS		B	SH
B011-G063	0:40:31.87	41:39:16.9	16.79	old	HS		B	SH
B012-G064	0:40:32.46	41:21:44.2	15.12	old	HS		B	SH
B196D	0:40:34.79	40:26:38.0	19.18±0.15	young	HS	5.1	L	SL
B448-D035	0:40:36.52	40:40:15.1	18.52±0.28	young	HS	7.7	L	SL
BH09	0:40:37.15	40:33:21.9	19.83±0.07	old	HS	3.8	L	SLH
B006D-D036	0:40:37.37	40:48:45.5	18.69±0.21	young	HS	5.1	L	SL
B007D	0:40:37.57	40:48:11.6	18.37±0.09			5.1	L	L
B013-G065	0:40:38.43	41:25:23.7	17.18	old	HS		B	SH
B335-V013	0:40:41.67	40:38:27.9	17.88±0.24	old	HS	11.6	L	SL
B449-V11	0:40:42.3	40:36:04.9	18.64±0.31	old	HS	5.1	L	SL
BH10	0:40:44.86	40:53:07.9	19.61±0.10	young	HS	3.8	L	SL
B008D	0:40:45.01	40:58:55.2	19.51±0.17			3.8	L	L
B015-V204	0:40:45.02	40:59:56.3	17.87±0.12	old	HS	11.6	L	SL
B016-G066	0:40:45.16	41:22:09.9	17.58	old	HS		B	S
PHF7-1	0:40:46.42	40:51:40.6	18.91±0.14			3.8	L	L
DAO38	0:40:47.01	40:40:57.9	19.06±0.27	old	HS	3.8	L	SLH
B336-G067	0:40:47.60	42:08:43.2	17.81	old	HS		B	S
V203	0:40:47.80	40:59:06.0	18.15±0.06	HII	HS	5.1	L	SL
V202	0:40:47.82	40:55:34.3	19.13±0.28	young	HS	5.1	L	SL
B452-G069	0:40:48.33	40:35:06.0	18.00±0.10	young	HS	7.7	L	SL
PHF7-2	0:40:48.38	40:51:58.2	18.43±0.20	young	HS	3.8	L	SL
B337-G068	0:40:48.47	42:12:11.0	16.73	old	HS		B	S
B017-G070	0:40:48.73	41:12:07.1	16.04±0.14	old	HS	7.7	L	SL
B018-G071	0:40:49.42	40:41:31.4	18.21±0.28	interm	HS	3.8	L	SLH
B009D	0:40:50.01	41:01:39.9	18.75±0.09			5.1	L	L
BH11	0:40:50.83	40:40:38.4	20.05±0.15	old	HS	3.8	L	SLH
B010D	0:40:51.1	41:15:04.9	18.92±0.08	young	HS	5.1	L	SL
B198D	0:40:51.47	40:33:27.8	18.13±0.22			7.7	L	L
B011D	0:40:51.63	40:44:06.1	18.04±0.25	young	HS	2.5	L	SLH
DAO40	0:40:51.96	40:36:02.8	20.35±0.07	HII	HS	2.5	L	SLH
B012D-D039	0:40:52.28	40:58:41.3	19.05±0.05	young	HS	3.8	L	SL
B246	0:40:52.29	40:53:55.9	18.63±0.14	old	HS	5.1	L	SL
B019-G072	0:40:52.52	41:18:53.8	14.98±0.08	old	HS	7.7	L	SLH
KHM31-74	0:40:52.99	40:35:19.8	19.04±0.29	old	HS	7.7	L	SLH
SK018A	0:40:53.64	41:16:15.1	19.48±0.07	young	HS	3.8	L	SL
KHM31-77	0:40:53.69	40:36:50.8	19.78±0.05	old	HS	5.1	L	SLH
B020-G073	0:40:55.26	41:41:25.2	14.91	old	HS		B	S
KHM31-81	0:40:55.72	40:35:22.1	21.16±0.40	young	HS	1.2	L	SLH
KHM31-85	0:40:56.61	40:34:24.6	19.62±0.38	young	HS	2.5	L	SLH
V212	0:40:58.53	41:03:32.4	19.14±0.12	HII	HS	3.8	L	SLH
KHM31-97	0:40:58.81	40:34:23.9	19.26±0.14	young	HS	5.1	L	SLH
B338-G076	0:40:58.87	40:35:47.9	14.22±0.10	old	HS	11.6	L	SLH
B021-G075	0:40:58.99	41:05:39.1	17.78±0.14	old	HS	7.7	L	SL
B022-G074	0:40:59.08	41:24:42.0	17.35	old	HS		B	S
B339-G077	0:41:00.71	39:55:54.2	16.87	old	HS		B	S
B014D	0:41:01.07	41:06:32.8	18.53±0.15	young	HS	7.7	L	SL
B023-G078	0:41:01.19	41:13:45.7	14.17±0.09	old	HS	11.6	L	SLH
V211	0:41:02.01	41:02:54.9	18.53±0.06	HII	HS	5.1	L	SLH
B247	0:41:02.27	41:00:32.0	18.26±0.40	old	HS	5.1	L	SL
KHM31-113	0:41:02.64	40:34:43.1	19.72±0.12	young	HS	3.8	L	SLH
B015D-D041	0:41:02.74	41:06:36.3	18.70±0.20	young	HS	5.1	L	SL
BH12	0:41:02.88	40:34:58.4	18.70±0.30	young	HS	3.8	L	SLH
B453-D042	0:41:03.27	41:00:56.9	18.30±0.05	young	HS	5.1	L	SL
B200D-D043	0:41:06.79	40:34:29.0	19.04±0.31	young	HS	3.8	L	SL
B248	0:41:07.94	40:53:01.0	18.06±0.05	old	HS	7.7	L	SL
B201D-D044	0:41:08.29	40:32:51.7	19.18±0.31	young	HS	3.8	L	SL

TABLE 1 — *Continued*

Object	RA	Dec	V	type	S[a]	Ap ″	P[b]	C[c]
		2000						
B341-G081[d]	0:41:09.15	40:35:52.8	16.27±0.03	old	HS	5.1	L	SL
B017D	0:41:10.01	40:58:10.6	18.23±0.19	old	HS	7.7	L	SL
B024-G082	0:41:11.86	41:45:49.1	16.79	old	HS		B	S
V031	0:41:12.26	41:05:29.1	18.37±0.30	young	HS	7.7	L	SLH
G083-V225	0:41:12.45	41:09:49.3	19.06±0.16	young	HS	3.8	L	SL
B025-G084	0:41:12.55	41:00:28.3	16.77±0.08	old	HS	5.1	L	SL
B249	0:41:12.58	41:01:12.7	18.16±0.26	old	HS	7.7	L	SL
G085-V015	0:41:12.79	40:34:17.4	18.04±0.22	young	HS	3.8	L	SL
SK020A	0:41:13.36	41:09:42.0	19.68±0.12	na	HS	5.1	L	SL
V014	0:41:13.81	40:33:57.9	17.72±0.33	young	HS	5.1	L	SL
B027-G087	0:41:14.54	40:55:50.9	15.61±0.06	old	HS	7.7	L	SLH
B026-G086	0:41:14.55	41:24:40.1	17.53	old	HS		B	S
V226	0:41:14.80	41:09:23.4	19.19±0.12	HII	HS	3.8	L	SL
B019D	0:41:16.13	41:05:07.8	18.93±0.13	interm	HS	5.1	L	SLH
B028-G088	0:41:16.50	40:59:03.2	16.90±0.09	old	HS	7.7	L	SL
B020D-G089	0:41:17.23	41:08:09.1	17.47±0.05	old	HS	7.7	L	SLH
B029-G090	0:41:17.82	41:00:23.0	16.65±0.13	old	HS	11.6	L	SL
B030-G091	0:41:18.74	40:57:15.6	17.32±0.05	old	HS	7.7	L	SLH
B031-G092	0:41:20.93	40:59:04.2	17.72±0.03	old	HS	5.1	L	SL
B032-G093	0:41:21.51	41:17:30.2	17.61±0.03	old	HS	7.7	L	SL
B342-G094	0:41:24.09	40:36:47.0	18.46±0.32	young	HS	5.1	L	SLH
B033-G095	0:41:26.40	41:00:14.0	17.68±0.08	old	HS	7.7	L	SL
B034-G096	0:41:28.12	40:53:49.6	15.40±0.10	old	HS	11.6	L	SL
B457-G097	0:41:29.23	42:18:37.1	16.91	old	HS		B	S
DAO47	0:41:29.49	40:45:16.8	19.07±0.13	young	HS	5.1	L	SL
V034	0:41:30.18	41:05:01.9	19.42±0.43	HII	HS	3.8	L	SL
LGS04131.1_404612	0:41:31.16	40:46:12.6	19.12±0.18	young	HS	3.8	L	SL
B035	0:41:32.58	41:38:32.7	17.47	old	HS		B	S
B036	0:41:32.83	41:26:05.1	17.31	old	HS		B	S
B024D	0:41:34.00	41:01:25.0	19.84±0.13			2.5	L	L
B037-V327	0:41:34.98	41:14:55.1	16.86±0.09	old	HS	11.6	L	SLH
B038-G098	0:41:35.95	41:19:14.8	16.51±0.06	old	HS	5.1	L	SL
G099-V022	0:41:36.86	40:47:25.2	19.35±0.80	young	HS	2.5	L	SL
B039-G101	0:41:37.87	41:20:50.1	16.17±0.11	old	HS	7.7	L	SL
B029D	0:41:38.43	41:43:13.4	18.50				G	
B040-G102	0:41:38.84	40:40:54.4	17.60±0.15	young	HS	7.7	L	SL
PHF8-1	0:41:39.50	40:40:33.5	19.26±0.11	young	HS	3.8	L	SL
B206D-D048	0:41:40.60	40:50:06.8	18.80±0.09	young	HS	3.8	L	SL
B041-G103	0:41:40.81	41:14:45.4	18.57±0.11	old	P	5.1	L	LH
B042-G104	0:41:41.69	41:07:26.2	16.16±0.07	old	HS	5.1	L	SLH
B521	0:41:41.71	40:52:01.5	19.08±0.09	young	HS	5.1	L	SL
B043-G106	0:41:42.31	40:42:40.0	17.01±0.13	young	HS	7.7	L	SL
B044-G107	0:41:42.91	41:20:06.2	16.84±0.07	old	HS	5.1	L	SL
B343-G105	0:41:43.10	40:12:22.4	16.34	old	HS		B	SH
B045-G108	0:41:43.11	41:34:20.3	15.71±0.10	old	HS	11.6	L	SLH
B458-D049	0:41:44.59	40:51:21.9	18.17±0.22	young	HS	7.7	L	SLH
B046-G109	0:41:44.60	41:46:27.7	17.80	old	HS		B	S
B048-G110	0:41:45.53	41:13:30.6	16.58±0.08	old	HS	7.7	L	SL
B047-G111	0:41:45.56	41:42:04.1	17.50	old	HS		B	S
B049-G112	0:41:45.57	40:49:54.7	17.68±0.10	young	HS	7.7	L	SLH
BH13	0:41:45.73	41:33:25.4	20.82±0.16			2.5	L	L
B032D	0:41:45.96	41:13:01.4	18.59±0.18	young	HS	3.8	L	SL
B050-G113	0:41:46.28	41:32:18.7	16.74±0.04	old	HS	7.7	L	SL
PHF6-2	0:41:46.48	41:18:47.8	19.88±0.29	HII	HS	3.8	L	SL
B051-G114	0:41:46.70	41:25:19.1	16.28±0.15	old	HS	7.7	L	SL
V245	0:41:46.74	41:18:46.8	19.53±0.20	HII	HS	3.8	L	SL
SK036A	0:41:47.40	40:51:08.6	19.72±0.19	old	HS	3.8	L	SL
B054-G115	0:41:47.68	41:00:55.3	18.16±0.04	old	HS	5.1	L	SL
KHM31-330	0:41:48.22	40:52:59.3	20.36±0.34			3.8	L	L
B055-G116[d]	0:41:50.39	41:12:12.4	16.65±0.10	old	HS	11.6	L	SL
B035D	0:41:50.46	41:20:03.2	18.48±0.10	young	HS	5.1	L	SL
B254	0:41:50.5	41:16:25.9	18.66±0.14	old	HS	5.1	L	SL
B522	0:41:50.95	40:52:48.2	18.66±0.14	old	HS	5.1	L	SL
B056-G117	0:41:51.16	40:57:40.2	17.29±0.11	old	HS	11.6	L	SLH
B057-G118	0:41:52.82	40:52:05.1	17.58±0.07	old	HS	5.1	L	SLH
KHM31-340	0:41:52.92	40:52:16.4	19.97±0.33			3.8	L	L
B058-G119	0:41:53.00	40:47:09.7	15.00±0.08	old	HS	7.7	L	SLH
KHM31-341	0:41:53.04	40:52:35.7	19.32±0.08	young	HS	3.8	L	SL
KHM31-345	0:41:53.85	40:50:09.8	20.02±0.25	young	HS	3.8	L	SL
B059-G120	0:41:54.11	41:11:00.7	17.18±0.06	old	HS	5.1	L	SL
KHM31-347	0:41:54.25	40:50:28.1	20.62±0.36			1.8	L	
KHM31-350	0:41:55.06	40:51:52.1	20.53±0.16			2.5	L	L
KHM31-152	0:41:56.93	40:46:31.9	19.56±0.17	young	HS	5.1	L	SLH
B060-G121	0:41:57.01	41:05:14.5	16.68±0.08	old	HS	7.7	L	SL
B255	0:41:59.96	40:48:33.7	18.28±0.19	young	HS	5.1	L	SL

TABLE 1 — *Continued*

Object	RA	Dec	V	type	S[a]	Ap	P[b]	C[c]
		2000				"		
B061-G122	0:42:00.14	41:29:35.7	16.59±0.10	old	HS	11.6	L	SLH
BH14	0:42:00.39	40:47:46.0	19.80±0.22	HII	HS	5.1	L	SLH
B038D	0:42:00.45	41:12:14.2	19.03±0.27			3.8	L	L
B063-G124	0:42:00.88	41:29:09.5	15.73±0.05	old	HS	7.7	L	SLH
B065-G126	0:42:01.93	40:40:13.1	16.83±0.10	old	HS	11.6	L	SL
B064-G125	0:42:01.93	41:11:07.5	16.30±0.07	old	HS	7.7	L	SL
B344-G127	0:42:02.97	41:52:02.2	15.95	old	HS		B	S
B066-G128	0:42:03.07	40:44:47.1	17.77±0.16	young	HS	5.1	L	SL
B067-G129	0:42:03.19	41:04:23.7	17.20±0.08	old	HS	7.7	L	SL
B068-G130	0:42:03.21	40:58:50.2	16.24±0.10	old	HS	11.6	L	SLH
B257-V219	0:42:03.28	40:58:13.9	17.76±0.07	old	HS	7.7	L	SLH
B461-G131	0:42:04.24	42:03:26.6	17.52	old	HS		B	S
B040D	0:42:04.3	41:18:07.0	18.55±0.06	young	HS	5.1	L	SL
B041D	0:42:04.72	41:16:47.3	18.23±0.13	old	HS	5.1	L	SL
B069-G132	0:42:05.54	41:26:09.3	19.02±0.39	young	HS	2.5	L	SLH
SK044A	0:42:06.38	40:53:16.8	19.47±0.22	na	HS	3.8	L	SLH
B070-G133	0:42:06.91	41:07:56.3	16.74±0.05	old	HS	5.1	L	SLH
B071	0:42:07.13	41:12:12.0	17.94±0.06	old	HS	3.8	L	SL
B073-G134	0:42:07.33	40:59:21.3	15.97±0.09	old	HS	11.6	L	SL
B072	0:42:07.44	41:22:47.6	17.84±0.17	old	HS	2.5	L	SL
B258	0:42:07.80	41:09:26.0	18.47±0.10			3.8	L	L
B074-G135	0:42:08.04	41:43:21.6	16.65	old	HS		B	S
B075-G136	0:42:08.83	41:20:21.3	17.56±0.21	old	HS	5.1	L	SL
G137	0:42:09.43	41:28:31.7	17.77±0.24	HII	HS	5.1	L	SLH
MITA140	0:42:09.51	41:17:45.6	17.00±0.04	old	HS	5.1	L	SL
B045D	0:42:09.87	41:21:14.5	18.97±0.09	old	HS	3.8	L	SL
B076-G138	0:42:10.24	41:05:22.0	16.67±0.09	old	HS	7.7	L	SLH
B047D	0:42:10.93	41:29:59.2	19.11±0.31	na		5.1	L	LH
B077-G139	0:42:11.14	41:07:33.9	17.25±0.09	old	HS	7.7	L	SLH
B078-G140	0:42:12.17	41:17:58.9	17.69±0.11	old	HS	5.1	L	SL
B080-G141	0:42:12.40	41:19:00.6	17.67±0.27	old	HS	3.8	L	SL
B081-G142	0:42:13.59	40:48:39.1	17.48±0.17	young	HS	3.8	L	SL
B345-G143	0:42:14.12	40:17:36.5	16.51	old	HS		B	S
B462	0:42:14.72	42:01:36.7	18.05	old	HS		B	S
B082-G144	0:42:15.84	41:01:14.4	16.13±0.29	old	HS	2.5		SLH
B083-G146	0:42:16.44	41:45:20.7	17.09	old	HS		B	S
B084	0:42:17.45	41:18:55.7	18.00±0.09	old	HS	5.1	L	SL
B085-G147	0:42:18.24	40:39:57.2	16.84±0.07	old	HS	7.7	L	SL
B086-G148	0:42:18.65	41:14:02.1	15.09±0.08	old	HS	7.7	L	SLH
B259	0:42:19.0	41:42:13.9	18.36	old	HS		G	S
SK049A	0:42:19.48	40:52:22.6	20.22±0.15	na	HS	2.5	L	SL
B087[e]	0:42:19.81	41:38:16.2	18.57±0.03	old	HS	5.1	L	SL
B051D	0:42:20.56	41:04:37.7	18.82±0.07	na	HS	3.8	L	SL
B088-G150	0:42:21.07	41:32:14.2	15.40±0.11	old	HS	11.6	L	SLH
B090	0:42:21.08	41:02:57.5	18.44±0.07	old	HS	5.1	L	SLH
SK050A	0:42:21.57	41:14:19.7	18.61±0.04	na	HS	2.5	L	SLH
B091-G151	0:42:21.73	41:22:05.2	17.92±0.12	young	HS	5.1	L	SLH
B092-G152	0:42:22.38	41:08:08.7	16.89±0.03	old	HS	7.7	L	SL
B347-G154	0:42:22.89	41:54:27.5	16.49	old	HS		B	S
B348-G153	0:42:22.92	41:52:28.4	16.79	old	HS		B	S
B093-G155	0:42:23.17	41:21:43.5	16.86±0.17	old	HS	5.1	L	SLH
B349	0:42:24.10	40:37:43.9	18.03±0.03	young	HS	7.7	L	SL
B053D-NB20	0:42:24.94	41:12:34.7	19.95±0.16			1.8	L	L
B094-G156	0:42:25.06	40:57:17.7	15.61±0.09	old	HS	7.7	L	SLH
B095-G157	0:42:25.80	41:05:36.3	16.20±0.04	old	HS	7.7	L	SL
B096-G158	0:42:26.1	41:19:14.8	16.62±0.07	old	HS	5.1	L	SL
B098	0:42:27.40	40:59:36.1	16.25±0.04	old	HS	5.1	L	SL
B097-G159	0:42:27.48	41:25:32.1	16.79±0.05	old	HS	7.7	L	SL
B099-G161	0:42:27.59	41:10:02.7	16.83±0.08	old	HS	5.1	L	SL
B515	0:42:28.05	41:33:24.5	18.60±0.22	na		7.7	L	LH
B056D	0:42:28.36	41:34:27.2	18.54±0.08	na	HS	7.7	L	SLH
B350-G162	0:42:28.44	40:24:51.1	16.74	old	HS		B	S
B100-G163	0:42:28.96	40:49:56.0	17.68±0.06	old	HS	7.7	L	SL
B101-G164	0:42:29.04	41:08:15.6	16.91±0.03	old	HS	5.1	L	SL
NB108	0:42:29.28	41:15:15.6	20.17±0.37			1.8	L	L
B103-G165	0:42:29.75	41:17:57.5	15.15±0.03	old	HS	7.7	L	SLH
B104-NB5	0:42:29.94	41:17:25.7	17.51±0.09	old	HS	5.1	L	SLH
B105-G166	0:42:30.75	41:30:27.3	17.33±0.12	old	HS	5.1	L	SL
B106-G168	0:42:31.04	41:12:18.3	16.37±0.18	old	HS	3.8	L	SL
B108-G167	0:42:31.19	41:08:51.3	17.30±0.08	old	HS	7.7	L	SL
B107-G169	0:42:31.27	41:19:38.9	15.79±0.08	old	HS	5.1	L	SL
NB24	0:42:31.81	41:15:45.1	19.70±0.23			1.8	L	L
B109-G170	0:42:32.16	41:10:27.9	16.34±0.04	old	HS	7.7	L	SLH
B061D	0:42:32.6	41:21:42.0	19.13±0.06	young	HS	3.8	L	SL
B110-G172	0:42:33.10	41:03:28.4	15.17±0.07	old	HS	5.1	L	SLH

TABLE 1   —   *Continued*

Object	RA	Dec	V	type	S[a]	Ap ″	P[b]	C[c]
		2000						
NB16	0:42:33.12	41:20:16.8	18.47±0.13	old	HS	2.5	L	SLH
B111-G173	0:42:33.17	41:00:26.5	16.66±0.04	old	HS	7.7	L	SL
B260	0:42:33.19	41:31:24.8	18.56±0.16	old	HS	7.7	L	SL
B112-G174	0:42:33.26	41:17:42.4	16.58±0.16	old	HS	3.8	L	SLH
B114-G175	0:42:34.30	41:12:44.9	17.04±0.09	old	HS	5.1	L	SLH
B117-G176	0:42:34.38	40:57:09.3	16.88±0.23	old	HS	2.5	L	SLH
NB17-AU014	0:42:34.40	41:17:31.4	19.45±0.28	na	HS	2.5	L	SLH
B115-G177	0:42:34.41	41:14:02.0	15.97±0.04	old	HS	5.1	L	SLH
B116-G178	0:42:34.54	41:32:51.4	16.83±0.06	old	HS	5.1	L	SL
NB35-AU4	0:42:34.55	41:18:40.4	19.35±0.07	old	HS	2.5	L	SLH
NB29	0:42:35.30	41:17:47.2	19.37±0.40	na		2.5	L	LH
B064D-NB6	0:42:35.54	41:14:34.3	16.41±0.07	old	HS	5.1	L	SLH
B119-NB14	0:42:36.11	41:17:35.4	17.47±0.09	old	HS	3.8	L	SLH
NB21-AU5	0:42:37.98	41:15:58.9	17.98±0.10	old	HS	2.5	L	SLH
B351-G179	0:42:37.98	42:11:30.7	17.55	old	HS		B	S
B352-G180	0:42:38.19	42:02:13.1	16.53	old	HS		B	S
B067D	0:42:38.99	41:36:43.2	19.11±0.06	young	HS	3.8	L	SLH
B068D	0:42:39.9	41:20:39.9	18.66±0.14	old	HS	3.8	L	SLH
B122-G181	0:42:40.11	41:33:46.8	17.65±0.03	old	HS	7.7	L	SL
B123-G182	0:42:40.66	41:10:33.4	17.38±0.08	old	HS	5.1	L	SLH
B124-NB10	0:42:41.44	41:15:23.7	14.73±0.07	old	HS	5.1	L	SLH
B125-G183	0:42:42.27	41:05:31.0	16.51±0.11	old	HS	7.7	L	SL
V270	0:42:42.39	41:31:54.6	18.90±0.08	HII	HS	3.8	L	SL
DAO55	0:42:42.5	40:29:27.0	18.68	old	HS		B	S
B126-G184	0:42:43.70	41:12:42.8	17.13±0.04	old	HS	5.1	L	SLH
NB62	0:42:44.21	41:14:23.1	19.53±0.13			1.8	L	LH
B127-G185	0:42:44.50	41:14:41.5	14.42±0.08	old	HS	7.7	L	SLH
NB89	0:42:44.78	41:14:44.2	17.51±0.20	na	HS	3.8	L	SLH
SK054A	0:42:45.08	41:08:15.1	18.37±0.09	na	HS	5.1	L	SL
B072D	0:42:45.79	41:27:27.0	19.06±0.08	old	HS	3.8	L	SLH
BH16	0:42:46.09	41:17:36.0	18.80±0.28			1.8	L	L
NB18	0:42:46.34	41:18:32.4	18.82±0.11	na	HS	2.5	L	SLH
B354-G186	0:42:47.64	42:00:24.7	17.81	old	HS		B	S
B128-G187	0:42:47.81	41:11:13.8	17.03±0.04	old	HS	5.1	L	SLH
NB41	0:42:48.18	41:16:00.6	18.09	na			G	H
B129	0:42:48.35	41:25:06.6	17.10±0.06	old	HS	7.7	L	SLH
NB39-AU6	0:42:48.55	41:15:47.6	18.32±0.27	na		1.8	L	LH
B130-G188	0:42:48.86	41:29:52.7	16.78±0.11	old	HS	11.6	L	SLH
AU008	0:42:48.97	41:18:11.2	18.15±0.30	na	HS	2.5	L	SLH
B262	0:42:50.05	41:19:28.1	17.74±0.11	old	HS	3.8	L	SL
BH18	0:42:50.73	41:10:33.4	18.10±0.09	old	HS	3.8	L	SL
B131-G189	0:42:50.81	41:17:07.3	15.37±0.03	old	HS	5.1	L	SLH
BH17	0:42:50.84	40:58:41.5	20.45±0.18	na		3.8	L	LH
B132-NB15	0:42:51.44	41:15:40.7	17.78±0.12	old	HS	2.5	L	SLH
B134-G190	0:42:51.65	41:14:03.6	16.68±0.17	old	HS	5.1	L	SLH
B078D	0:42:51.91	41:22:05.2	19.35±0.04	old	HS	2.5	L	SL
B135-G192	0:42:51.98	41:31:08.3	15.94±0.04	old	HS	7.7	L	SL
B264-NB19	0:42:53.19	41:16:14.4	17.70±0.10	old	HS	3.8	L	SLH
B136-G194	0:42:53.64	41:19:34.4	16.95±0.07	old	HS	5.1	L	SL
B137-G195	0:42:54.0	41:32:14.4	17.67±0.06	old	HS	7.7	L	SL
B081D	0:42:55.22	41:03:07.4	18.27±0.05	young	HS	7.7	L	SLH
B138	0:42:55.62	41:18:35.1	16.94±0.09	old	HS	3.8	L	SLH
B524	0:42:55.89	41:03:13.1	19.31±0.11	old		3.8	L	LH
B086D	0:42:56.71	40:51:22.7	19.21±0.49	na		5.1	L	LH
AU010	0:42:58.13	41:16:52.7	17.54±0.03	old	HS	3.8	L	SL
NB34-AU15	0:42:58.45	41:14:55.4	18.73±0.15	HII		3.8	L	L
B140-G196[f]	0:42:58.75	41:08:52.7	17.84±0.25	old	HS	3.8	L	SLH
B087D	0:42:58.92	41:09:08.8	17.54±0.06	old	HS	5.1	L	SL
B141-G197	0:42:59.29	41:32:47.5	16.83±0.08	old	HS	11.6	L	SL
B088D	0:42:59.38	41:04:17.5	18.63±0.24			3.8	L	LH
B143-G198	0:42:59.66	41:19:19.3	15.98±0.04	old	HS	7.7	L	SLH
B144	0:42:59.87	41:16:05.7	16.79±0.09	old	HS	3.8	L	SLH
B090D	0:43:01.23	41:16:10.4	17.37±0.08	old	HS	3.8	L	SL
B089D	0:43:01.36	41:26:24.1	18.90±0.06	young	HS	5.1	L	SL
B091D-D058	0:43:01.44	41:30:17.5	15.44±0.07	old	HS	5.1	L	SL
B145	0:43:01.59	41:12:26.9	18.37±0.09	old	HS	3.8	L	SLH
B092D	0:43:01.70	41:13:08.9	18.92±0.24	old	HS	3.8	L	SLH
B265	0:43:01.92	40:53:01.8	18.42±0.06	old	HS	5.1	L	SL
B146	0:43:02.94	41:15:22.6	16.99±0.06	old	HS	3.8	L	SLH
B147-G199[g]	0:43:03.30	41:21:21.5	15.71±0.13	old	HS	11.6	L	SLH
B266	0:43:03.52	41:40:31.2	18.27±0.07	old	HS	7.7	L	SLH
BH23	0:43:03.79	41:20:28.1	18.51±0.16	na	HS	3.8	L	SLH
B148-G200	0:43:03.87	41:18:04.8	15.77±0.05	old	HS	5.1	L	SLH
B220D	0:43:04.38	39:50:05.3	16.97				B	
B149-G201	0:43:05.48	41:34:27.3	17.03±0.13	old	HS	11.6	L	SL

TABLE 1 — *Continued*

Object	RA	Dec	V	type	S[a]	Ap ″	P[b]	C[c]
		2000						
B467-G202	0:43:06.45	42:01:49.1	17.43	old	HS		B	S
B268	0:43:07.19	41:11:47.8	18.33±0.07	old	HS	3.8	L	SLH
B269	0:43:07.38	41:27:32.9	18.83±0.16	old	HS	5.1	L	SLH
B150-G203	0:43:07.52	41:20:19.6	16.62±0.04	old	HS	7.7	L	SL
PHF6-1	0:43:08.02	41:18:18.3	17.67±0.07	old	HS	3.8	L	SLH
B223D	0:43:09.55	42:24:59.2	17.75				G	
B151-G205	0:43:09.56	41:21:32.1	14.77±0.04	old	HS	7.7	L	SLH
B152-G207	0:43:10.02	41:18:16.1	16.09±0.09	old	HS	7.7	L	SLH
B356-G206	0:43:10.36	41:50:31.3	16.89±0.10	old	HS	11.6	L	SL
B153	0:43:10.63	41:14:51.4	16.13±0.05	old	HS	5.1	L	SLH
BH25	0:43:11.99	41:02:49.0	18.93±0.30	na		3.8	L	LH
B154-G208	0:43:12.46	41:16:04.9	16.70±0.08	old	HS	5.1	L	SLH
B357-G209	0:43:13.23	40:10:56.3	16.61	old	B		B	
B155-G210	0:43:13.39	41:03:28.3	17.90±0.09	old	HS	5.1	L	SLH
B225D	0:43:13.40	40:01:14.9	18.36				B	
B156-G211	0:43:13.73	41:01:17.9	16.86±0.03	old	HS	7.7	L	SLH
B157-G212	0:43:14.00	41:11:19.7	17.59±0.12	old	HS	5.1	L	SL
B095D	0:43:14.03	41:08:44.8	18.97±0.06	young	HS	3.8	L	SL
B158-G213	0:43:14.41	41:07:21.2	14.65±0.06	old	HS	7.7	L	SLH
B159	0:43:14.65	41:25:13.5	17.35±0.04	old	HS	7.7	L	SLH
B160-G214	0:43:14.93	41:01:35.6	18.03±0.09	old	HS	5.1	L	SLH
B227D	0:43:15.29	40:15:42.9	16.91				G	
B161-G215	0:43:15.43	41:11:25.0	16.30±0.05	old	HS	5.1	L	SL
SK063A	0:43:16.09	41:27:57.0	18.38±0.13	na	HS	5.1	L	SLH
B162-G216	0:43:16.41	41:24:04.5	17.54±0.07	old	HS	5.1	L	SLH
B097D	0:43:16.69	41:06:33.4	18.33±0.12	young	HS	7.7	L	SL
B098D	0:43:17.4	41:31:30.0	18.83±0.06	young	HS	3.8	L	SL
B163-G217	0:43:17.64	41:27:45.0	15.00±0.11	old	HS	11.6	L	SLH
B358-G219	0:43:17.86	39:49:13.1	15.12	old	B		B	
B164-V253	0:43:18.14	41:12:29.3	17.78±0.04	old	HS	5.1	L	SL
B165-G218	0:43:18.22	41:10:54.7	16.44±0.08	old	HS	7.7	L	SL
B167	0:43:21.13	41:14:08.3	17.34±0.07	old	HS	3.8	L	SLH
B168	0:43:22.52	41:44:05.6	18.41±0.19	old	HS	5.1	L	SL
B169	0:43:23.00	41:15:25.4	17.27±0.03	old	HS	5.1	L	SLH
B271	0:43:23.07	41:25:26.4	18.35±0.08	interm	HS	7.7	L	SL
B170-G221	0:43:23.47	40:50:41.8	17.40±0.05	old	HS	5.1	L	SL
SK066A	0:43:24.08	41:38:42.2	19.55±0.11	na	HS	5.1	L	SLH
B272-V294	0:43:25.52	41:37:11.7	18.23±0.12	old	HS	11.6	L	SL
B171-G222	0:43:25.61	41:15:37.2	15.26±0.08	old	HS	7.7	L	SLH
B172-G223	0:43:26.00	41:21:31.6	16.71±0.07	old	HS	5.1	L	SL
SK068A	0:43:28.15	41:00:22.0	19.95±0.09	old	HS	3.8	L	SL
B173-G224	0:43:28.76	41:22:37.0	17.45±0.06	old	HS	5.1	L	SL
B174-G226	0:43:30.31	41:38:56.2	15.40±0.03	old	HS	15.4	L	SLH
B176-G227	0:43:30.45	40:49:11.1	16.86±0.19	old	HS	5.1	L	SL
B177-G228	0:43:30.49	41:05:42.4	18.30±0.09	old	HS	7.7	L	SL
B178-G229	0:43:30.79	41:21:16.4	14.97±0.10	old	HS	15.4	L	SL
B179-G230	0:43:31.10	41:18:14.7	15.34±0.11	old	HS	11.6	L	SL
B180-G231	0:43:31.72	41:07:46.4	16.27±0.15	old	HS	3.8	L	SL
B181-G232	0:43:32.46	41:29:07.4	16.93±0.09	old	HS	7.7	L	SL
V254	0:43:34.87	41:09:55.3	17.34±0.46	HII	HS	5.1	L	SL
B182-G233	0:43:36.66	41:08:12.2	15.42±0.09	old	HS	7.7	L	SL
B183-G234	0:43:36.94	41:02:02.4	15.99±0.09	old	HS	7.7	L	SL
B185-G235	0:43:37.28	41:14:43.6	15.58±0.08	old	HS	5.1	L	SLH
B184-G236	0:43:37.52	41:36:34.5	17.46±0.14	old	HS	5.1	L	SL
B186	0:43:38.23	41:36:24.1	19.14±0.63	old	HS	3.8	L	SL
B187-G237	0:43:38.64	41:29:47.1	17.29±0.13	old	HS	5.1	L	SL
B274	0:43:39.36	41:31:18.4	18.77±0.22	old	HS	7.7	L	SL
B233D	0:43:41.31	39:36:45.9	16.17				G	
B188-G239	0:43:41.51	41:24:25.6	17.04±0.11	old	HS	7.7	L	SL
B189-G240	0:43:42.42	41:35:23.3	17.06±0.22	old	HS	11.6	L	SL
B190-G241	0:43:43.39	41:34:06.0	16.91±0.10	old	HS	7.7	L	SL
B192-G242	0:43:44.52	41:37:26.7	18.54±0.09	young	HS	7.7	L	SL
M001	0:43:45.09	41:18:12.0	19.12±0.09	young	HS	3.8	L	SL
B194-G243	0:43:45.18	41:06:08.7	17.24±0.11	old	HS	5.1	L	SL
B193-G244	0:43:45.52	41:36:57.6	15.33±0.03	old	HS	15.4	L	SL
SK071A	0:43:46.40	41:39:28.8	20.07±0.26	na	HS	3.8	L	SL
SK072A	0:43:46.69	41:22:28.2	17.59±0.07	na	HS	3.8	L	SL
B103D-G245	0:43:47.54	41:27:08.0	17.73±0.05	old	HS	7.7	L	SL
B472-D064	0:43:48.42	41:26:53.2	15.21±0.06	old	HS	7.7	L	SL
SK073A	0:43:48.52	41:07:48.4	18.07±0.08	na	HS	5.1	L	SL
B195	0:43:48.56	41:02:28.0	18.55±0.09	young	HS	5.1	L	SL
B196-G246	0:43:48.57	40:42:36.8	17.40	old	HS		B	S
B197-G247	0:43:49.72	41:30:10.1	17.77±0.09	old	HS	7.7	L	SL
B199-G248	0:43:49.83	40:58:14.8	17.52±0.05	old	HS	7.7	L	SLH
LGS04350.1_410223	0:43:50.05	41:02:23.2		na	HS			SL

TABLE 1 — *Continued*

Object	RA	Dec	V	type	S[a]	Ap ″	P[b]	C[c]
		2000						
B198-G249	0:43:50.11	41:31:52.6	17.91±0.16	old	HS	7.7	L	SLH
B200	0:43:50.44	41:29:22.9	18.29±0.16	old	HS	7.7	L	SL
B201-G250	0:43:52.83	41:09:58.1	16.18±0.12	old	HS	7.7	L	SL
M003	0:43:54.28	41:14:11.7	18.47±0.12	young	HS	5.1	L	SL
B106D	0:43:54.45	41:15:14.5	18.28±0.14	young	HS	5.1	L	SLH
B202-G251	0:43:54.69	41:00:32.5	17.77±0.03	old	HS	7.7	L	SLH
B203-G252	0:43:55.83	41:32:35.1	16.69±0.07	old	HS	11.6	L	SLH
B204-G254	0:43:56.42	41:22:02.9	15.68±0.07	old	HS	5.1	L	SL
B361-G255	0:43:57.10	40:14:01.2	17.10	old	HS		B	S
B108D	0:43:57.11	41:45:32.9	18.63±0.17	young	HS	5.1	L	SL
M005	0:43:58.00	41:21:32.9	19.93±0.12	young	HS	2.5	L	SL
B205-G256	0:43:58.17	41:24:38.3	15.44±0.09	old	HS	11.6	L	SL
B206-G257	0:43:58.63	41:30:18.1	15.06±0.07	old	HS	7.7	L	SLH
B110D-V296	0:43:59.14	41:36:41.3	18.60±0.09	old	HS	3.8	L	SLH
LGS04359.1_413843	0:43:59.17	41:38:43.8	18.36±0.13		HS	5.1	L	SLH
B207-G258	0:43:59.44	41:06:10.7	17.27±0.05	old	HS	7.7	L	SL
B208-G259	0:44:00.08	41:23:11.6	18.05±0.07	old	HS	7.7	L	SL
M009	0:44:00.83	41:17:12.5	18.01±0.12	old	HS	5.1	L	SL
G260	0:44:00.85	42:34:48.4	17.01	old	B		B	
B209-G261	0:44:02.63	41:25:26.7	16.60±0.06	old	HS	7.7	L	SL
B210-M11	0:44:02.75	41:14:24.6	17.79±0.09	young	HS	5.1	L	SLH
M012	0:44:02.83	41:21:40.3	18.93±0.25	old	HS	5.1	L	SL
B211-G262	0:44:02.92	41:20:04.8	16.80±0.13	old	HS	5.1	L	SL
B212-G263	0:44:03.05	41:04:56.4	15.39±0.10	old	HS	11.6	L	SL
B213-G264	0:44:03.52	41:30:38.7	16.83±0.07	old	HS	7.7	L	SLH
B214-G265	0:44:03.96	41:26:18.6	17.65±0.07	old	HS	5.1	L	SL
B111D-D065	0:44:04.90	41:39:05.5	18.60±0.27	young	HS	3.8	L	SLH
B215-G266	0:44:06.40	41:31:43.7	17.23±0.09	old	HS	7.7	L	SLH
B240D-D066	0:44:06.85	41:40:28.1	18.54±0.26	young	HS	2.5	L	SL
M016	0:44:08.00	41:23:54.0	19.53±0.04	young	HS	3.8	L	SL
B216-G267	0:44:08.80	41:37:56.0	17.33±0.13	young	HS	7.7	L	SL
G268	0:44:10.01	42:46:57.8	16.63	old	B		B	
DAO67	0:44:10.29	41:58:51.5	18.80±0.16	HII	HS	5.1	L	SL
B217-G269	0:44:10.60	41:23:51.2	16.52±0.07	old	HS	7.7	L	SL
M019	0:44:11.71	41:23:54.0	18.35±0.09	old	HS	5.1	L	SL
SK084A	0:44:12.35	41:21:11.0	19.42±0.17	na	HS	3.8	L	SLH
M020	0:44:13.94	41:22:18.9	18.53±0.03	young	HS	5.1	L	SL
B218-G272	0:44:14.33	41:19:19.4	14.76±0.11	old	HS	11.6	L	SL
B219-G271	0:44:15.04	40:56:47.3	16.39	old	HS		B	S
B277-M22	0:44:16.90	41:14:16.0	19.36±0.12	old	HS	3.8	L	SL
B363-G274	0:44:17.25	40:33:35.1	17.86	old	HS		B	S
M023	0:44:18.95	41:21:10.1	19.38±0.31	young	HS	3.8	L	SLH
B220-G275	0:44:19.44	41:30:35.0	16.51±0.13	old	HS	11.6	L	SLH
M025	0:44:19.60	41:24:09.0	18.88±0.14	young	HS	5.1	L	SL
M026	0:44:20.25	41:27:19.9	20.05±0.12	na	HS	3.8	L	SL
B112D-M27	0:44:21.23	41:19:09.8	18.57±0.09	old	HS	5.1	L	SLH
M028	0:44:22.06	41:33:40.1	19.14±0.16			5.1	L	L
B246D	0:44:22.83	42:04:32.9	16.52±0.08	young	HS	5.1	L	S
B221-G276	0:44:23.07	41:33:06.4	16.77±0.09	old	HS	11.6	L	SL
B278-M30	0:44:23.33	41:35:04.1	18.79±0.08	young	HS	5.1	L	SL
M031	0:44:24.26	41:33:58.6	19.37±0.13	young	HS	5.1	L	SL
B222-G277	0:44:25.35	41:14:12.0	17.54±0.20	young	HS	11.6	L	SL
SK086A	0:44:26.07	41:35:14.5	18.88±0.57	na	HS	5.1	L	SL
B115D-M33	0:44:26.52	41:38:57.5	18.53±0.25	na		5.1	L	L
B223-G278	0:44:27.05	41:34:37.1	18.51±0.16	young	HS	7.7	L	SL
B224-G279	0:44:27.10	41:28:49.9	15.31±0.03	old	HS	15.4	L	SLH
B279-D068	0:44:27.99	41:44:10.3	18.60±0.18	old	HS	5.1	L	SLH
B225-G280	0:44:29.55	41:21:35.8	14.15	old	HS		B	SH
M039	0:44:31.34	41:30:04.8	19.18±0.12	young	HS	5.1	L	SLH
M040	0:44:31.51	41:27:55.2	19.71±0.09	old	HS	3.8	L	SL
B228-G281	0:44:33.21	41:41:27.8	16.79±0.08	old	HS	11.6	L	SLH
B229-G282	0:44:33.83	41:38:28.5	17.17±0.03	old	HS	15.4	L	SLH
M042	0:44:33.9	41:21:03.0	18.87±0.07	young	HS	5.1	L	SL
M043	0:44:34.36	41:23:11.5	20.16±0.14	old	HS	2.5	L	SL
M044	0:44:34.44	41:24:09.6	19.68±0.08			2.5	L	L
DAO69	0:44:34.80	41:53:27.7	18.32±0.48	young	HS	2.5	L	SL
B230-G283	0:44:35.18	40:57:12.2	16.04	old	HS		B	S
M045	0:44:36.4	41:35:32.9	19.25±0.32	old	HS	5.1	L	SLH
B365-G284	0:44:36.46	42:17:20.9	16.89±0.15	old	HS	7.7	L	SL
M046	0:44:36.67	41:27:14.2	18.93±0.19	na		5.1	L	LH
M047	0:44:37.8	41:28:51.9	19.16±0.19	old	HS	7.7	L	SLH
B231-G285	0:44:38.59	41:27:47.0	17.26±0.03	old	HS	5.1	L	SLH
BH28	0:44:39.10	41:44:26.0	20.33±0.23	na		2.5	L	LH
B118D	0:44:39.66	41:24:28.2	19.16±0.42	young	HS	2.5	L	SL
B232-G286	0:44:40.23	41:15:00.7	15.62±0.08	old	HS	7.7	L	SLH

TABLE 1 — *Continued*

Object	RA 2000	Dec	V	type	S[a]	Ap ʺ	P[b]	C[c]
M050	0:44:40.67	41:30:06.6	19.47±0.27	young	HS	5.1	L	SLH
B233-G287	0:44:42.12	41:43:54.6	15.83±0.09	old	HS	11.6	L	SLH
B281-G288	0:44:42.85	41:20:08.6	17.54±0.04	old	HS	15.4	L	SL
B234-G290	0:44:46.38	41:29:17.8	16.81±0.08	old	HS	7.7	L	SLH
B366-G291	0:44:46.72	42:03:50.5	16.48±0.19	old	HS	7.7	L	SLH
B367-G292	0:44:47.19	42:05:31.9	18.11±0.10	young	HS	7.7	L	SLH
B368-G293	0:44:47.80	41:51:09.2	18.08±0.09	old	B	7.7	L	LH
B255D-D072	0:44:48.52	42:06:12.9	18.97±0.48	na		3.8	L	LH
KHM31-234	0:44:49.37	41:19:35.0	20.74±0.23	young	HS	3.8	L	SLH
B121D	0:44:54.42	41:09:28.9	18.94±0.04			3.8	L	L
KHM31-246	0:44:54.73	41:28:51.3	19.78±0.10	interm	HS	3.8	L	SLH
B283-G296	0:44:55.37	41:17:00.2	18.01±0.12	old	HS	7.7	L	SL
V298	0:44:55.70	41:29:19.3	18.63±0.24			11.6	L	LH
B475-V128	0:44:56.06	41:54:00.5	17.84±0.30	young	HS	7.7	L	SL
M052	0:44:56.20	41:41:36.0	20.83±0.34			2.5	L	L
M053	0:44:57.29	41:48:02.0	19.25±0.13	old	HS	5.1	L	SL
B235-G297	0:44:57.93	41:29:24.0	16.42±0.12	old	HS	7.7	L	SL
B256D	0:44:58.7	41:54:36.7	17.35±0.17	young	HS	2.5	L	SL
M054	0:44:59.17	41:42:25.6	19.96±0.16			3.8	L	L
B257D-D073	0:44:59.36	41:54:47.3	18.48±0.35	na		2.5	L	L
M055	0:44:59.63	41:33:39.4	19.36±0.04	na		7.7	L	LH
V300	0:45:00.65	41:28:36.1	18.84±0.05	HII	HS	3.8	L	SL
M056	0:45:01.56	41:39:04.5	19.98±0.29	na		3.8	L	LH
M057	0:45:02.75	41:47:02.4	19.76±0.24	old	HS	3.8	L	SL
M058	0:45:03.36	41:40:05.5	19.43±0.45	old	HS	3.8	L	SLH
M059	0:45:04.08	41:46:20.8	18.78±0.09	young	HS	3.8	L	SL
KHM31-264	0:45:05.86	41:35:43.3	20.47±0.19	old	HS	2.5	L	SLH
KHM31-267	0:45:07.14	41:37:18.3	19.00±0.15		HS	3.8	L	SLH
B476-D074	0:45:07.18	41:40:31.1	18.59±0.06	old	HS	7.7	L	SL
M062	0:45:07.6	41:45:30.9	20.20±0.22	young	HS	2.5	L	SL
B477-D075	0:45:08.4	41:39:38.0	18.29±0.16	young	HS	7.7	L	SLH
B236-G298	0:45:08.90	40:50:28.6	17.38	old	HS		B	SH
B237-G299	0:45:09.22	41:22:34.6	17.31±0.25	old	HS	11.6	L	SL
M065	0:45:09.96	41:42:23.4	19.37±0.20			5.1	L	L
V133	0:45:10.50	42:00:12.0	18.58±0.22	young	HS	5.1	L	SL
M068	0:45:11.0	41:38:55.9	20.37±0.15	young	HS	2.5	L	SL
M069	0:45:11.3	41:49:20.0	20.26±0.28	young	HS	2.5	L	SL
M070	0:45:11.79	41:40:19.8	19.86±0.26	old	HS	3.8	L	SLH
M072	0:45:13.79	41:42:25.9	18.56±0.03	young	HS	5.1	L	SL
M071	0:45:13.80	41:42:34.0	20.30±0.20			2.5	L	L
B370-G300	0:45:14.39	41:57:40.8	16.28±0.09	old	HS	7.7	L	SL
B238-G301	0:45:14.67	41:19:37.1	16.41±0.09	old	HS	11.6	L	SL
M073	0:45:15.15	41:47:32.2	19.89±0.05	young	HS	3.8	L	SL
B239-M74	0:45:15.6	41:35:17.2	17.19±0.05	old	HS	7.7	L	SL
M075	0:45:15.80	41:44:46.1	19.98±0.14			3.8	L	L
M076	0:45:16.1	41:43:22.0	19.92±0.24	young	HS	3.8	L	SL
M077	0:45:17.39	41:39:33.0	20.25±0.18	HII	HS	2.5	L	SLH
M078	0:45:17.77	41:41:52.5	20.10±0.09	young	HS	3.8	L	SL
M079	0:45:17.80	41:40:58.2	19.70±0.19	young	HS	3.8	L	SL
M080	0:45:19.59	41:48:30.0	19.46±0.15	young	HS	3.8	L	SL
M081	0:45:22.29	41:47:57.0	20.75±0.21	old	HS	2.5	L	SL
B240-G302	0:45:25.04	41:06:22.1	15.23	old	HS		B	SH
M082	0:45:26.2	41:45:52.0	19.58±0.07	young	HS	3.8	L	SL
M083	0:45:26.93	41:45:43.8	19.90±0.26			3.8	L	L
B371-G303	0:45:27.15	41:43:44.9	18.27±0.21	young	HS	7.7	L	SL
M085	0:45:28.0	41:42:03.9	19.86±0.30	young	HS	3.8	L	SL
M086	0:45:28.49	41:49:29.3	18.98±0.25	young	HS	5.1	L	SL
B287	0:45:28.49	41:30:04.8	18.08±0.34	old	HS	7.7	L	SL
M087	0:45:32.05	41:49:32.0	18.85±0.40	young	HS	3.8	L	SL
M089	0:45:32.46	41:43:33.6	20.27±0.51	old		2.5	L	L
M088	0:45:32.54	41:43:31.1	20.07±0.49	young	HS	2.5	L	SL
M090	0:45:32.98	41:48:23.0	20.22±0.10			3.8	L	L
M091	0:45:33.11	41:42:19.3	19.00±0.12	young	HS	5.1	L	SLH
B372-G304	0:45:33.39	42:00:24.4	16.56±0.15	old	HS	7.7	L	SL
M092	0:45:35.60	41:45:18.0	19.34±0.17	young	HS	3.8	L	SL
BH30	0:45:36.75	41:43:34.9	20.50±0.24			2.5	L	LH
BH29	0:45:37.31	41:36:45.3	19.64±0.12	na		5.1	L	LH
M093	0:45:37.47	41:40:11.4	19.76±0.10	interm	HS	5.1	L	SL
M094	0:45:39.74	41:46:34.6	20.01±0.18			3.8	L	L
M095	0:45:39.85	41:44:41.6	19.61±0.39			3.8	L	L
B373-G305	0:45:41.85	41:45:33.6	15.70±0.09	old	HS	7.7	L	SL
B374-G306	0:45:44.53	41:41:54.9	18.35±0.14	young	HS	5.1	L	SLH
V129-BA4	0:45:44.69	41:51:59.4	17.05±0.03	old	HS	7.7	L	SL
B480-V127	0:45:45.55	41:45:52.4	18.24±0.09	young	HS	5.1	L	SL
B375-G307	0:45:45.58	41:39:42.4	17.51±0.10	old	HS	11.6	L	SL

TABLE 1 — *Continued*

Object	RA	Dec	V	type	S[a]	Ap ″	P[b]	C[c]
		2000						
M101	0:45:46.28	41:48:20.9	19.48±0.33	young	HS	3.8	L	SL
M102	0:45:46.8	41:45:23.0	20.26±0.06	HII	HS	3.8	L	SL
B377-G308	0:45:48.28	40:38:04.2	17.14	old	HS		B	S
B376-G309	0:45:48.40	41:42:40.1	18.03±0.07	young	HS	7.7	L	SL
M104	0:45:48.84	41:48:20.2	18.82±0.12	young	HS	3.8	L	SL
M105	0:45:49.70	41:39:26.0	20.18±0.43	old	HS	2.5	L	SL
B484-G310	0:45:53.89	41:47:37.0	18.36±0.09	young	HS	5.1	L	SL
B483-D085	0:45:53.92	42:02:18.1	18.43±0.16	young	HS	7.7	L	SL
B378-G311	0:45:57.24	41:53:31.1	17.56±0.07	old	HS	7.7	L	SL
B379-G312	0:45:58.83	40:42:31.3	16.13	old	HS		B	SH
B380-G313	0:46:06.20	42:00:53.0	17.53±0.27	young	HS	7.7	L	SL
B381-G315	0:46:06.54	41:20:58.8	15.76	old	HS		B	S
B486-G316	0:46:08.62	40:58:03.6	17.52	old	HS		B	S
B382-G317	0:46:10.32	41:37:40.5	17.36±0.06	old	HS	7.7	L	SL
B383-G318	0:46:11.94	41:19:41.4	15.33	old	HS		B	S
B384-G319	0:46:21.93	40:16:59.6	15.79	old	HS		B	SH
BH32	0:46:23.55	42:00:58.5	20.26±0.27	na		3.8	L	LH
SH20	0:46:26.04	41:03:16.0	16.81				G	
B386-G322	0:46:27.00	42:01:52.8	15.69±0.09	old	HS	7.7	L	SLH
SH21	0:46:31.79	39:23:56.1	16.51				G	
B387-G323	0:46:33.51	40:44:13.4	16.98	old	HS		B	S
B488-G324	0:46:34.28	42:11:42.7	16.78±0.17	HII	HS	5.1	L	SL
B489	0:46:36.36	40:00:26.8	17.35				G	
DAO88	0:46:41.98	42:15:45.9	19.82±0.15	HII	HS	3.8	L	SL
G327-MVI	0:46:49.49	42:44:46.7	15.94	old	B		B	
B297D	0:46:55.68	42:19:44.9	17.78±0.16			7.7	L	L
B391-G328	0:46:58.10	41:33:56.5	17.28	old	HS		B	S
B392-G329[d]	0:47:00.94	41:54:44.5	16.80±0.03	young	HS	15.4	L	SL
B393-G330	0:47:01.20	41:24:06.3	16.93	old	HS		B	S
BA28	0:47:14.22	42:21:42.2	19.10±0.41			7.7	L	L
B495-G334	0:47:24.69	41:55:11.5	17.97±0.22			7.7	L	L
B396-G335	0:47:25.15	40:21:42.1	17.38	old	HS		B	S
B397-G336	0:47:27.23	41:12:10.4	16.53	old	HS		B	S
BA10	0:47:56.28	42:28:43.5	19.10±0.03			7.7	L	L
B398-G341	0:47:57.78	41:48:45.6	17.46	old	HS		B	S
B399-G342	0:47:59.55	41:35:28.3	17.28	old	HS		B	S
B400-G343	0:48:01.45	42:25:33.2	16.50±0.08	old	B	7.7	L	L
B401-G344	0:48:08.50	41:40:41.9	16.83	old	HS		B	S
B329D	0:48:19.40	42:08:26.7	16.61±0.29			11.6	L	L
B332D	0:48:29.33	41:38:10.9	17.21				G	
B402-G346	0:48:36.11	42:01:34.8	17.42±0.13	old	P	7.7	L	L
B503	0:48:37.41	39:31:03.4	16.30				G	
BA11	0:48:45.59	42:23:37.7	17.66	old	P		B	
DAO99	0:48:48.30	42:32:43.9	19.03				B	
B334D	0:48:54.84	39:35:56.0	17.56				G	
B335D-D100	0:49:01.25	42:15:39.0	17.29				G	
B337D	0:49:11.20	41:07:21.0	18.23	old	HS		B	S
B338D	0:49:15.76	40:46:23.4	17.91				G	
B403-G348	0:49:17.62	41:35:08.1	16.22	old	HS		B	S
B506	0:49:34.90	40:00:28.9	17.04				G	
B405-G351	0:49:39.80	41:35:29.7	15.20	old	HS		B	S
B345D	0:49:52.55	40:53:10.1	17.25				G	
B509-D108	0:49:52.84	42:09:43.3	17.52				G	
B406-D109	0:49:59.32	42:15:55.9	17.19				G	
B407-G352	0:50:09.95	41:41:00.9	16.09	old	B		B	
B347D	0:50:13.80	40:56:24.2	16.84				G	
G353-BA13	0:50:18.21	42:35:44.1	17.15	old	P		B	
B348D	0:50:19.21	40:58:02.7	18.14				G	
B349D	0:50:32.00	41:13:20.3	16.68				G	
B350D	0:50:48.85	42:21:43.9	17.77				G	
EXT8	0:53:14.53	41:33:24.4			B			
VDB00	01:16:04.1	49:36:36.2	16.07				G	

[a] Source of velocity: HS=this paper; B=Barmby et al. (2000); P=Perrett et al. (2002)

[b] Source of photometry: L=this paper; B=Barmby et al. (2000); G=Galleti et al. (2007), H=Huxor et al. (2005)

[c] Source of classification as a cluster: S=spectrum from this paper indicates a cluster; L=LGS image indicates non-stellar; H=HST image indicates a cluster; objects with blank entries in this column and in the velocity source column should still be considered "candidates"

[d] not a cluster in Barmby et al. (2000)

[e] not a cluster in Crampton et al. (1985)

[f] not a cluster in Racine (1991)

[g] Dubath & Grillmair (1997) probably observed a different object

TABLE 2
Young Clusters, Ordered by Mass

Object	E(B−V)	Vel km s^{-1}	Log Age yr	Log Mass M$_\odot$	χ^2	Comments
B316-G040	0.20	-359.1±15	9.0	5.2	0.7	
B392-G329	0.25	-72.8±16	8.9	5.2	0.7	
B324-G051[f,i]	0.28	-218.2±15	8.8	5.1	1.4	NGC205-HubV
VDB0-B195D[b]	0.28	-551.8±20	7.6	5.1	2.7	emiss
B315-G038[e,g,h,j]	0.35	-555.2±17	8.2	5.0	1.1	
B222-G277[g,i]	0.28	-287.4±12	8.9	5.0	0.9	
B307-G030[g]	0.25	-454.6±20	9.0	4.9	0.4	
DAO30	0.25	-504.4±18	9.0	4.9	0.5	
B325[c,d]	0.25	-654.0±29	8.8	4.9	0.5	
B271	0.33	-351.6±35	9.1	4.8	0.3	
B349	0.28	-405.7±15	8.9	4.8	1.2	
BH05	0.28	-569.5±23	7.4	4.7	4.2	
B018-G071	0.20	-592.9±14	9.0	4.7	0.7	
B081-G142[g]	0.28	-368.1±14	8.5	4.7	1.6	
B097D	0.30	-327.7±9	8.9	4.7	0.7	emiss
B319-G044[e,g,j]	0.28	-540.0±21	8.6	4.7	0.8	
B049-G112[g]	0.25	-448.3±20	8.6	4.6	0.5	emiss
B040D	0.40	-318.4±15	8.8	4.6	0.7	
B043-G106[e,g]	0.25	-420.4±13	8.1	4.6	1.6	emiss
M087	0.65	-103.1±34	8.5	4.6	0.4	
B374-G306[g]	0.30	-107.2±24	8.8	4.5	0.4	
B475-V128[g]	0.28	-95.2±20	8.5	4.5	0.8	emiss
B216-G267[a,e,g,h]	0.25	-50.1±11	8.3	4.5	1.0	emiss
B019D	0.30	-416.1±14	9.0	4.5	0.6	
B458-D049[g]	0.25	-494.8±22	8.7	4.5	0.5	emiss
B303-G026[g]	0.22	-486.2±16	8.6	4.5	0.7	
B448-D035[g]	0.55	-550.1±18	8.4	4.5	0.5	
B015D-D041[g]	0.65	-457.6±18	8.2	4.5	0.7	
B327-G053[e,f,g,i]	0.25	-546.4±22	7.7	4.5	1.4	emiss
B380-G313[a,f,g,i]	0.28	-66.5±20	8.7	4.5	1.0	
B255	0.25	-433.4±23	8.7	4.5	0.5	
B040-G102[g]	0.25	-416.4±13	8.3	4.4	1.6	
B480-V127[g]	0.25	-110.4±17	8.7	4.4	0.5	
B014D	0.50	-433.5±24	8.4	4.4	0.7	
B371-G303	0.20	-59.8±17	8.7	4.4	0.6	
SK018A	0.50	-304.3±34	8.9	4.4	0.8	
B195	0.18	-360.2±12	8.9	4.4	0.8	
B091-G151[g]	0.25	-298.3±22	8.4	4.4	0.4	
B108D	0.38	-164.0±22	8.6	4.4	0.4	
M091	0.30	-143.7±43	8.9	4.4	0.5	
B484-G310[g,h]	0.30	-85.2±12	8.5	4.3	0.8	
B010D	0.25	-361.0±16	8.9	4.3	0.6	
B477-D075	0.30	-110.4±12	8.5	4.3	2.6	emiss
B318-G042[e,g]	0.14	-593.4±20	8.1	4.3	0.9	
V031[g,h]	0.30	-464.8±16	8.5	4.3	0.7	emiss
B032D	0.20	-325.7±16	8.8	4.3	0.5	
B210-M11[g,h]	0.35	-237.0±13	8.0	4.3	2.5	
M092	0.50	-74.6±20	8.7	4.3	0.6	
B035D	0.25	-311.6±14	8.6	4.3	0.9	emiss
B483-D085[g]	0.20	-61.5±20	8.7	4.3	0.8	
B089D	0.25	-172.0±17	8.8	4.3	0.7	emiss
B431-G027[g]	0.20	-507.1±23	8.4	4.3	0.5	
B323[d]	0.21	-499.8±25	8.4	4.3	0.4	emiss
B012D-D039[g]	0.52	-499.3±24	8.4	4.3	0.6	
B367-G292[g]	0.25	-111.9±20	8.3	4.3	0.9	
B376-G309[e,g]	0.23	-109.9±18	8.3	4.3	1.0	
KHM31-37	0.33	-521.4±28	8.2	4.3	1.9	
M059	0.25	-57.8±18	8.7	4.2	0.6	
B206D-D048[g]	0.25	-492.4±28	8.7	4.2	0.3	emiss
B321-G046[e,f,g,i]	0.20	-520.6±19	8.3	4.2	0.6	
B256D	0.28	-74.4±28	7.7	4.2	3.8	
V014	0.17	-450.4±16	8.2	4.2	1.0	
B452-G069	0.25	-507.4±19	8.2	4.2	0.8	
G085-V015	0.25	-444.3±20	8.2	4.2	0.5	
M093	0.28	-217.2±38	9.0	4.2	0.4	
M003	0.62	-239.3±31	7.7	4.2	0.8	
M086	0.18	-31.7±23	8.8	4.2	0.8	emiss
B322-G049[f,g,i]	0.28	-585.4±23	8.1	4.2	0.8	emiss
M072	0.25	-94.9±20	8.4	4.1	0.9	
M104	0.15	-39.5±21	8.7	4.1	0.9	
B442-D033	0.29	-563.2±19	8.1	4.1	0.6	
B201D-D044	0.25	-446.7±35	8.7	4.1	1.0	

TABLE 2 — *Continued*

Object	E(B−V)	Vel km s^{-1}	Log Age yr	Log Mass M$_\odot$	χ^2	Comments
KHM31-246	0.22	-173.6±19	9.1	4.1	0.6	
M101	0.25	-52.3±25	8.9	4.1	0.4	
B067D	0.28	-227.7±17	8.6	4.1	0.7	
KHM31-152	0.38	-405.7±52	8.7	4.1	0.3	
B314-G037[a,e,f,g,i]	0.18	-459.0±17	8.7	4.1	0.6	
B521	0.38	-515.8±33	8.4	4.1	0.4	
DAO47[g]	0.20	-515.8±18	8.7	4.1	0.4	
B278-M30	0.20	-42.7±18	8.5	4.1	0.6	
B006D-D036[g]	0.33	-543.8±19	8.2	4.0	0.5	
B189D-G047[g]	0.28	-560.0±18	8.2	4.0	1.0	
G083-V225	0.50	-331.9±22	8.1	4.0	0.7	
B106D	0.28	-311.6±36	8.0	4.0	0.4	
B342-G094[g,j]	0.23	-479.7±26	8.2	4.0	0.5	
G099-V022[d]	0.30	-458.4±21	8.6	4.0	0.8	
B069-G132[g]	0.18	-204.9±18	8.6	4.0	0.7	emiss
B095D	0.25	-304.0±17	8.5	4.0	0.4	
B066-G128[e,g]	0.15	-404.6±16	7.9	4.0	1.1	emiss
BH12[d]	0.25	-453.4±19	8.3	4.0	0.6	
B098D	0.25	-159.0±16	8.3	4.0	0.7	
B192-G242	0.10	-124.2±16	8.4	4.0	0.7	
M042	0.10	-232.9±23	8.6	4.0	0.5	
M001	0.20	-205.4±20	8.6	4.0	0.7	
M025	0.20	-166.3±18	8.4	4.0	0.4	
M088	0.33	-95.8±20	8.8	4.0	0.5	
B223-G278[a,g,h]	0.15	-33.0±10	8.3	3.9	1.1	emiss
BH10	0.25	-541.0±21	8.7	3.9	0.4	
PHF7-2	0.25	-588.0±25	8.0	3.9	0.5	emiss
B011D	0.28	-480.6±46	7.5	3.9	1.0	
KHM31-341	0.28	-484.3±50	8.5	3.9	0.4	
LGS04131.1_404612	0.20	-495.0±32	8.5	3.9	1.5	
M023	0.35	-222.1±19	8.4	3.9	0.4	
B061D	0.30	-214.4±31	8.3	3.9	0.4	
B111D-D065[g]	0.15	-99.1±14	8.3	3.9	0.8	
M079	0.30	-121.1±26	8.6	3.9	0.5	
B081D	0.32	-374.3±22	7.5	3.9	1.1	emiss
V202	0.28	-474.8±33	8.3	3.9	0.5	
M050	0.25	-156.6±32	8.6	3.9	0.4	
M085	0.25	-119.9±37	8.8	3.9	0.6	
M039	0.18	-82.4±22	8.5	3.8	0.5	
B200D-D043	0.29	-469.2±20	8.1	3.8	0.5	
M016	0.08	-194.2±19	8.7	3.8	0.6	
KHM31-97	0.25	-470.7±25	8.3	3.8	1.5	
DAO69	0.22	-132.1±16	7.6	3.7	0.9	emiss
B453-D042[g]	0.19	-526.0±18	7.8	3.7	0.9	
B443-D034[g]	0.20	-541.2±23	8.2	3.7	0.5	emiss
M005	0.25	-205.6±24	8.6	3.7	0.5	
M031	0.25	2.3±36	8.3	3.7	0.8	
PHF8-1	0.28	-403.5±20	8.0	3.6	0.5	
B118D	0.28	-212.3±36	8.0	3.6	0.6	emiss
KHM31-234	0.29	-184.1±34	8.8	3.6	0.4	
M082	0.25	-98.7±30	8.2	3.6	0.4	
V133	0.10	-57.9±16	7.9	3.6	0.6	emiss
KHM31-22	0.36	-550.0±52	8.3	3.6	0.3	
KHM31-85	0.25	-552.3±46	8.2	3.6	1.6	
M073	0.28	-84.7±19	8.3	3.5	0.6	emiss
M078	0.28	-110.2±35	8.4	3.5	0.4	
M076	0.25	-32.9±44	8.3	3.5	0.4	
KHM31-113	0.20	-534.3±25	8.2	3.5	2.3	
KHM31-345	0.15	-449.3±38	8.4	3.4	0.6	
M069	0.28	-87.1±40	8.3	3.4	0.4	
M080	0.25	-88.8±24	7.6	3.3	0.8	emiss
B246D	0.15	-159.5±44	6.5	3.3	6.1	
M062	0.25	-95.7±45	8.2	3.3	0.5	
M020	0.15	-220.1±30	7.1	3.3	0.6	
M068	0.28	-110.9±38	8.1	3.3	0.6	
WH2	0.20	-575.0±31	8.4	3.2	1.2	
KHM31-81	0.20	-500.9±38	7.9	2.7	1.1	emiss
B240D-D066	0.10	-129.0±29	6.6	2.6	0.6	
B196D	0.21	-507.4±15	6.3	2.4	1.0	emiss

TABLE 2 — *Continued*

Object	E(B−V)	Vel km s^{-1}	Log Age yr	Log Mass M$_\odot$	χ^2	Comments

[a] Not a cluster in Cohen et al. (2005)
[b] Star in field
[c] Noted as young in van den Bergh (1969)
[d] Noted as young in Hodge (1979)
[e] Noted as young in Elson & Walterbos (1988)
[f] Noted as young in Barmby et al. (2000)
[g] Noted as young in Fusi Pecci et al. (2005)
[h] Noted as young in Burstein et al. (2004)
[i] Noted as young in Beasley et al. (2004)
[j] Noted as young in Williams & Hodge (2001a)

TABLE 3
STARS

Object[a]	RA	Dec	Vel[b]	V	P[c]	C[d]
		2000	km s^{-1}			
B133D	0:34:10.99	39:50:50.2		18.18	G	B
BH01	0:34:11.92	39:24:11.6				H
B135D	0:35:32.39	41:19:47.5		17.76	G	B
DAO3	0:35:51.90	40:20:55.7	-83.8±36			S
B137D	0:36:20.90	40:56:00.0		18.51	G	B
B145D-G013	0:36:38.76	42:16:28.5	-84.6±20	17.53	G	S
B146D	0:36:42.42	41:38:19.9		18.07	G	B
B153D-G017	0:37:12.55	39:50:16.8	-4.6±24	16.66±0.04	L	SL
G018	0:37:18.45	40:21:19.5	14.9±22	17.28±0.08	L	SL
DAO16	0:37:57.25	40:24:49.7	-37.6±32	19.33±0.10	L	S
B164D	0:37:57.36	40:32:19.8	-1.5±22	17.55	G	S
G020	0:37:58.30	42:31:48.1	-64.0±35	17.96	G	S
B430-G025	0:38:42.9	41:44:00.0	-51.2±15	18.52	B	S
DAO023x	0:38:54.34	40:26:46.5	-38.0±24	19.25±0.11	L	SL
B178D	0:39:21.07	41:26:52.5	-27.0±23	18.11	G	S
B179D	0:39:25.42	41:27:24.7	3.9±22	18.00	G	S
B180D-D029	0:39:26.61	41:54:15.1	18.7±25	16.90	G	S
B182D	0:39:31.50	41:27:35.5	-32.2±21	17.25	G	S
B185D	0:40:00.05	40:34:22.9	-46.5±27	18.11±0.08	L	SLH
SK008A	0:40:00.45	40:43:53.7	-108.9±28	19.05±0.09	L	SLH
SK038B	0:40:03.72	40:44:04.2		17.48±0.09	L	LH
B441	0:40:07.90	41:43:36.0		19.14	G	B
B191D	0:40:17.89	42:25:23.9		17.95	G	B
DAO32	0:40:19.37	40:32:43.0	-31.3±20	15.90±0.05	L	SL
B445	0:40:21.80	41:46:57.0		18.88	G	B
B444	0:40:21.83	41:41:46.9	-6.2±25	19.14	G	SH
B326[f]	0:40:23.71	41:41:10.2	-54.3±23	17.98	B	SH
B193D-G055[f]	0:40:25.08	41:42:54.7	-142.7±23			S
B332	0:40:26.50	41:39:55.9		18.83	G	H
BH06x	0:40:31.22	40:44:52.5	30.3±24	16.62±0.09	L	SLH
B005D	0:40:32.86	41:34:42.3	-42.8±13	18.70	G	S
BH08	0:40:34.42	41:39:04.2	-61.4±15	18.66	G	SH
VB203x	0:40:48.47	40:59:11.6	81.7±33	19.69±0.08	L	SL
SK061B	0:40:57.98	41:03:38.7		18.72±0.09	L	LH
SK064B	0:41:01.95	41:08:21.9				LH
SK093C	0:41:03.47	40:46:06.7		19.42±0.11	L	LH
SK065B	0:41:05.10	41:11:06.1				LH
B201Dx	0:41:08.57	40:32:53.3	-43.4±43	19.67±0.09	L	SL
G083x	0:41:11.85	41:09:54.9	-0.2±13	17.56±0.03	L	SL
B018D	0:41:14.46	41:45:15.8	-9.0±32	17.40	G	S
SK075B	0:41:14.70	41:08:45.0		17.55±0.06	L	LH
B021D	0:41:25.77	41:10:19.1	-0.1±22	17.92±0.04	L	SL
B203D	0:41:25.99	40:35:18.7	-106.9±23	18.07±0.10	L	SL
SK031A	0:41:35.20	40:53:41.5				LH
B027D	0:41:37.03	41:45:27.4	-43.3±17	17.60	G	S
B028D-G100	0:41:37.75	40:52:03.7	-352.4±36	18.70±0.30	L	S
028D-100x	0:41:38.32	40:52:12.1	-503.8±22	21.70±0.29	L	SH
SK082B	0:41:38.53	40:52:33.7				LH
B030Dx	0:41:41.01	41:03:17.1	-4.4±26	17.40±0.09	L	SL
041-103x	0:41:41.23	41:14:42.9	-70.2±16	18.24±0.09	L	SLH
B030D[g]	0:41:41.49	41:03:08.0	-747.8±18	19.10±0.08	L	SL
B053	0:41:47.25	41:22:45.3	-17.1±22	18.28±0.07	L	SLH
B033D	0:41:47.89	41:04:00.1	-114.5±18	17.54±0.06	L	S
B253[f]	0:41:49.73	40:53:00.0	-463.7±22	19.46±0.06	L	SH
B034D	0:41:50.13	40:51:46.8	-31.1±23	18.38±0.09	L	SLH
SK088B	0:41:51.49	40:47:07.4		17.18±0.08	L	LH
B460	0:41:54.81	39:35:25.5		18.35	G	B
SK102C	0:41:55.94	40:50:20.4		15.24±0.04	L	LH
B036D	0:41:58.69	41:45:05.1	-67.6±19	17.10	G	S
BH14x	0:42:00.14	40:47:55.5	-20.3±16	14.20±0.04	L	SH
B039D	0:42:01.97	40:47:48.8	-416.8±35	19.10±0.08	L	SH
SK093B	0:42:06.58	40:52:01.9				LH
B044Dx	0:42:07.80	41:00:10.8	-0.7±17	15.20±0.09	L	SL
B072x	0:42:07.88	41:22:39.7	-14.6±20			S
DAO52	0:42:08.79	40:50:51.5		20.08±0.37	L	H
B046D[f]	0:42:10.41	41:15:50.4	-294.2±24	18.78±0.33	L	SH
047D-000x	0:42:11.31	41:29:54.2	-28.4±19	17.73±0.12	L	SLH
048D-000x	0:42:13.19	40:48:35.2	-380.2±16	20.17±0.11	L	S
SK107C	0:42:14.24	41:34:26.8		18.03±0.11	L	LH
B049D	0:42:16.18	41:08:09.1	-37.1±32	17.75±0.07	L	SL
B050D	0:42:17.31	41:07:41.0	-35.7±21	17.27±0.09	L	SL
B089	0:42:21.30	41:39:47.0	-264.6±9	18.18	B	S
B209D	0:42:23.55	42:13:54.2		18.17	G	B
SK105B	0:42:25.00	41:21:12.2		18.73±0.11	L	LH

TABLE 3 — *Continued*

Object[a]	RA	Dec	Vel[b]	V	P[c]	C[d]
		2000	km s^{-1}			
NB36	0:42:26.04	41:17:35.6		20.02±0.20	L	H
B095x	0:42:26.08	41:05:45.8	-45.7±50			S
B054D-NB33	0:42:26.19	41:19:05.4	-60.4±22	18.57±0.08	L	SLH
NB73	0:42:26.27	41:17:13.5		19.87±0.16	L	LH
NB56	0:42:26.68	41:13:48.3		18.17±0.06	L	LH
NB79	0:42:26.81	41:15:05.8	-150.2±31	18.37±0.09	L	SLH
NB83	0:42:27.00	41:13:19.9	-75.1±16	16.81±0.14	L	SLH
NB32	0:42:27.02	41:17:10.0		18.57±0.04	L	BLH
B055D	0:42:27.34	40:49:29.1	-82.4±12	19.67±0.09	L	SL
NB84	0:42:28.62	41:13:15.1		19.45±0.18	L	LH
NB102	0:42:28.88	41:17:50.6	-70.2±26	18.85±0.16	L	SLH
NB46	0:42:29.44	41:19:59.3	-8.3±28	17.54±0.05	L	SL
B210D	0:42:29.50	39:52:52.5		17.09	G	B
NB85	0:42:29.79	41:13:03.2	-118.6±34	19.75±0.05	L	SLH
B102	0:42:29.85	41:34:18.0	-211.2±17	16.57±0.03	L	SH
NB54	0:42:29.86	41:13:36.6		19.96±0.23	L	H
SK109C	0:42:30.05	41:23:26.0		17.86±0.04	L	LH
NB70	0:42:30.11	41:18:41.7	-15.1±22	14.93±0.06	L	SH
058D-000x	0:42:30.34	41:22:44.2	77.6±16	17.29±0.07	L	SLH
B057D	0:42:30.80	41:20:52.3	-239.5±33	19.62±0.12	L	S
B059D	0:42:30.95	40:54:18.0	-24.7±24	18.89±0.10	L	SL
B058D	0:42:30.97	41:22:37.7		18.58±0.10	L	H
NB51-AU2	0:42:31.05	41:13:34.6	40.2±26	18.01±0.09	L	SLH
NB43	0:42:31.41	41:20:20.1		19.51±0.08	L	H
NB81	0:42:31.47	41:13:37.0	-28.6±19	16.12±0.05	L	SLH
NB61[e]	0:42:31.69	41:19:48.0	-51.9±19	18.78±0.07	L	SL
NB82	0:42:31.75	41:13:28.2	-95.6±28	18.41±0.05	L	SLH
B060D	0:42:31.88	41:20:42.6	-180.3±25	19.10±0.12	L	SLH
NB48	0:42:32.21	41:19:21.7		17.75±0.07	L	LH
NB37	0:42:32.99	41:16:14.1		19.88±0.23	L	H
NB75	0:42:33.13	41:16:28.9	-65.7±20	15.78±0.07	L	SLH
NB76	0:42:33.47	41:15:50.2				LH
B113	0:42:33.54	41:21:38.5	-11.7±18	17.19±0.07	L	SL
NB47-AU3	0:42:33.98	41:19:28.9	23.0±51	19.02±0.10	L	SLH
NB67-AU13	0:42:34.15	41:19:46.6	-23.1±16	15.88±0.06	L	SLH
NB55	0:42:34.46	41:17:01.9		19.60±0.08	L	H
B118-NB78	0:42:34.54	41:15:08.4		16.82±0.07	L	LH
NB86	0:42:34.78	41:11:50.3	-29.5±22	17.60±0.04	L	SLH
NB64	0:42:35.19	41:19:58.8		18.21±0.09	L	LH
SK109B	0:42:35.21	40:52:23.5		18.06±0.09	L	LH
NB53	0:42:35.22	41:14:50.7		19.72±0.08	L	LH
B261-NB72	0:42:36.06	41:17:41.0	-58.0±29	18.06±0.07	L	SLH
NB80	0:42:36.88	41:14:22.5	-163.1±29	17.48±0.08	L	SLH
B120-NB71	0:42:36.99	41:18:28.6	-62.2±8	17.87±0.10	L	SLH
NB28	0:42:37.10	41:17:46.3		19.82±0.13	L	H
NB38	0:42:37.44	41:13:28.2		19.26±0.15	L	LH
NB68	0:42:37.49	41:19:18.1	-58.8±19	15.57±0.09	L	SLH
NB105	0:42:37.54	41:18:26.4		19.58±0.09	L	LH
NB27	0:42:38.16	41:13:36.7		18.72±0.13	L	H
B065D-NB69	0:42:38.40	41:18:47.9		18.50±0.08	L	LH
NB74	0:42:38.45	41:16:46.8	-60.0±12	20.04±0.24	L	H
B121	0:42:38.68	41:20:21.0	9.8±22	16.86±0.07	L	SLH
B211D	0:42:38.71	40:02:10.6		17.58	G	B
SK111B	0:42:39.08	41:16:58.8		17.28±0.04	L	LH
NB25	0:42:39.31	41:13:39.7	-75.6±18	18.39±0.04	L	SL
NB91	0:42:39.56	41:13:05.4	-81.0±20	15.65±0.05	L	SL
B069D	0:42:40.45	41:21:44.4		18.87±0.09	L	LH
B212D	0:42:41.4	40:18:54.9	-108.4±17	17.88	G	S
NB58	0:42:42.06	41:15:12.6		19.78±0.36	L	H
B213D	0:42:42.89	42:16:07.0	7.7±22	17.07	G	S
B215D-D056	0:42:43.28	41:12:02.7	-31.4±20	16.52±0.06	L	SL
B214D	0:42:43.40	42:22:04.0		17.77	G	B
B070D	0:42:43.7	41:21:21.9	-413.3±36	19.12±0.14	L	SLH
NB87	0:42:45.08	41:19:01.9	18.7±15	15.66±0.09	L	SL
SK113C	0:42:45.10	41:17:52.0				LH
NB90	0:42:45.11	41:13:30.8	-67.0±22	13.85±0.04	L	SH
B071D	0:42:45.32	41:21:43.1	3.0±26	18.66±0.08	L	SLH
NB30	0:42:45.89	41:17:53.2		19.10±0.20	L	H
B073D	0:42:46.19	40:48:36.0	-22.9±23	18.93±0.04	L	SL
NB92	0:42:46.97	41:12:08.4	-7.7±22	16.69±0.05	L	SLH
B074D-NB88	0:42:47.83	41:14:54.4		17.10±0.04	L	LH
NB95	0:42:48.04	41:15:36.9	-36.0±20	15.32±0.05	L	SLH
NB52	0:42:48.57	41:12:09.6	-0.5±21	20.24±0.35	L	SH
B075D-NB96	0:42:48.82	41:15:13.0	35.7±16	14.59±0.07	L	SH
AU007	0:42:48.95	41:16:40.5	-73.8±31	18.31±0.18	L	SLH

TABLE 3 — *Continued*

Object[a]	RA	Dec	Vel[b]	V	P[c]	C[d]
		2000	km s^{-1}			
B076D	0:42:49.39	40:52:50.9	-69.1±25	19.36±0.09	L	SL
NB45-AU9	0:42:49.45	41:13:39.9		18.64±0.10	L	BLH
NB94	0:42:49.56	41:15:40.7		17.85±0.17	L	BH
B077D	0:42:50.31	40:50:49.4		18.96±0.07	L	LH
NB101	0:42:50.89	41:12:30.8				LH
BH18x	0:42:51.41	41:10:38.1	-77.2±18	14.16±0.04	L	S
B133-G191[f]	0:42:51.64	41:23:29.9	-151.2±39	17.79±0.10	L	SH
NB50	0:42:51.88	41:12:56.2	-65.3±24	19.10±0.11	L	SLH
B263	0:42:52.2	40:47:56.0	-64.0±23	19.41±0.08	L	SL
NB40	0:42:53.28	41:12:46.4	-313.6±20	19.52±0.19	L	SH
B079D	0:42:53.92	40:46:44.0	-77.6±27	18.57±0.05	L	SL
B080D-NB93	0:42:54.15	41:16:14.0		17.57±0.10	L	LH
B083D-V232	0:42:55.29	41:02:11.3	-43.7±11	16.67±0.06	L	SLH
NB97	0:42:55.69	41:14:33.3	16.8±27	18.71±0.05	L	SLH
NB49	0:42:55.83	41:13:50.6		19.23±0.21	L	BH
SK114B	0:42:56.10	40:59:54.5				LH
NB99	0:42:56.16	41:13:27.0	-23.0±22	17.07±0.09	L	SLH
B139	0:42:56.41	41:18:22.3	-61.9±22	17.62±0.10	L	SLH
B084D	0:42:56.48	41:18:12.0		18.42±0.09	L	LH
B085D	0:42:56.6	40:52:12.9	-155.5±23	18.79±0.06	L	SLH
086D-000x	0:42:56.80	40:51:21.9	-20.6±25	18.82±0.12	L	SH
NB98	0:42:57.11	41:14:20.6		18.79±0.06	L	LH
NB100	0:42:57.19	41:13:11.4	-13.0±22	16.92±0.06	L	SLH
NB26	0:42:57.28	41:12:53.8		19.66±0.22	L	H
PHF4-2	0:42:57.81	41:18:24.4		19.94±0.06	L	H
BH20	0:42:58.02	40:56:45.3	-4.0±23	17.78±0.04	L	SLH
NB106	0:42:58.40	41:14:11.6	-102.9±20	16.13±0.09	L	SLH
B088Dx	0:42:59.02	41:04:21.6	-7.3±13			SH
B142	0:42:59.28	41:21:27.1	-44.6±22	17.60±0.09	L	SL
B218D	0:42:59.3	42:06:47.0	-70.5±21	18.19	G	S
B465-D057	0:42:59.93	41:14:43.7	-126.4±18	16.52±0.07	L	SL
B219D	0:43:00.0	42:14:02.9	-99.4±26	18.25	G	S
BH21	0:43:01.27	40:54:17.6	-66.7±16	18.55±0.08	L	SLH
B093D	0:43:01.89	40:49:54.9	-53.7±25	19.17±0.09	L	SH
B094D	0:43:05.56	41:11:49.0	-8.1±35	18.81±0.04	L	SH
SK119B	0:43:05.73	41:15:58.3				LH
B221D	0:43:05.84	42:18:55.6	-20.2±23	17.77	G	S
SK120B	0:43:05.98	41:23:08.5		17.67±0.08	L	LH
B222D	0:43:07.89	40:17:37.3		17.38	G	B
G204	0:43:08.08	41:16:52.7	-66.5±22	15.72±0.09	L	SLH
SK123B	0:43:09.28	41:34:01.6				LH
BH25x	0:43:12.25	41:02:47.2	47.7±15	16.30±0.06	L	SLH
V272	0:43:12.61	41:28:10.5	-183.4±15	18.73±0.09	L	SLH
B224D	0:43:14.12	42:14:00.5	-73.2±26	18.23	G	S
B226D	0:43:14.88	41:58:42.9	-11.8±24	17.89	G	S
B096D	0:43:16.31	41:37:30.4	-184.1±29	18.47±0.04	L	SL
B166	0:43:20.48	41:12:33.6	-24.7±12	16.74±0.06	L	SLH
B229D	0:43:21.66	39:49:39.0		17.32	G	B
DAO60	0:43:24.37	41:45:54.8	7.2±28	16.80±0.07	L	SL
SK132B	0:43:26.60	41:40:41.2				LH
DAO62	0:43:27.02	40:47:26.8	-41.8±41	17.63±0.05	L	S
B175	0:43:30.10	41:14:36.9	-11.6±13	16.74±0.03	L	SLH
B231D	0:43:33.9	42:17:26.9	-28.5±24	18.40	G	S
SK127C	0:43:34.28	41:40:46.1		18.52±0.09	L	LH
B232D	0:43:36.33	40:38:53.7	-8.0±16	17.85	G	S
B235D	0:43:48.78	41:51:25.5	-4.2±17	17.88±0.06	L	SL
B236D	0:43:49.34	39:54:35.9	-74.7±20	17.23	G	S
B105D[f]	0:43:51.99	41:15:50.4	-251.5±34	18.49±0.10	L	S
M003x	0:43:53.71	41:14:14.9	-98.7±17	17.84±0.06	L	SL
B202x	0:43:54.67	41:00:22.1	-14.4±22			SH
B107D	0:43:56.39	41:42:55.7	-81.9±20	18.66±0.04	L	SL
G253	0:43:56.71	41:26:19.2	-26.9±16	15.21±0.07	L	SL
B108Dx	0:43:57.77	41:45:29.6	-29.0±29	18.35±0.04	L	SL
M004	0:43:57.78	41:13:52.7	-265.6±39	17.48±0.04	L	S
B109D	0:43:58.97	40:42:17.0	27.2±14	17.00	G	S
B239D	0:44:02.04	42:18:18.2	-90.5±22	18.40	G	S
SK079A	0:44:04.59	41:32:09.2	-258.4±26	19.14±0.08	L	SLH
B362	0:44:09.34	41:41:39.1	-66.8±18	17.69±0.04	L	SL
B242D	0:44:13.27	39:48:52.9	5.0±22	17.81	B	S
M020x	0:44:14.05	41:22:27.9	8.3±24	18.27±0.05	L	SL
M028x	0:44:22.30	41:33:48.7	-91.7±22	20.42±0.08	L	S
BH26	0:44:23.77	41:45:02.7		21.11±0.29	L	H
BH27	0:44:25.20	41:45:29.0		20.59	G	H
B114D	0:44:25.59	41:44:14.8		19.36±0.14	L	LH
B473-M36	0:44:27.49	41:11:34.0	15.3±16	17.45±0.06	L	SL

TABLE 3 — *Continued*

Object[a]	RA	Dec	Vel[b]	V	P[c]	C[d]
		2000	km s^{-1}			
SK172B	0:44:28.99	41:20:10.5		17.79±0.09	L	LH
SK173B	0:44:30.93	41:18:22.4		18.26±0.09	L	LH
B116D	0:44:32.30	40:48:16.9	-163.9±17	17.50	G	S
B117D	0:44:32.51	40:45:52.2	-117.4±26	18.30	G	S
B248D-D070	0:44:40.63	41:40:43.5	-1.3±24	18.39±0.06	L	S
B251D	0:44:43.30	39:59:32.0		18.59	G	B
B282	0:44:43.69	40:44:15.6	-45.7±20	18.20	B	S
B252D	0:44:44.34	42:10:07.5	-31.2±16	17.67±0.06	L	SL
G289	0:44:45.75	41:17:08.0	-59.8±15			S
B254D	0:44:47.38	41:51:56.9	-55.5±16	16.55±0.05	L	SLH
B255Dx	0:44:48.68	42:06:08.0	11.5±40	19.76±0.08	L	SLH
SK181B	0:44:48.69	42:06:08.1				LH
G295	0:44:52.69	41:25:10.8	-22.9±15			S
SK183B	0:44:54.32	41:32:14.4				LH
B123D	0:44:55.56	41:12:50.1	-12.4±17	18.91±0.07	L	SL
B284	0:44:57.05	40:58:00.2	-71.3±13	19.23	B	S
SK094A	0:44:59.35	41:33:05.2				LH
WH23	0:45:00.86	41:30:58.9	-159.4±15	19.87±0.32	L	SH
B125D	0:45:08.03	40:51:40.0	-67.7±17	18.00	G	SH
B259D	0:45:08.88	40:17:02.1				B
B259Dx	0:45:09.20	40:17:03.2	-3.3±25			S
B258D	0:45:09.29	42:02:39.3	7.4±24	17.46±0.07	L	SL
SK168C	0:45:14.97	41:40:12.3		19.34±0.11	L	LH
B126D	0:45:15.70	41:10:12.0	-59.2±23	18.00	G	S
B262D-D077	0:45:19.95	41:19:11.5	-14.0±24	18.51±0.06	L	SL
B286	0:45:25.55	40:59:24.6	-22.7±12	18.45	G	S
B265D	0:45:26.51	40:39:07.4	-80.1±13	16.39	G	SH
M085x	0:45:27.26	41:42:10.7	-76.6±44	21.21±0.11	L	S
M083x	0:45:27.42	41:45:41.2	-81.4±51	21.78±0.12	L	S
287-000x	0:45:28.26	41:29:58.7	14.4±21	15.59±0.07	L	SL
B132D	0:45:35.59	41:18:12.5	-41.9±32	19.98±0.12	L	S
B272D	0:45:54.65	40:17:09.0	-26.3±22	16.34	G	S
G314	0:46:06.41	41:20:50.3		15.72	G	B
B275D	0:46:07.06	41:38:18.8	-9.7±22	18.23±0.04	L	SL
B278D	0:46:12.87	42:10:34.0	-55.2±19	18.12±0.06	L	SL
B279D	0:46:21.06	40:51:10.4	-47.9±12	17.97	G	S
BH31	0:46:21.76	42:06:31.0	24.6±26	18.63±0.04	L	SLH
B280D	0:46:22.38	40:40:23.5	-45.5±16	17.29	G	S
B487-G320	0:46:24.17	40:30:11.0	-13.1±17	16.71	G	S
B282D	0:46:26.12	40:50:26.7	-67.7±16	17.78	G	S
B286D	0:46:29.59	40:33:17.4	-23.6±20	17.76	G	S
B287D	0:46:29.63	40:33:22.3	-12.6±20			S
B288D	0:46:30.75	41:58:19.7	-15.0±22	18.10±0.08	L	SL
B388	0:46:40.95	41:38:11.6	-19.7±47	20.01±0.46	L	S
G325	0:46:41.3	41:50:00.8	-37.0±23	17.65±0.06	L	SL
B294D	0:46:51.09	40:01:43.6	-9.0±16	17.37	G	S
B390	0:46:51.63	40:23:46.9	-44.1±18	17.18	G	S
B296D	0:46:53.77	40:49:39.1	-8.5±16	17.67	G	S
B302D	0:47:04.51	40:01:36.9	-25.1±22	17.76	G	S
B308D	0:47:23.6	41:45:45.0	-104.3±17	17.96±0.04	L	SL
B309D	0:47:23.86	40:19:31.8	-18.6±19	17.31	G	S
B313D	0:47:31.02	40:27:07.8	0.8±23	17.65	G	S
B316D	0:47:35.01	40:26:27.0	-28.6±18	16.93	G	SH
B318D	0:47:37.82	40:25:27.3	-103.4±20	17.20	G	SH
B319D	0:47:39.09	40:25:04.3	-53.1±23	17.49	G	S
G339-BA30	0:47:50.21	43:09:16.4	33.0±26	17.19	B	S
B323D	0:47:50.37	40:07:40.9	-28.3±21	16.31	G	S
B324D	0:47:54.2	41:45:33.0	-60.0±33	18.74	G	S
325D-D095x	0:47:57.3	42:06:57.8	50.4±23	18.95±0.15	L	SL
B502	0:48:29.91	39:39:18.6		17.60	G	B
B504	0:48:45.16	40:08:45.9		17.83	G	B
B336D	0:49:09.80	41:17:23.3	-18.6±22	18.28	G	S
B508	0:49:45.80	41:23:22.8	-74.8±20	17.12	G	S
B510	0:50:33.90	41:49:20.4		17.71	G	B
B409	0:50:39.18	41:17:35.3		12.52	G	B
B511	0:50:43.41	40:11:13.3		17.27	G	B
B512	0:50:46.32	39:53:19.9		17.45	G	B

TABLE 3 — *Continued*

Object[a]	RA	Dec	Vel[b]	V	P[c]	C[d]
		2000	km s^{-1}			

[a] The suffix "x" indicates that coords correspond to a real object, but which was wrongly identified in the initial input catalog.

[b] All velocities from Hectospec

[c] Source of photometry: L=this paper; B=Barmby et al. (2000); G=Galleti et al. (2007)

[d] Source of classification as a star: S=spectrum from this paper indicates a star; L=LGS image indicates stellar FWHM; H=HST image indicates a star; B=Barmby et al. (2000) indicated a star

[e] NB61 is an M star, the velocity of -646 listed Galleti et al. (2007) was likely the result of a velocity template mismatch.

[f] Multiple stars or asterisms in M31.

[g] The velocity of this F supergiant star indicates is it probably a member of the M31 giant stream. Details to be presented in a subsequent paper.

TABLE 4
Possible Stars

Object[a]	RA	Dec 2000	Vel km s^{-1}	V	S[b]	P[c]	C[d]
SK015B	0:37:09.77	40:11:36.7		16.15±0.07		L	L
SK024B	0:38:11.02	40:38:52.3		19.13±0.08		L	L
B172D	0:38:42.20	40:12:12.0	-90.4±22	17.72±0.04	HS	L	SL
SK059C	0:38:53.74	40:38:30.4		18.50±0.04		L	L
B177D	0:38:56.19	40:03:14.9	-150.6±21	17.66±0.07	HS	L	SL
SK068C	0:39:23.47	40:14:40.4		16.93±0.06		L	L
B183D	0:39:42.29	40:40:32.0		18.14±0.03		L	L
SK034B	0:39:51.23	40:45:33.1		19.60±0.09		L	L
SK072C	0:39:59.11	40:28:17.2		18.35±0.09		L	L
SK037B	0:40:00.40	40:48:51.1		18.47±0.09		L	L
B190D-G048	0:40:16.90	40:39:31.0		19.18±0.05		L	L
SK013A	0:40:22.41	40:50:07.6	-104.5±53	19.82±0.09	K	L	L
SK046B	0:40:25.07	40:37:58.2		19.56±0.13		L	L
SK085C	0:40:33.28	40:51:53.6		19.52±0.25		L	L
SK052B	0:40:37.92	40:38:03.7		19.39±0.07		L	L
B451-D037	0:40:46.84	40:51:33.8		18.68±0.09		L	L
B016D	0:41:07.29	40:50:13.0		18.77±0.07		L	L
SK024A	0:41:19.70	40:39:29.7	-465.9±38	19.60±0.10	K	L	L
B022D	0:41:30.01	41:17:19.4		18.30±0.07		L	L
SK081B	0:41:37.38	40:59:19.2		15.57±0.04		L	L
SK099C	0:41:39.74	40:56:33.1					L
B459	0:41:49.27	42:07:42.5	-128.6±18	18.17	HS	G	S
SK039A	0:41:51.09	41:20:14.7	-246.1±35	18.39±0.09	K	L	L
B037D	0:41:59.10	41:21:58.5	-109.6±29	19.03±0.03	HS	L	SL
SK091B	0:41:59.95	40:46:04.1		17.00±0.10		L	L
SK092B	0:42:03.81	40:47:36.6		19.04±0.13		L	L
SK045A	0:42:09.56	40:47:44.0	-543.8±52	15.88±0.04	K	L	L
B048D	0:42:12.54	40:48:38.0		18.61±0.14		L	
SK047A	0:42:14.30	40:50:07.8					L
SK095B	0:42:14.60	40:51:12.4		18.48±0.12		L	L
SK098B	0:42:16.85	40:51:43.1		19.12±0.45		L	L
SK099B	0:42:19.60	41:27:02.7		17.94±0.06		L	L
SK100B	0:42:20.32	40:51:22.9		19.00±0.11		L	L
B052D	0:42:20.93	41:04:35.2		19.14±0.12		L	L
SK101B	0:42:21.57	41:27:59.1		17.92±0.10		L	L
SK103B	0:42:24.13	41:37:34.0		15.69±0.04		L	L
NB31	0:42:25.10	41:17:54.9	-2.4±22	19.30±0.04	HS	L	SL
NB66	0:42:25.7	41:19:47.0	-201.6±29	18.73±0.06	HS	L	SL
NB22	0:42:26.30	41:19:57.1		18.77±0.06		L	L
SK106B	0:42:28.21	40:51:37.1		17.73±0.04		L	L
NB65	0:42:29.68	41:19:53.3	5.0±16	16.26±0.07	HS	L	SL
NB107	0:42:30.28	41:15:19.7		18.68±0.04		L	L
NB77	0:42:30.92	41:15:38.2	-139.7±32	18.70±0.03	HS	L	SL
NB63	0:42:31.24	41:20:11.8	-64.5±17	17.38±0.05	HS	L	SL
SK051A	0:42:32.14	40:53:34.8					L
B063D	0:42:35.00	40:48:39.0		18.53±0.04		L	L
SK112C	0:42:44.53	40:54:28.9		17.74±0.07		L	L
B216D	0:42:46.50	41:51:43.9	-90.5±13	18.10±0.06	HS	L	SL
SK115C	0:42:49.82	41:22:36.0		15.92±0.09		L	L
NB59	0:42:51.13	41:14:36.6		19.31±0.12		L	L
SK116C	0:42:51.20	41:23:15.7		17.29±0.03		L	L
B355-G193	0:42:52.88	41:57:59.1	-81.8±12	17.76	HS	B	S
NB103	0:42:53.99	41:15:20.7		19.31±0.08		L	L
B082D	0:42:55.55	41:20:29.7	-91.9±21	19.07±0.11	HS	L	SL
B217D	0:42:58.05	41:54:49.7	-157.8±11	17.88	HS	G	S
SK057A	0:42:58.06	41:23:02.7	-220.6±20		K		L
SK118B	0:43:00.02	41:20:43.5		17.24±0.05		L	L
SK058A	0:43:05.95	41:50:59.7	-301.0±54	19.20±0.04	K	L	L
SK119C	0:43:08.94	41:07:31.9					L
SK121B	0:43:08.94	41:25:55.0		16.68±0.10		L	L
SK125C	0:43:27.23	41:07:54.1					L
SK135B	0:43:33.17	41:34:05.9		18.24±0.09		L	L
B100D	0:43:35.42	40:53:19.5	-55.7±12	17.84±0.04	HS	L	SL
SK137B	0:43:39.27	41:10:19.3					L
SK139B	0:43:41.38	41:48:47.5		19.15±0.06		L	L
SK129C	0:43:42.81	41:46:31.1		18.72±0.08		L	L
SK130C	0:43:44.41	41:47:05.3		18.67±0.11		L	L
B102D	0:43:44.93	41:20:27.4		19.12±0.03		L	L
SK142B	0:43:45.09	41:12:28.1					L
B104D-M2	0:43:49.10	41:14:16.1	-272.4±17	18.35±0.06	HS	L	S
SK143B	0:43:51.33	41:46:49.4		18.05±0.10		L	L
SK144B	0:43:52.19	41:42:39.2		18.81±0.09		L	L
SK146B	0:43:52.86	41:49:50.3		18.65±0.06		L	L
SK077A	0:43:56.36	41:19:47.9	-149.6±56	18.11±0.04	K	L	L

TABLE 4 — *Continued*

Object[a]	RA	Dec	Vel	V	S[b]	P[c]	C[d]
		2000	km s^{-1}				
B237D	0:43:57.31	41:59:55.5		18.27±0.07		L	L
SK151B	0:43:57.78	41:35:19.8		18.11±0.07		L	L
SK152B	0:43:59.39	40:48:04.1		18.72±0.06		L	L
B238D	0:43:59.99	41:51:45.9		18.00±0.07		L	L
SK153B	0:44:00.06	41:48:34.1		17.83±0.07		L	L
SK080A	0:44:06.85	41:49:04.3	-145.7±22	18.82±0.17	K	L	L
SK159B	0:44:10.61	41:17:59.5		17.54±0.08		L	L
H126	0:44:12.11	41:58:50.2	13.7±17	16.65±0.06	HS	L	SL
B241D	0:44:12.13	42:00:47.2	-45.4±22	17.10±0.08	HS	L	SL
SK161B	0:44:12.14	41:36:37.3		18.86±0.08		L	L
G270	0:44:12.17	41:33:24.2		17.29±0.09		L	L
SK141C	0:44:17.37	41:49:17.4		18.65±0.16		L	L
B243D	0:44:18.05	41:52:08.9	-71.8±29	18.24±0.07	HS	L	SL
B245D	0:44:20.43	41:47:31.0	-24.9±21	18.16±0.04	HS	L	SL
SK085A	0:44:20.63	41:41:45.0	-55.3±34	19.09±0.13	K	L	L
SK143C	0:44:26.97	41:38:34.4		19.32±0.09		L	L
SK170B	0:44:27.25	41:37:15.5		19.20±0.09		L	L
SK144C	0:44:29.76	41:55:37.2		18.93±0.07		L	L
SK146C	0:44:31.35	41:36:49.3		17.04±0.08		L	L
SK176B	0:44:36.75	41:52:48.8		19.16±0.09		L	L
SK177B	0:44:38.98	41:55:11.2		19.63±0.13		L	L
SK154C	0:44:40.77	41:56:47.0		18.59±0.05		L	L
SK178B	0:44:42.86	41:25:05.9					L
SK179B	0:44:42.88	41:33:26.2		17.78±0.05		L	L
B253D	0:44:46.29	40:36:44.9	-70.7±13	17.68	HS	G	S
B119D	0:44:47.45	41:24:09.5		18.17±0.09		L	L
SK188B	0:44:59.29	41:53:18.8					L
SK096A	0:45:02.25	41:23:36.7	-312.9±52	18.47±0.04	K	L	L
SK163C	0:45:07.00	42:17:47.5		18.97±0.07		L	L
SK098A	0:45:07.55	41:35:15.9					L
SK198B	0:45:10.47	41:50:20.0		18.41±0.09		L	L
B260D-M66	0:45:10.98	41:40:23.1	-105.4±25	17.11±0.08	HS	L	SL
B127D	0:45:16.91	41:24:41.5		18.72±0.06		L	L
B261D	0:45:17.15	42:10:57.4	-115.5±17	17.58±0.04	HS	L	SL
SK178C	0:45:24.55	41:27:41.7		19.21±0.09		L	L
B131D	0:45:29.63	41:22:46.8		18.87±0.06		L	L
B267D	0:45:35.87	40:35:34.6	-86.8±13	17.28	HS	G	S
SK206B	0:45:36.92	41:44:18.3		16.70±0.06		L	L
SK208B	0:45:41.14	41:55:08.2		18.84±0.07		L	L
SK191C	0:45:44.19	41:42:53.8		17.93±0.09		L	L
B270D	0:45:49.21	41:01:49.2	50.4±16	17.50	HS	G	S
DAO83	0:45:49.86	41:48:18.3		19.86±0.12		L	L
SK106A[e]	0:45:52.17	42:05:26.6	-889.9±38	19.50±0.15	K	L	L
B276D	0:46:10.33	40:50:32.3	-13.7±15	17.60	HS	G	S
B281D	0:46:22.27	40:18:08.0	-61.6±16	18.12	HS	G	S
B283D	0:46:28.57	41:53:05.1	-143.6±26	17.66±0.10	HS	L	SL
B289D	0:46:38.71	42:16:24.9	-181.0±40	18.30±0.06	B	L	L
SK224B	0:46:38.77	41:59:31.7		18.00±0.06		L	L
SK209C	0:46:39.70	41:51:35.4		19.90±0.12		L	L
B291D	0:46:41.27	40:03:02.0	-82.9±26	18.12	HS	G	S
SK225B	0:46:42.65	41:58:35.7		18.93±0.09		L	L
B292D	0:46:45.69	42:21:15.6		17.86±0.06		L	L
B293D	0:46:48.09	40:02:21.7	-52.9±21	17.91	HS	G	S
SK210C	0:46:48.19	41:45:40.3		18.08±0.06		L	L
SK211C	0:46:49.75	41:45:44.1		18.41±0.08		L	L
SK228B	0:46:55.53	42:20:50.3		17.81±0.05		L	L
SK218C	0:47:22.00	42:26:57.8		18.59±0.04		L	L
SK220C	0:47:28.80	41:53:50.4		17.38±0.04		L	L
SH24	0:48:10.67	42:25:22.9		16.77±0.05		L	L

[a] The suffix "x" indicates that coords correspond to a real object, but which was wrongly identified in the initial input catalog.

[b] Source of velocity: HS=this paper; B=Barmby et al. (2000); K=Kim et al. (2007); P=Perrett et al. (2002)

[c] Source of photometry: L=this paper; B=Barmby et al. (2000); G=Galleti et al. (2007)

[d] Source of classification as a star: S=spectrum from this paper exists but is inconclusive; L=LGS image indicates stellar FWHM; B=Barmby et al. (2000) indicated a star

[e] The colors of SK106A indicate it is an M star, the velocity of -890 reported in Kim et al. (2007) was likely the result of a velocity template mismatch (see also Lee et al. 2008)

TABLE 5
Galaxies

Object	RA	Dec	Z[a]
	2000		
G006	0:35:04.77	42:35:32.2	0.06568
G007	0:35:13.70	42:35:18.5	0.08222
DAO1	0:35:18.89	40:09:11.1	0.20722
B136D-G008	0:35:52.43	39:57:08.0	0.10042
B414	0:36:19.3	42:16:30.9	0.08603
B294-G012	0:36:32.94	40:24:53.4	0.03588
B143D-D005	0:36:35.68	40:28:15.2	0.09974
B296-G015	0:36:46.88	40:30:47.1	0.10004
B415	0:36:51.05	40:30:38.4	0.09992
B297-G016	0:36:51.47	39:38:37.8	0.09383
B149D-D006	0:36:56.04	40:08:52.1	0.13675
B416-D007	0:37:01.43	39:48:34.9	0.13748
B151D-D008	0:37:02.26	39:48:05.0	0.13770
B417	0:37:05.54	42:02:34.5	0.17738
B152D	0:37:06.11	42:25:41.1	0.12812
B418	0:37:17.78	40:06:51.3	0.06431
B154D	0:37:20.64	42:18:49.4	0.11941
B155D-D009	0:37:25.82	40:04:54.2	0.14373
B419-D010	0:37:27.22	39:43:08.7	0.13888
DAO11	0:37:29.18	39:57:01.2	0.13357
B158D	0:37:36.71	39:50:11.0	0.05610
DAO12	0:37:39.54	39:46:30.8	0.17826
B159D-D013	0:37:46.08	40:05:12.7	0.13297
B160D-D014	0:37:50.59	40:10:39.8	0.13653
B161D-D015	0:37:51.35	40:10:06.3	0.13660
B162D	0:37:53.49	40:03:38.2	0.12807
B163D	0:37:55.16	39:53:54.0	0.10156
B424-D017	0:38:03.07	39:45:23.0	0.15199
B425	0:38:17.68	39:37:19.1	0.05641
B300	0:38:18.65	39:39:58.8	0.12294
B427-D019	0:38:22.71	39:58:09.7	0.09570
B168D-D020	0:38:25.00	39:40:50.9	0.12873
B169D	0:38:25.45	39:52:07.0	0.05602
B170D-D021	0:38:28.1	39:44:06.0	0.12456
B428	0:38:36.24	40:45:01.6	0.05624
B171D	0:38:37.41	40:39:18.9	0.04633
B173D	0:38:43.73	40:41:46.7	0.07281
B174D-V009	0:38:47.81	40:41:05.6	
B175D	0:38:48.42	40:04:32.4	0.13348
DAO22	0:38:53.76	39:51:30.5	0.09597
432-000x	0:38:59.1	41:43:16.0	0.14604
B433	0:39:02.49	40:00:10.0	0.14700
DAO25	0:39:13.32	40:07:31.8	0.15254
B434-D026	0:39:15.17	41:29:15.6	0.12857
B435-D028	0:39:18.42	40:48:25.7	0.09929
B308-V001	0:39:18.94	40:29:33.2	0.04650
B437	0:39:32.94	39:55:15.8	0.10203
B438	0:39:35.50	40:00:00.6	0.14612
B439-G034	0:39:40.15	41:02:14.8	0.08888
B184D	0:39:48.78	42:23:12.0	0.11898
B241	0:39:55.45	41:15:07.0	0.13816
B242	0:40:00.98	41:00:57.6	0.09967
B243	0:40:01.76	41:09:22.1	0.19105
B440	0:40:02.29	42:09:56.3	0.14476
B002D	0:40:03.62	41:33:03.8	0.12041
B187D-D031	0:40:05.63	41:34:39.5	0.13959
B320	0:40:15.70	41:48:30.6	0.17970
B192D	0:40:24.72	40:37:49.8	0.05512
B329	0:40:24.75	41:47:23.6	0.09403
B004D-V223	0:40:26.28	41:13:42.6	0.05186
B194D	0:40:26.59	39:58:50.3	0.12960
B447	0:40:26.67	40:07:06.5	0.07911
B446	0:40:27.24	41:36:55.1	0.11343
B007-G059	0:40:27.27	41:29:09.8	0.13964
BH07	0:40:30.70	41:26:27.0	
B245-V213	0:40:36.09	41:07:33.2	0.05262
B014-V222	0:40:38.60	41:12:45.8	0.09936
B197D	0:40:41.07	39:58:31.1	0.12953
B013D	0:40:57.22	41:27:23.9	0.13906
B199D	0:41:03.52	40:29:53.2	0.12867
B454-G079	0:41:03.99	40:01:30.5	0.10194
B202D	0:41:14.07	40:06:16.0	0.10489
B250	0:41:15.18	41:33:57.6	0.12719
B456-D045	0:41:21.41	40:15:08.1	0.07504
DAO46	0:41:22.99	40:28:33.8	0.10795

TABLE 5 — *Continued*

Object	RA	Dec	Z[a]
		2000	
B204D	0:41:33.51	42:20:36.3	0.09266
B023D	0:41:33.62	41:21:32.3	0.11434
B025D-V217	0:41:34.29	41:01:05.9	0.17570
B026D-V216[b]	0:41:34.37	41:00:49.9	0.17558
B251	0:41:36.60	41:00:18.2	0.17802
G099x	0:41:36.78	40:47:23.4	0.15351
B205D	0:41:38.08	40:34:10.2	0.09937
B252	0:41:39.26	41:30:35.2	0.26806
B207D-D050	0:41:44.95	40:16:06.7	0.12205
B052-V266	0:41:46.96	41:38:09.7	0.10034
B208D	0:41:48.43	40:13:06.5	0.09232
DAO51	0:41:56.59	40:22:59.4	0.07286
B062-G123	0:42:00.29	41:38:32.4	0.12727
B256	0:42:01.06	41:38:11.1	0.19107
B042D	0:42:06.08	41:02:47.7	0.19288
B043D-V246[b]	0:42:06.57	41:18:06.2	0.05176
B044D-V228	0:42:07.11	41:00:16.5	0.11924
DAO53	0:42:09.86	40:38:04.1	0.12792
DAO54	0:42:11.03	40:18:55.4	0.10366
B079	0:42:12.17	41:29:27.8	0.10072
G145	0:42:16.12	40:19:35.9	0.10266
B346-G149	0:42:20.16	40:30:30.6	0.12729
NB23	0:42:26.66	41:18:04.6	0.18340
B463-G160	0:42:27.51	40:35:52.4	0.12762
BH15	0:42:27.60	40:33:30.0	
B464	0:42:30.69	42:00:13.1	0.11911
B062D	0:42:33.99	40:54:15.2	0.11878
B066D	0:42:38.50	40:49:48.5	0.14587
BH19	0:42:57.08	40:49:17.1	
BH22	0:43:04.3	40:51:28.9	0.28429
B267	0:43:05.65	40:46:04.7	0.17478
BH24	0:43:11.8	40:53:03.1	0.28412
B270	0:43:17.42	40:55:45.6	
B228D	0:43:18.99	40:24:12.6	0.12756
B469-G220	0:43:19.33	42:10:18.3	0.07201
B230D-D061	0:43:24.56	40:24:51.8	0.12624
B273	0:43:26.51	40:51:51.6	0.18069
SK067A	0:43:27.50	41:35:34.8	0.15485
A0043281+410739	0:43:28.12	41:07:38.5	0.27176
B099D	0:43:34.80	40:55:42.2	0.12253
B470-D063	0:43:37.54	42:09:47.4	0.13297
SK070A	0:43:39.75	41:29:16.3	0.11186
B101D	0:43:41.25	40:54:45.6	0.17700
B471-G238	0:43:41.63	42:07:57.0	0.10277
B234D	0:43:42.01	39:46:28.6	0.09353
B191	0:43:43.54	40:43:41.8	0.10416
SK075A	0:43:52.37	41:38:30.0	0.07363
B360	0:43:55.73	40:01:23.3	0.07300
B275x	0:43:56.12	40:58:52.9	0.12126
B275	0:43:56.46	40:58:50.5	0.12111
SK078A	0:43:58.56	41:25:02.4	0.17779
B276	0:44:02.70	41:02:17.7	0.12156
V285-M18	0:44:11.23	41:25:22.7	0.12076
B364	0:44:18.86	39:45:21.5	0.06485
B244D	0:44:19.17	42:25:10.8	0.12887
B113D	0:44:22.96	40:46:27.0	0.12701
B280	0:44:27.42	40:50:17.9	0.17543
B226-M38	0:44:30.51	41:10:59.3	0.10057
B247D	0:44:30.81	40:05:54.9	0.12651
B227	0:44:31.24	40:44:19.9	0.12777
B249D	0:44:42.64	39:46:06.0	0.11900
B250D-D071	0:44:43.95	42:07:30.1	0.12011
B120D	0:44:48.24	41:16:17.0	0.18097
B474	0:44:50.28	41:09:22.8	0.12076
PHF4-1	0:44:53.67	41:16:57.0	0.18398
B122D	0:44:55.06	41:16:15.8	0.10979
B124D	0:45:04.70	41:08:55.1	0.23155
B369	0:45:12.10	39:52:53.2	0.12802
B478-D076	0:45:12.73	42:24:08.2	0.12046
B263D-D078	0:45:22.22	42:20:56.6	0.11101
B264D	0:45:22.51	39:38:59.3	0.04798
B128D-D079	0:45:23.39	41:21:27.6	0.11052
B285	0:45:25.03	41:05:18.9	0.11230
B129D	0:45:27.91	40:48:03.3	0.05498
B479-D080	0:45:27.94	42:07:03.0	0.05183

TABLE 5 — *Continued*

Object	RA	Dec	Z[a]
		2000	
B130D	0:45:29.04	41:20:37.9	0.09282
B266D	0:45:29.15	40:05:49.3	0.12495
DAO81	0:45:30.08	42:14:18.9	0.11211
B288	0:45:41.11	41:06:31.4	0.11072
B268D-D082	0:45:44.13	41:40:06.1	0.11053
B269D	0:45:46.25	39:49:32.4	0.12835
B481	0:45:48.19	40:23:29.8	0.16685
B271D	0:45:51.80	40:30:15.6	0.09650
DAO84	0:45:52.33	41:42:49.2	0.31014
B482	0:45:53.21	41:19:17.9	0.09551
B273D	0:45:59.37	40:36:40.0	0.10662
B274D	0:45:59.39	40:38:08.1	0.10588
B485	0:46:06.50	40:47:09.1	0.05149
B277D	0:46:10.11	40:02:53.3	0.10568
B385-G321	0:46:24.90	41:35:09.4	0.09505
B284D	0:46:29.18	41:02:57.1	0.04874
B285D	0:46:29.26	41:03:46.4	0.04825
A0046383+410729	0:46:38.32	41:07:28.5	0.02515
B290D	0:46:38.77	39:27:01.8	0.06698
B490	0:46:40.74	41:32:56.9	0.12711
B389-G326	0:46:43.81	41:49:10.1	0.12576
B491	0:46:51.35	41:09:45.0	0.12890
B295D	0:46:52.17	41:15:09.1	0.10772
B298D	0:46:59.50	40:19:51.5	0.13566
B299D	0:47:00.30	40:59:37.8	0.10699
B300D	0:47:00.34	40:40:36.8	0.13182
B492	0:47:02.54	41:10:12.6	0.10734
B303D	0:47:04.51	39:42:01.1	0.16578
B394-G331	0:47:05.62	41:08:11.9	0.05170
B395-G332	0:47:06.08	41:12:25.4	0.10713
B304D	0:47:06.47	41:35:44.2	0.10847
B305D	0:47:08.24	39:48:18.2	0.09912
B306D	0:47:14.48	39:45:14.4	0.28800
B493-D090	0:47:14.48	42:17:05.7	0.15354
B494-G333	0:47:20.43	41:54:57.2	0.07397
B307D	0:47:20.58	39:44:13.9	0.09509
B310D	0:47:26.89	40:54:21.7	0.12726
B312D	0:47:29.4	40:02:14.0	0.12983
B496	0:47:29.45	39:40:23.7	0.09529
B311D-G337	0:47:29.69	41:43:20.9	0.12857
B314D	0:47:31.69	40:53:11.1	0.12472
B315D	0:47:33.23	39:56:45.8	0.11053
B317D	0:47:36.08	40:22:30.3	0.13476
B320D	0:47:41.43	42:04:14.0	0.07917
B497-G338	0:47:44.85	40:11:37.1	0.11000
B321D	0:47:45.45	41:15:27.7	0.05482
B322D	0:47:45.69	39:44:41.7	0.10572
B498-G340	0:47:49.40	41:39:09.5	0.10803
B325D-D095	0:47:57.31	42:07:02.4	
B499	0:48:03.53	39:42:14.1	0.13698
B326D	0:48:09.08	39:30:02.4	
B327D	0:48:10.79	41:32:26.6	0.10837
B328D	0:48:16.68	40:21:50.8	0.13245
B501-G345	0:48:23.55	40:29:21.5	0.13271
B330D	0:48:26.96	41:38:07.5	0.12759
B331D	0:48:29.24	41:35:10.1	0.10791
B333D	0:48:36.32	41:20:42.1	0.10256
B341D	0:49:32.01	41:39:00.7	0.12557

[a] All redshifts from Hectospec. Median velocity error is 17 km s^{-1} . Entries without redshifts were classified background based on images.
[b] Perrett et al. (2002) had velocity indicating M31 membership

TABLE 6
MISSING OBJECTS OR BAD COORDINATES

Object	RA	Dec
		2000
SH05	0:38:55.20	41:10:28.0
SH06	0:39:19.30	41:10:29.0
SH08	0:40:31.40	40:26:27.0
B450	0:40:46.8	41:40:27.0
NB60	0:42:26.68	41:18:10.7
V229	0:42:34.50	40:55:44.0
NB57	0:42:36.13	41:13:13.2
NB44	0:42:46.52	41:17:58.4
NB42	0:42:46.97	41:17:35.2
B353-CFA1	0:42:47.41	41:15:40.5
NB104	0:42:56.22	41:14:14.8
SH14	0:44:14.8	41:55:23.9
M060	0:45:06.83	41:38:57.8
DAO93	0:47:46.20	41:44:55.0
SH25	0:51:58.70	41:35:17.0

TABLE 7
Comparison of ages

Object	Age (Gyr) CMD	Age (Gyr) Spec	ref
B049-G112	0.35	0.44	this paper
B315-G038	0.10	0.13	Williams & Hodge (2001a)
B318-G042	0.056	0.12	Williams & Hodge (2001b)
B319-G044	0.10	0.28	Williams & Hodge (2001a)
B342-G094	0.16	0.15	Williams & Hodge (2001a)
B367-G292	0.20	0.20	this paper
B458-D049	0.25	0.51	this paper

B049-G112 0.35 0.44 this paper
B315-G038 0.10 0.13 Williams & Hodge (2001a)
B318-G042 0.056 0.12 Williams & Hodge (2001b)
B319-G044 0.10 0.28 Williams & Hodge (2001a)
B342-G094 0.16 0.15 Williams & Hodge (2001a)
B367-G292 0.20 0.20 this paper
B458-D049 0.25 0.51 this paper